Time-varying, serotype-specific force of infection of dengue virus

Robert C. Reiner, Jr.[a,b,1], Steven T. Stoddard[a,b], Brett M. Forshey[c], Aaron A. King[a,d], Alicia M. Ellis[a,e], Alun L. Lloyd[a,f], Kanya C. Long[b,g], Claudio Rocha[c], Stalin Vilcarromero[c], Helvio Astete[c], Isabel Bazan[c], Audrey Lenhart[h,i], Gonzalo M. Vazquez-Prokopec[a,j], Valerie A. Paz-Soldan[k], Philip J. McCall[h], Uriel Kitron[a,j], John P. Elder[l], Eric S. Halsey[c], Amy C. Morrison[b,c], Tadeusz J. Kochel[c], and Thomas W. Scott[a,b]

[a]Fogarty International Center, National Institutes of Health, Bethesda, MD 20892; [b]Department of Entomology and Nematology, University of California, Davis, CA 95616; [c]US Naval Medical Research Unit No. 6 Lima and Iquitos, Peru; [d]Department of Ecology and Evolutionary Biology, University of Michigan, Ann Arbor, MI 48109; [e]Rubenstein School of Environment and Natural Resources, University of Vermont, Burlington, VT 05405; [f]Department of Mathematics and Biomathematics Graduate Program, North Carolina State University, Raleigh, NC 27695; [g]Department of Biology, Andrews University, Berrien Springs, MI 49104; [h]Liverpool School of Tropical Medicine, Liverpool, Merseyside L3 5QA, United Kingdom; [i]Entomology Branch, Division of Parasitic Diseases and Malaria, Center for Global Health, Centers for Disease Control and Prevention, Atlanta, GA 30333; [j]Department of Environmental Sciences, Emory University, Atlanta, GA 30322; [k]Global Health Systems and Development, School of Public Health and Tropical Medicine, Tulane University, New Orleans, LA 70112; and [l]Institute for Behavioral and Community Health, Graduate School of Public Health, San Diego State University, San Diego, CA 92182

Edited by Burton H. Singer, University of Florida, Gainesville, FL, and approved April 16, 2014 (received for review August 15, 2013)

Infectious disease models play a key role in public health planning. These models rely on accurate estimates of key transmission parameters such as the force of infection (FoI), which is the per-capita risk of a susceptible person being infected. The FoI captures the fundamental dynamics of transmission and is crucial for gauging control efforts, such as identifying vaccination targets. Dengue virus (DENV) is a mosquito-borne, multiserotype pathogen that currently infects ∼390 million people a year. Existing estimates of the DENV FoI are inaccurate because they rely on the unrealistic assumption that risk is constant over time. Dengue models are thus unreliable for designing vaccine deployment strategies. Here, we present to our knowledge the first time-varying (daily), serotype-specific estimates of DENV FoIs using a spline-based fitting procedure designed to examine a 12-y, longitudinal DENV serological dataset from Iquitos, Peru (11,703 individuals, 38,416 samples, and 22,301 serotype-specific DENV infections from 1999 to 2010). The yearly DENV FoI varied markedly across time and serotypes (0–0.33), as did daily basic reproductive numbers (0.49–4.72). During specific time periods, the FoI fluctuations correlated across serotypes, indicating that different DENV serotypes shared common transmission drivers. The marked variation in transmission intensity that we detected indicates that intervention targets based on one-time estimates of the FoI could underestimate the level of effort needed to prevent disease. Our description of dengue virus transmission dynamics is unprecedented in detail, providing a basis for understanding the persistence of this rapidly emerging pathogen and improving disease prevention programs.

disease ecology | emerging infections | arthropod-borne virus

The force of infection (FoI) describes the per-capita rate at which susceptible individuals become infected with a pathogen (1, 2). An accurate estimate of the FoI is essential for parameterizing disease models (3). It can be used to calculate key quantities such as the basic reproductive number ($\mathcal{R}_0$) (2, 4) and the critical vaccination coverage threshold (p_c) of a pathogen (5), which are frequently used to guide disease control programs and for determining the control effort required to eliminate a disease (6).

Dengue, a mosquito-borne disease whose incidence and geographic range have increased considerably in the past 50 y (7, 8), is caused by any of four related but antigenically distinct virus serotypes (DENV-1, DENV-2, DENV-3, and DENV-4). Previous estimates of the FoI for DENV are few and uncertain owing to limitations inherent to most available DENV datasets, including difficulty in specifying when an individual DENV infection occurred. Given the growing public health need for optimal vector management strategies and the growing potential for deployment of a dengue vaccine in the near future (9), there is a pressing need for accurate, serotype-specific estimates of the FoI and p_c for DENV. Here, we use a unique, long-term serological dataset from Iquitos, Peru to provide to our knowledge the first such estimates.

Basic mathematical models of pathogen transmission, such as the catalytic model where the FoI was initially introduced (1), make simplifying assumptions about the parameters governing transmission, including the frequent assumption that parameters do not vary through time in epidemiologically important ways (10). The assumption that the FoI is constant in time is, however, inconsistent with current understanding of DENV epidemiology because transmission clearly varies seasonally and year to year (8, 11–14). Resolving the magnitude of temporal variations in the quantities that govern or summarize transmission requires (*i*) adequate, temporally resolved incidence data and (*ii*) development of an estimation approach specifically designed to use such a dataset to compute time-varying quantities.

Significance

Using mathematical models to extend knowledge of pathogen transmission and recommend optimized control efforts is dependent on the accuracy of model parameters. The rate at which susceptible individuals become infected [the force of infection (FoI)] is one of the most important parameters, but due to data constraints it is often incorrectly assumed to be constant over time. Using a bespoke method for a 12-y longitudinal dataset of serotype-specific dengue virus (DENV) infections, we estimated time-varying, serotype-specific FoIs for all four DENV serotypes. The FoI varied markedly in time, which implies that DENV transmission dynamics are complex and are best summarized using time-dependent transmission parameters. Our results provide more accurate measures of virus transmission dynamics and a basis for improving selection of control and disease prevention strategies.

Author contributions: R.C.R., S.T.S., B.M.F., H.A., A.L., G.M.V.-P., V.A.P.-S., P.J.M., U.K., J.P.E., E.S.H., A.C.M., T.J.K., and T.W.S. designed research; R.C.R., S.T.S., B.M.F., A.A.K., A.M.E., K.C.L., C.R., S.V., H.A., I.B., A.L., G.M.V.-P., V.A.P.-S., P.J.M., U.K., E.S.H., A.C.M., T.J.K., and T.W.S. performed research; R.C.R., A.A.K., and A.L.L. contributed new reagents/analytic tools; R.C.R., S.T.S., B.M.F., A.A.K., A.M.E., A.L.L., and A.C.M. analyzed data; and R.C.R., S.T.S., and T.W.S. wrote the paper.

The authors declare no conflict of interest.

This article is a PNAS Direct Submission.

Freely available online through the PNAS open access option.

[1]To whom correspondence should be addressed. E-mail: rcreiner@ucdavis.edu.

This article contains supporting information online at www.pnas.org/lookup/suppl/doi:10.1073/pnas.1314933111/-/DCSupplemental.

Review of approaches for estimating the FoI of dengue (3) shows that, mostly owing to data limitations, two approaches have predominated over the last 30 y (2): (*i*) methods intended for use with data collected passively from clinics and hospitals (clinical cases) and (*ii*) methods for use with data actively collected from age-stratified serologic surveys. Data that are collected from verified clinical cases are temporally resolved but only capture clinically apparent infections. Not accounting for the potentially large proportion of undetected, inapparent infections can greatly diminish the accuracy of FoI estimates (15). Indeed, the ratio of DENV infections that are subclinical (i.e., inapparent*) to those that are clinically apparent can be variable and often quite large, ranging from 0.9:1–40:1 and higher (11, 16–18).

Thus, estimates of the DENV FoI based on verified clinical cases (e.g., refs. 19–21) are uncertain. In contrast, serological surveys theoretically capture all (or most) infections in a study population. The tradeoff is that the actual time of the infection cannot be defined from a single blood sample, and so the individual's age is used instead. An important complication for multistrain pathogens, like DENV, is that the infecting strain is often not determined in serological surveys. Investigators in several studies estimated the FoI of DENV using single serological surveys (e.g., refs. 4, 13, and 22), but cross-reactive antibodies obscure identification of the infecting serotype. Thus, in most dengue endemic settings one cannot resolve potentially important relationships among serotypes such as antigenic-dependent enhancement (23) using single blood specimens from cross-sectional surveys. Owing to limitations of both serology and reported clinical case data, current estimates of the FoI for DENV are uncertain and potentially inaccurate.

Prospective, longitudinal studies generate serial samples from the same individuals over several years that can be used to validate serological results and derive serotype-specific infection information (11). A longitudinal study design, therefore, provides data that are amenable to estimating the FoI, particularly if the FoI changes from year to year and is serotype-specific (24). Because existing FoI estimation approaches were not designed to use longitudinal data, we developed a spline-based modeling approach to analyze a 12-y longitudinal serology dataset (11,703 participants and 38,416 blood samples) from the city of Iquitos, Peru and produced the first, to our knowledge, time-varying, serotype-specific FoI estimates for DENV.

Methods

Approval of Experiments Involving Human Subjects. This study used information from participants in five overlapping cohorts. Each had separate human subjects protocols (see *SI Appendix*, Table S1 for protocol numbers) that were in compliance with US federal regulations governing the protections of human subjects. All protocols received approval from the institutional review boards (IRBs) of all participating institutions and from a Peruvian Ethics Committee that ensured that all Peruvian regulations governing the protection of human subjects were followed. Starting in 2007, the Naval Medical Research Center Detachment (now NAMRU-6) formed an IRB that is registered with the Department of Defense, the Office Human Research Protection, and the Peruvian Ethics Committee. In addition, all protocols were reviewed and approved by the Loreto Regional Health Department, which oversees health-related research in Iquitos. In all instances, written consent was provided by study participants.

Data and Seroconversion Identification. Iquitos is an isolated city of ∼370,000 inhabitants located in the Amazon basin of northeastern Peru. It has been well described elsewhere (11). All four DENV serotypes have been introduced into Iquitos and subsequently circulated endemically: DENV-1 in 1990 (25), DENV-2 in 1995 (26), DENV-3 in 2001 (11), and DENV-4 in 2008 (27, 28). Our analysis includes 12 y (1999–2010) of data from five longitudinal dengue cohorts involving Iquitos residents >5 y of age (see *SI Appendix*, section S1 and Table S1 for details; Fig. 1). In each cohort, participants provided blood samples for testing by plaque reduction neutralization tests (PRNTs) at 6–9 mo intervals. In some circumstances, studies overlapped in time and space (*SI Appendix*, section S1). For our analysis, we combined all cohorts into a single subsample of the Iquitos population with extensive turnover of individuals throughout the study period. Some of the later cohort studies recruited individuals that were either not yet born or too young to qualify for inclusion in the first cohort (i.e., aged less than 5 y in 1999). As such, to maintain a comparable subpopulation (and avoid confounding effects of birth and a changing population size in Iquitos), we removed individuals from consideration who were born after 1995. This resulted in the removal of 1,465 children from consideration. Thus, our analyses were based on the subpopulation of individuals born before 1995, which henceforth we will refer to as the sample population.

All blood samples from 1999 through 2010 were analyzed for the presence of DENV neutralizing antibodies by serotype-specific PRNT (11) in baby hamster kidney BHK21 cells using a carboxymethyl cellulose overlay. Samples were considered positive when plaques were reduced 70% or more (PRNT70) using dilutions of 1:60, 1:80, 1:60, and 1:40 for DENV-1, DENV-2, DENV-3, and DENV-4, respectively (11) (*SI Appendix*, section S2). Chronological sets of PRNT70 results, coupled with knowledge of the timing of DENV serotype introductions into Iquitos, provided confidence in our interpretation of serologic results (29). On this basis, we designed an algorithm to identify infections that minimized the probability of false-positive results by (*i*) using serotype-specific thresholds, (*ii*) ignoring all transient positive results (e.g., negative–postive–negative), and (*iii*) eliminating all participants who had any instance of seroconversion to more than one serotype in the same blood sampling interval (see *SI Appendix*, section S2 for details). Completely eliminating such participants from all analyses is quite conservative, but our method of identifying seroconversions relies on investigating the entire serohistory of an individual. As such, any possibly erroneous PRNT casts doubt on results for all serotypes. This conservative approach means our estimates of FoIs are biased low. Our approach allowed us to identify tertiary and quaternary DENV infections (29) in part because of sequential introductions of two novel serotypes. Simultaneous virus isolation and identification from dengue cases (i.e., case data) (30) provided independent validation of the patterns we describe (*Discussion* and *SI Appendix*, section S2).

Model Description. For likelihood-based inference, we estimated the proportion of the study population that had already been infected by time t [denoted $F(t)$], rather than estimating the FoI directly. Defining $\lambda(t)$ as the FoI at time t, we have (*SI Appendix*, section S3)

$$F(t) = 1 - \exp\left\{-\int_{-\infty}^{t} \lambda(u)du\right\}. \quad [1]$$

This equation implicitly assumes that the population is homogeneous and well mixed (i.e., every individual is equally at risk to be infected by of any infectious individual). This assumption is imperfect and some of its consequences are discussed below. The data were left-censored (*SI Appendix*, Fig. S1*A*), interval-censored (Fig. 1), and right-censored (*SI Appendix*, Fig. S1*B*), corresponding to individuals who entered the study already seroconverted, seroconverted between two blood draws, and left the study having never seroconverted, respectively. Using the probability density function of the infection times of infected people, $f = dF/dt$, the likelihood for the three types of censored data are given in *SI Appendix*, Table S3 (where I denotes the time of infection) (31). We considered each individual's infection status to be independent of others, which permitted us to take the likelihood of the data as the product of each individual's likelihood (*SI Appendix*, section S3).

To estimate the FoI through time, we used a nonparametric spline-based approach (32). Specifically, we defined a set of B-splines (33) as basis functions for f. The advantages of B-splines over other bases, such as monomials and trigonometric functions, are that they are flexible and do not a priori assume periodicity. Based on deviation information criterion (DIC; for details see *SI Appendix*, section S5 and Table S2), we identified six B-splines per year (72 total) as the optimal basis for f for the four serotypes and present these results in the main text. A model using four B-splines per year (48 total) also worked well (*SI Appendix*, Table S2, section S6, and Figs. S2–S11). There were no qualitative differences between results obtained when using a model with four B-splines per year compared with a model with six B-splines per year.

*Throughout the manuscript, the terms "inapparent" and "clinically apparent" are used to differentiate between asymptomatic infections or infections with mild symptoms that do not result in detection through passive case detection (inapparent) and infections severe enough that the individual seeks medical attention (clinically apparent).

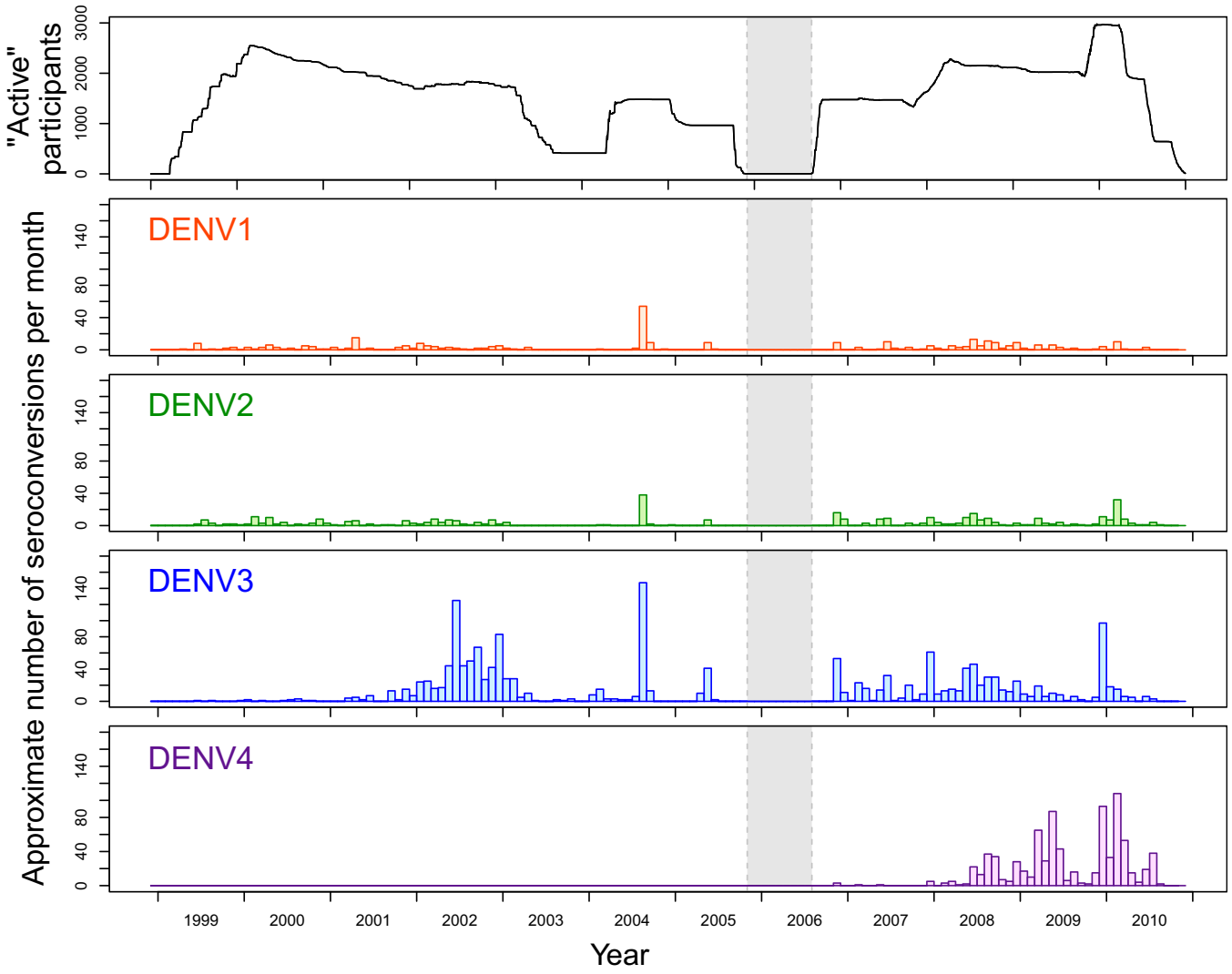

Fig. 1. Summary of participants and interval-censored infections. The top panel shows the total number of active participants across cohort studies from 1999 to 2010. The absence of a cohort study from late 2005 to mid-2006 is indicated by the gray shaded region. Remaining panels: After applying the seroconversion identification algorithm to the raw data the number of interval censored infections are plotted against time. For all, the midpoint of the interval over which the infection was censored is used to time infections.

We could not estimate the function f before 1999 because we did not have data before that date. Seroconversions that occurred before 1999 were left-censored, allowing estimation of the proportion of the population that was exposed before the beginning of the study. We defined κ as the proportion of the population that had seroconverted before 1999:

$$\kappa = \int_{-\infty}^{t_0} f(u)du, \qquad [2]$$

with t_0 representing the beginning of the study. Using Eq. **2**, the likelihood of both right-censored and left-censored observations was rewritten using κ.

Model-Fitting Procedure. To estimate the pdf f, we used a Markov chain Monte Carlo (MCMC) approach, specifically an adaptive, Metropolis-within-Gibbs algorithm (34, 35) (for complete details on the fitting procedure, see *SI Appendix*, section S4 and Figs. S12–S15). We ran 10 chains, each of length 100,000, and evaluated convergence primarily by monitoring scale reduction factors (*SI Appendix*, Fig. S13) (36, 37), trace plots (*SI Appendix*, Fig. S14), and acceptance probability plots (*SI Appendix*, Fig. S15). For our analysis, we combined the last 15,000 steps of each chain and randomly sampled 1,000 steps to remove autocorrelation. The parameters were not independent of each other, so to create credible regions for f (and later the FoI and $\mathcal{R}_0$) we used the 1,000 sampled steps of the chain to create 1,000 estimates of f. This formed an empirical estimate of the posterior distribution of f. For each day, we then selected the middle 90% of the estimates to form our Bayesian credible interval (BCI) at that point. Throughout, in addition to BCIs, we present the posterior medians. There were two parameters that a priori we knew would have identifiability and convergence issues: the parameters corresponding to the very beginning and very end of the study. We, therefore, truncated our estimates to the region where our chains converged (*SI Appendix*, section S4 and Figs. S16 and S17). All analyses were done with R (38) and the R package fda (39). We evaluated convergence with the R package CODA (40).

Parameter and Quantity Estimation. With our estimates of f we computed the proportion of our study population (those born before 1995) still susceptible at time t, denoted $s(t)$, as

$$s(t) = 1 - \left(\kappa + \int_{t_0}^{t} f(u)du\right). \qquad [3]$$

The FoI, $\lambda(t)$, was then (*SI Appendix*, section S3)

$$\lambda(t) = \frac{f(t)}{s(t)}. \qquad [4]$$

The number of secondary infections caused by a single infectious person at any time t was the effective reproductive number, denoted $R(t)$. To estimate $R(t)$ for the entire population of Iquitos, we used our FoI estimates to calculate the fraction of the entire population susceptible at any time t, denoted $s_P(t)$ (*SI Appendix*, section S3). Using the estimated mean time between successive DENV infections (i.e., serial interval) of 15–17 d (41), we approximated $R(d)$ on day d as the ratio of the number of infections that occurred between day d and day $d+1$ and the average number of infections 15–18 d in the future as follows (*SI Appendix*, section S3):

$$R(d) \approx \hat{R}(d) = \frac{\int_{d+15}^{d+18} s_P(u)\lambda(u)du}{3 \cdot \int_{d}^{d+1} s_P(u)\lambda(u)du}. \quad [5]$$

We assessed the sensitivity of $\mathcal{R}_0$ to this interval in *SI Appendix*, section S5. We then used this approximation of the effective reproductive number to calculate an estimate of the basic reproductive number, $\mathcal{R}_0$, on day d by scaling our approximation by the fraction of the entire population that is susceptible, $s_P(d)$:

$$\mathcal{R}_0(d) = \frac{\hat{R}(d)}{s_P(d)}. \quad [6]$$

$\mathcal{R}_0$ was used to calculate the critical vaccination coverage required to eliminate a pathogen. Specifically, the critical vaccination coverage level, p_c, satisfies the following relationship (5):

$$p_c \geq 1 - \frac{1}{\mathcal{R}_0}. \quad [7]$$

Results

Serotype-Specific Infections. The final dataset included 38,416 blood samples that provided serotype-specific infection information for 11,703 individuals. Participants provided 1 to 13 (mean = 3.3) sequential samples an average of 249.5 d apart. We identified 22,301 serotype-specific DENV infections, 3,276 of which were interval-censored (Table 1). Because DENV-1 and DENV-2 had already circulated in Iquitos for several years before the study began, the number of left-censored infections for those serotypes was higher than for DENV-3 and DENV-4. Conversely, the number of interval-censored infections for DENV-3 and DENV-4 was higher, with DENV-3 accounting for more than half of all interval-censored infections. Even though DENV-4 was not detected in clinics until 2008, there was still enough transmission for more than 800 individuals that joined the study after 2008 to seem to have already had neutralizing antibody against DENV-4 (Table 1). Using the mid date between sample pairs to time when seroconversions occurred, we found the number of observed infections per month varied markedly through time (Fig. 1). Testing conducted in 2004 was not spread out throughout the year and instead occurred at two times. As such, the mid date of many individuals occurred within same month (July 2004) which does not necessarily mean that all of these individuals were actually infected in July. Owing to the gap between cohort studies from late 2005 to mid-2006 (indicated by the shaded region in Fig. 1), we have no information on infections that occurred during that period (*SI Appendix*, section S1). In total, 84.0% of the 11,703 study participants seroconverted to at least one DENV serotype by the time they left the study. Transmission varied year to year and across serotypes, with a steady increase in the number of postsecondary infections (tertiary and quaternary) later in the study (Fig. 2). Overall, the majority of DENV-3 and DENV-4 infections were tertiary or quaternary (65.2% and 77.4%, respectively). For 36.2% of all individuals who seroconverted to DENV-4, it was their fourth infection with a DENV.

Table 1. Summary of censored data type by serotype

Data type	DENV-1	DENV-2	DENV-3	DENV-4
Left-censored	7,714	7,464	2,980	867
Interval-censored	342	408	1,701	825
Right-censored	2,527	2,724	5,800	4,658

For each serotype, the number of individuals that were either left-, interval-, or right-censored. Left-censored individuals entered the study already seroconverted to the specific serotype. Interval-censored individuals became infected to the specific serotype during their time in the study period. Right-censored individuals left the study having never been infected to the specific serotype. Note that none of the above columns adds up to 11,703 (the total number of participants). For some individuals, no PRNT test was conclusive for certain serotypes, and as such they were removed from consideration toward the calculations concerning that serotype. Additionally, DENV-4 was not tested for until 2006, and the smaller number of censored individuals for DENV-4 reflects this.

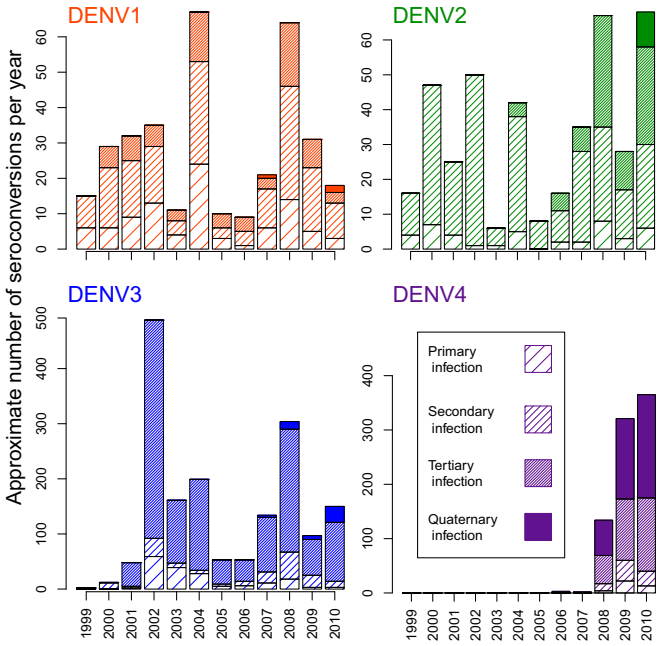

Fig. 2. Number and order of interval censored infections by serotype. For each serotype the number of interval-censored infections are plotted against year. Note that for comparison purposes the scale of the y axis is not the same in each panel. Per individual, these infections are broken down by which infection they constitute (primary, secondary, tertiary, or quaternary). Because both DENV-1 and DENV-2 cocirculated before the beginning of the study period, the majority of individuals were already exposed to at least one of these serotypes and thus most interval-censored infections were not primary infections. For this same reason (the cocirculation of DENV-1 and DENV-2 before 1999), there are considerably fewer DENV-1 and DENV-2 interval-censored infections than DENV-3 and DENV-4 interval-censored infections.

Model Parameter Estimates. The proportion of the population infected before 1999, κ (*SI Appendix*, Fig. S18), was 55.4% (90% BCI: 53.8–57%) for DENV-1 (*SI Appendix*, Fig. S18*A*) and 52.7% (90% BCI: 51.5–54%) for DENV-2 (*SI Appendix*, Fig. S18*B*). Conversely, κ was essentially 0 for DENV-3 and DENV-4 [0.004% (*SI Appendix*, Fig. S18*C*) and 0.004% (*SI Appendix*, Fig. S18*D*), respectively], which were introduced later. It is important to note, however, that DENV-4 was not included in our PRNT assays until 2006. The fact that these estimates were not exactly 0 was likely an artifact of the fitting procedure because no individuals were identified with a left- or interval-censored DENV-3 or DENV-4 infection until after the respective introductions of those viruses. Our estimates of the daily probability of infection, f, showed rough seasonal fluctuations in magnitude across serotypes (*SI Appendix*, Fig. S19). These estimates were greatest for DENV-3, particularly in 2002–2003. Over the period of study, the susceptible proportion of the study subpopulation, $s(t)$

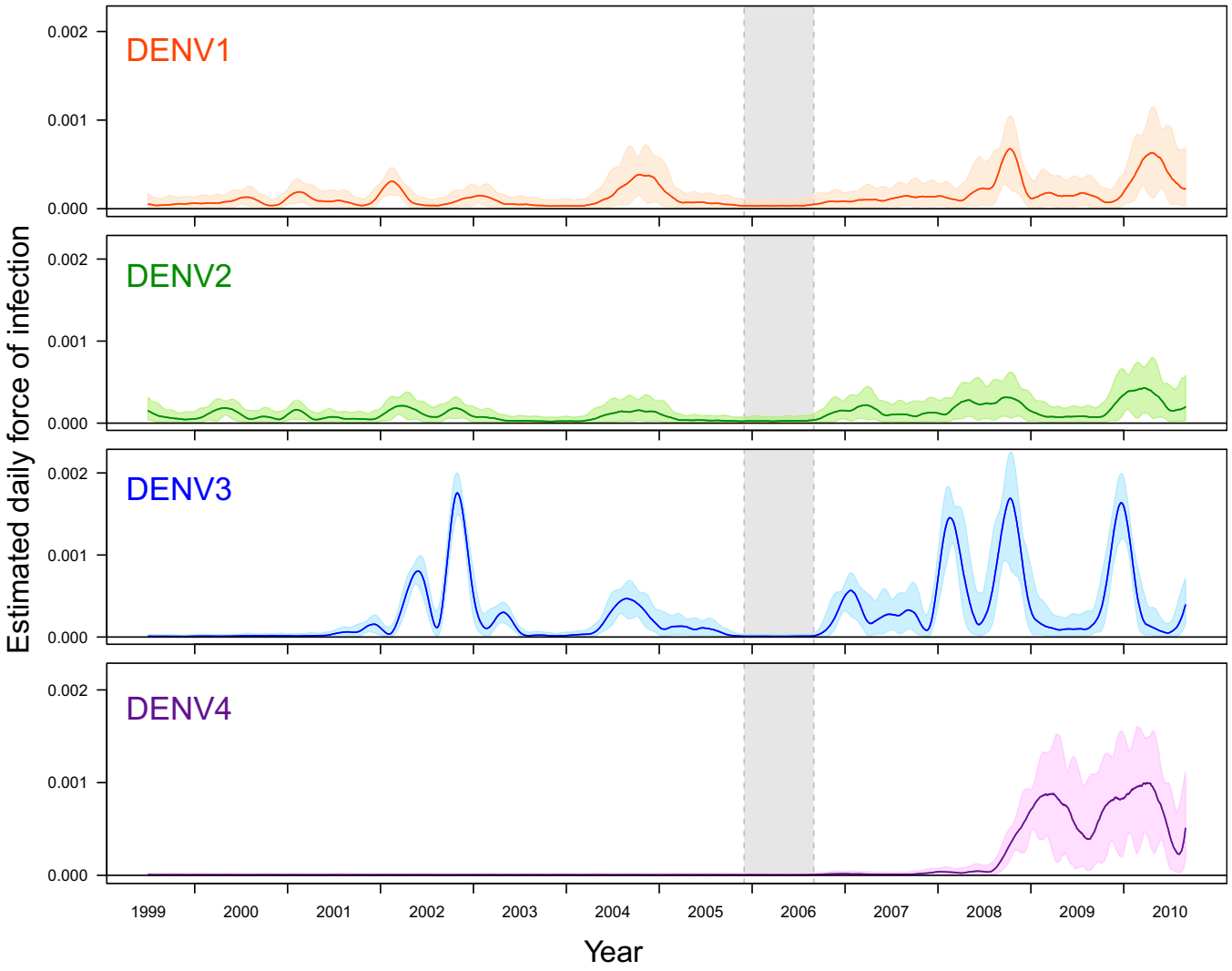

Fig. 3. Daily estimates of FoI. For each serotype, daily estimates of FoI as well as the 90% BCI are plotted against time. The absence of a cohort study from late 2005 to mid-2006 is indicated by the gray shaded region.

(*Methods*), decreased for all serotypes (*SI Appendix*, Fig. S20). At the end of the study, $s(t)$ was reflective of the order of serotype introductions into Iquitos: DENV-1 (first reported in 1990) = 22.9% (90% BCI: 21.9–23.9%), DENV-2 (first reported in 1995) = 26.8% (90% BCI: 26.8–28.7%), DENV-3 (first reported in 2001) = 32.0% (90% BCI: 30.9–33.2%), and DENV-4 (first reported in 2008) = 56.7% (90% BCI: 54.4–58.6%). Unlike estimates for the sample population, the susceptible proportion of the entire population of Iquitos, $s_P(t)$, was relatively stable for DENV-1 and DENV-2 (*SI Appendix*, Fig. S21). However, susceptible estimates within Iquitos for the invading serotypes (DENV-3 and DENV-4) decreased at rates similar to those within the sample population (*SI Appendix*, Fig. S21). The estimated age distribution of infections skewed toward younger individuals the longer the serotype circulated within Iquitos (*SI Appendix*, Figs. S22 and S23 and section S5).

FoI. Depending on year and serotype, daily FoI estimates ranged from 0 to 0.002 (Fig. 3), with the highest estimates being for DENV-3 and DENV-4. Although there was a gap between cohorts from late 2005 to mid-2006, we did identify nonzero point estimates of the FoI owing to the slight systematic increase in the proportion of left-censored individuals that occurred after that period compared with before. After analyzing the consistency of estimates across this gap (*SI Appendix*, section S5 and Fig. S24), we found that the loss of data increased median values and credible intervals of estimates around the gap. Away from the gap, estimated FoI values were consistent with those in Fig. 3. Further, the large credible intervals and timing of the estimated peak FoI for 2004 (July 2004) may be an artifact of the synchronized timing of blood draws in 2004.

Our longitudinal studies captured the introduction of a novel DENV serotype twice. In late 2001/early 2002, the FoI of the recently introduced DENV-3 was estimated to be significantly nonzero, indicating circulation (11). Owing to the regular testing of the longitudinal cohort participants, the timing of this increase was distinguishable from that of DENV-1 and DENV-2 (Fig. 3). This pattern was repeated at the time of the introduction of DENV-4 in late 2008/early 2009. In both instances, the novel serotype replaced the existing serotype(s). Weekly and monthly estimates of the FoI (*SI Appendix*, Fig. S25 *A* and *B*) displayed similar patterns.

There were periods when transmission of multiple serotypes seemed to synchronize. We computed Spearman rank correlations on daily estimates of the FoI between serotypes and found that DENV-1, DENV-2, and DENV-3 were all highly correlated (DENV-1/DENV-2: $\rho_{12} = 0.77$, DENV-1/DENV-3: $\rho_{13} = 0.54$,

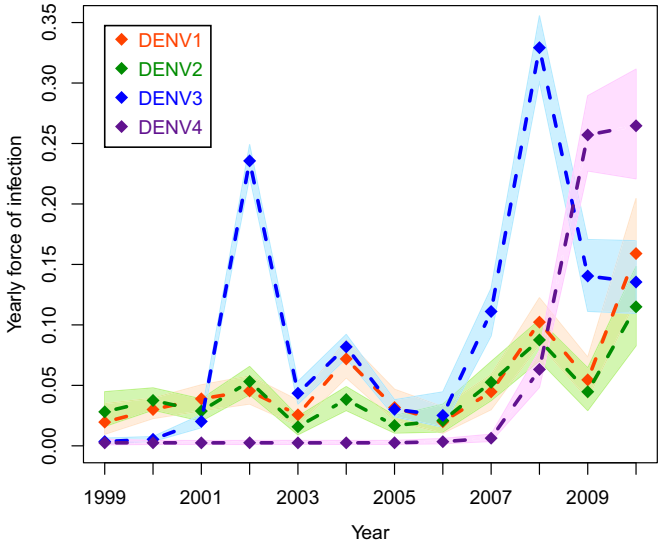

Fig. 4. Yearly estimates of FoI. For each serotype yearly estimates of FoI as well as the 90% BCI are plotted against time. The absence of a cohort study from late 2005 to mid-2006 does not preclude the estimation of yearly FoI estimates for either 2005 or 2006, as evidenced by nonzero FoI estimates for the circulating serotypes for both of those years.

and DENV-2/DENV-3: $\rho_{23} = 0.78$). DENV-4, having been introduced in late 2008, does not display high, if any, correlation with the other serotypes ($\rho_{14} = -0.068$, $\rho_{24} = 0.25$, and $\rho_{34} = -0.037$). FoIs for all serotypes were elevated, however, in late 2009/early 2010, with DENV-1, DENV-2, and DENV-4 reaching their local maxima at almost the same time in early 2010.

Aggregating our estimates by year indicated that the FoIs for DENV-3 and DENV-4 were highest (Fig. 4). For both, there were two years where the yearly FoI exceeded 0.2. The largest yearly FoI for any serotype was the 2008 estimate for DENV-3 [0.33 (90% BCI: 0.3–0.36)]. Every serotype had at least one year with a yearly FoI that exceeded 0.1, corresponding to seroconversion in 10% of members of the study population that were still susceptible to that serotype in that year. The FoIs for multiple serotypes were relatively high in 2002, 2004, 2008, and 2010. Conversely, the FoIs of multiple serotypes were simultaneously relatively low during 2001, 2003, 2005, and 2006 (relative to serotype-specific values for the surrounding years). The yearly FoIs of DENV-1, DENV-2, and DENV-3 were all correlated (Spearman rank correlations: DENV-1/DENV-2, $\rho_{12} = 0.79$; DENV-1/DENV-3, $\rho_{13} = 0.73$; and DENV-2/DENV-3, $\rho_{23} = 0.75$). Spearman rank correlations with DENV-4 were not informative because there were only three estimated yearly FoIs for DENV-4. As noted above with the daily FoI estimates, the yearly estimates for all four serotypes were high in 2010, each exceeding 0.1.

Serotype-Specific $\mathcal{R}_0$ and Vaccination Thresholds. Our estimates of $R(t)$ and $\mathcal{R}_0$ for each serotype fluctuated temporally (*SI Appendix*, Figs. S26 and S27, respectively). Small variations in the daily estimates of s_P resulted in large variations in $\mathcal{R}_0$ because s_P appeared in the denominator of Eq. **6**. This resulted in wide BCIs; the posterior distributions had long upper tails (*SI Appendix*, Fig. S27). Thus, for the purposes of comparison, we plotted estimates of $\mathcal{R}_0$ with the corresponding 50% BCI (Fig. 5) to truncate extreme values on the upper end of the posterior distribution. We investigated the sensitivity of these results to our definition of the serial interval and found that the estimated values were robust to changes in this interval (*SI Appendix*, section S5 and Figs. S28 and S29).

We did not estimate a value of $\mathcal{R}_0$ under 1 for DENV-1 or DENV-2, except for a small portion of the credible interval in a few instances. The median values of $\mathcal{R}_0$ for DENV-1 ranged from 1.40 to 3.64. The median values for DENV-2 were lower (1.36–3.49). Our estimates of DENV-3 ranged from below 1 to 4.72 by 2010. For DENV-4, $\mathcal{R}_0$ stayed below 2 until 2010, when it increased to 3.19 (Fig. 5). Weekly and monthly estimates of $\mathcal{R}_0$ (*SI Appendix*, Fig. S25 *C* and *D*) resulted in similar, slightly lower values. There was a considerable amount of fine-scale temporal variation in all four $\mathcal{R}_0$ estimates. Computing the cross-correlation between the FoI and $\mathcal{R}_0$ revealed a systematic lag of ∼60–80 d (Pearson correlation, *SI Appendix*, Fig. S30*A* and Spearman correlation, *SI Appendix*, Fig. S30*B*). Plotting $\mathcal{R}_0$ against the FoI (*SI Appendix*, Fig. S31) illustrates that sharp increases in the FoI were preceded by sharp spikes in $\mathcal{R}_0$.

Analogous to the computation of yearly FoI estimates, we computed yearly average $\mathcal{R}_0$ values (*SI Appendix*, Fig. S32) by taking the weighted average of the daily $\mathcal{R}_0$ estimates (weighted by relative number of infections). As with the daily $\mathcal{R}_0$ estimates, the yearly estimates for DENV-1 and DENV-2 were relatively similar, with DENV-1 estimates slightly higher. The yearly $\mathcal{R}_0$ estimate of DENV-3 experienced the largest jumps from one year to the next (2005–2006: 1.38–1.97 and 2008–2009: 1.82–2.61). Averaging over an entire year ignores seasonality, and the highest yearly $\mathcal{R}_0$ estimates were lower than the highest daily estimates for all serotypes. For DENV-2 and DENV-3, the highest yearly $\mathcal{R}_0$ estimates occurred in 2010 [DENV-2: 2.54 (50% BCI: 2.45–2.63) and DENV-3: 2.61 (50% BCI: 2.55–2.69)], and the highest yearly $\mathcal{R}_0$ estimate for DENV-1 and DENV-4 occurred in 2010 [DENV-1: 2.62 (50% BCI: 2.56–2.68) and DENV-4: 1.43 (50% BCI: 1.39–1.47)].

From serotype to serotype and across years, values of $\mathcal{R}_0$ and, in turn, p_c, varied. When DENV-3 or DENV-4 were first introduced (when the entire study population was susceptible), the estimated $\mathcal{R}_0$ was effectively 1 [DENV-3: 50% BCI: (0.80–1.45); DENV-4: 50% BCI: (0.76, 1.44)], giving $p_c \approx 50\%$. Using the upper bound on the 90% credible interval for DENV-4 at the time of its introduction (2.18), we found $p_c = 54\%$. In the first 4 y of the study, the largest median $\mathcal{R}_0$ calculated was 3.64 for DENV-1 in 2001. In the next 4 y, the largest identified was 3.07 for DENV-2 in 2004. In the last 4 y, the largest identified $\mathcal{R}_0$ was 4.72 for DENV-3 in 2010. These values result in recommendations of vaccination coverage of 73, 67, and 79% of the population, respectively. Using the largest yearly $\mathcal{R}_0$ estimate (2.61 for DENV-3 in 2009), 62% of the population would need to react to vaccination with a protective immune response. Conservatively, following the highest estimated $\mathcal{R}_0$ overall (4.72 for DENV-3 in 2010), our results indicate a vaccine should be distributed to 79% of the population.

Discussion

Our results quantify temporal variation in the FoI for each DENV serotype over a 12-y period, highlighting marked differences in transmission intensity both intra- and interannually. We found that FoI estimates for the recently introduced serotypes DENV-3 and DENV-4 were higher than those of DENV-1 and DENV-2, which caused outbreaks before but not during the period investigated (1990 and 1995, respectively). Overall, there was high correlation between FoIs across serotypes. There were years of relatively high (e.g., 2002, 2004, 2008, and 2010) and relatively low (e.g., 2001, 2003, 2005, and 2006) transmission, pointing to common drivers of DENV transmission dynamics. Our estimates for $\mathcal{R}_0$ varied from ∼1 to over 5, depending on year and serotype. During the years following its invasion, DEN-4 $\mathcal{R}_0$ estimates were less than those for other serotypes. This is consistent with the notion that DENV-4 is less transmissible than the other three serotypes (42, 43). It should be noted, however, that $\mathcal{R}_0$ for DENV-4 appeared to be increasing as our study period ended. $\mathcal{R}_0$ was variable across seasons, warning against quick estimates for critical

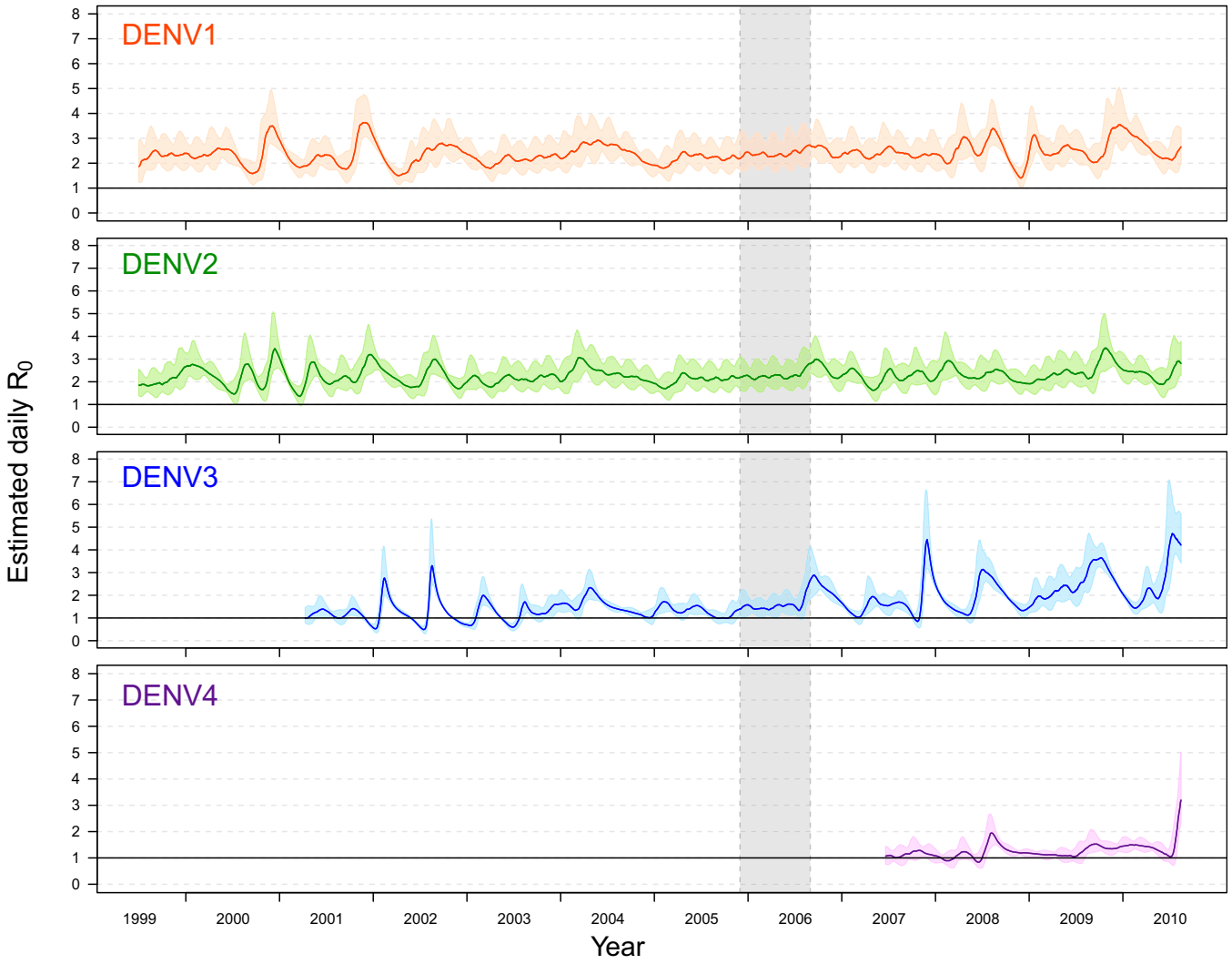

Fig. 5. Daily estimates of $\mathcal{R}_0$. For each serotype daily estimates of $\mathcal{R}_0$ as well as the 50% BCI are plotted against time. The absence of a cohort study from late 2005 to mid-2006 is indicated by the gray shaded region. The estimates for both DENV-3 and DENV-4 are truncated, excluding estimation before their respective introductions.

vaccination coverage. Using the highest estimated $\mathcal{R}_0$ values (for DENV-3 from 2010), we conservatively calculated p_c to be 79%.

Our yearly DENV FoI estimates mostly fell within the wide range of previously calculated estimates conducted in a variety of locations using an array of methods and datasets that often aggregated across DENV serotypes. Yearly FoI estimates ranged from 0.07– 0.14 (19) to 0.2–0.25 (4, 22) in Thailand to 0–0.3 (13) in Brazil. Similar to the FoI, our estimates of the $\mathcal{R}_0$ of DENV fell within the wide range of previously published values (1.3–6.3) (44). As detailed in a review of previous $\mathcal{R}_0$ estimation efforts (44), only three estimation methods used serotype-specific data (4, 19, 45), and only one of those was based on serological surveys (a study using single blood samples from 1,009 children all collected in early 1980) (4). Our estimates indicate dengue is slightly more transmissible than directly transmitted diseases such as severe acute respiratory syndrome ($\mathcal{R}_0 \sim 2$–5) (46) and influenza ($\mathcal{R}_0 \sim 2$–3) (47) and less transmissible than fast-spreading diseases such as measles and pertussis ($\mathcal{R}_0 \sim 12$–18 and ~12–18, respectively) (48). Although our estimated critical vaccination percentage of 79% was high, it was considerably lower (and thus vaccination would be a more reasonable control option) than that for measles and pertussis (~92–94%).

Our serotype-specific approach revealed synchronous dynamics among DENV serotypes. There were high correlations in both the daily and yearly estimates of FoI between DENV-1, DENV-2, and DENV-3. DENV-1, DENV-2, and DENV-4 all achieved their local maxima at essentially the same time in 2010. There were several transmission seasons when, independent of the size of the serotype-specific susceptible pool, there seemed to be more than 40 seroconversions to at least three different serotypes (Fig. 2), specifically in 2004, 2008, and 2010, even though for at least 2004 surveillance data suggested a single serotype dominated (30). Even under stricter schemes for identification of seroconversions (*SI Appendix*, section S2 and Fig. S33), there remained periods where multiple serotypes seemed to circulate concurrently. This emphasizes the potential for differences between patterns of disease (i.e., clinically apparent infections) and patterns of infection. A study identifying the timing of serotype-specific outbreaks of dengue in Thailand (49) similarly identified seasonal synchronization across serotypes, specifically between DENV-1, DENV-2, and DENV-3. DENV-4, however, was reported to be out-of-phase. Our estimated FoIs for DENV-1, DENV-2, and DENV-4 were at or close to their highest values at almost the exact same time in 2010, indicating

that the interserotypic immune reactions that drive patterns of transmission among serotypes may vary in their influence in different contexts. We also noted that invading serotypes replaced the existing serotype(s) that had been previously circulating at relatively high levels. Novel serotype invasions are rare events, in our case two over 12 y, which prevented us from performing statistical tests on serotype replacement patterns.

The synchrony between serotypes indicates there are common drivers. DENV is dependent on a mosquito population to complete its transmission cycle. Interannual variation in climate drivers can thus impose variation on transmission dynamics through their influence on mosquito biology and ecology. As in many cities with endemic dengue, Iquitos employs various mosquito control strategies in response to increases in dengue cases. We are currently investigating relationships between interannual variation in potential climate drivers, vector control efforts, and FoI estimates.

Although we computed daily estimates of $\mathcal{R}_0$, there was no inherent reason why these estimates should not all be equal. By investigating which assumptions were violated to produce such temporally fluctuating estimates and, in particular, produce the lagged patterns observed between our estimates of $\mathcal{R}_0$ and the FoI, it was possible to indirectly deduce characteristics of transmission dynamics. For instance, the repeating pattern of a sharp spike in $\mathcal{R}_0$ followed by a relatively slower increase and then decrease of the FoI was consistent with violation of the assumption of a well-mixed, spatially homogeneous population. We considered the Iquitos cohort to be one subpopulation, but in reality people (and their exposure to *Aedes aegypti* bites in locations other than their home) were nonhomogeneously distributed across the city (28, 50). These heterogeneities can have important implications for epidemiological prediction and inference (51). Localized outbreaks occur in Iquitos (52), and thus focal outbreaks would best be scaled by focal levels of human immunity. Perhaps if we incorporated the relatively rapid depletion of locally susceptible individuals there would be a more gradual change in the estimated values of $\mathcal{R}_0$. Another spatial heterogeneity that could contribute to the patterns we observed was the variation in individual movements. Some people may have contributed more to transmission than others by moving about more, being bitten by more mosquitoes, being more infectious, or some combination of these factors (53). Perhaps once an outbreak was initiated the pathogen spread to less-transmissible individuals, decreasing the aggregated $\mathcal{R}_0$ estimates.

Certain caveats exist with our approach. First, cross-reacting anti-DENV antibodies can result in false-positive PRNT results (54, 55). We compensated for this by excluding individuals who seemed to seroconvert to multiple serotypes in the same time period and by using an individual's entire serohistory to guard against transient false positives. This does not guarantee that we completely controlled for incorrectly serotyping an infection owing to a cross-reaction. Although there were periods of synchrony between the serotypes, increases, for example, in the number of DENV-3 seroconversions were not systematically accompanied by an increase in DENV-1 seroconversions. As such, we concluded that it is unlikely that cross-reacting antibodies, rather than cocirculation of multiple serotypes of DENV, were responsible for our results. Second, although the virus isolation and PCR data confirm certain patterns (e.g., the timing of the DENV-3 and DENV-4 invasions), virus detection was not always concordant with the longitudinal serological data. Virus detection in cell culture and PCR indicated that one or at most two predominant serotypes at a time produced clinically apparent infections. The patterns of inapparent infections do not by definition exactly match those of apparent infections (15). Considering the complex interplay between order of infection and severity of disease, especially for tertiary and quaternary infections (29, 56), it was not surprising that virus isolation/PCR data and the longitudinal serologic data did not always perfectly agree. Third, we modeled each serotype independently, ignoring the potential effects of temporary cross-protection. Following a DENV infection, an individual has temporary immunity to heterologous DENV infection (57), which may have affected our estimates (44). Correcting for cross-protection would result in a systematic increase in our FoI estimates because temporarily immune individuals would be removed from the heterologous susceptible pool in the denominator of Eq. **4**. Likewise, incorporating death would increase our estimates.

Although they require considerable effort, time, and resources, longitudinal studies provide valuable detailed information on pathogen transmission, especially when rates of asymptomatic infection are high, like they are for DENV (16). Because most estimation attempts are not based on longitudinal data, the methods to use such detail are not well developed. As noted earlier, the use of likelihood-based fitting of smooth functions for the FoI has been developed for data from a single serological survey of individuals within the study population (2). By combining a spline-based approach with equations previously derived in the field of reliability (31) we developed an estimation method that incorporates the detailed information provided by a longitudinal study and allows for temporal flexibility in FoI estimates. Our method was designed to work with a particular dataset but could be adapted to other longitudinal studies for dengue and other infectious diseases.

Our analysis and the interpretation of serological data were facilitated by the two novel DENV introductions that took place during the period of study. In both cases, the novel serotype initially displaced the preexisting serotypes. After this initial phase, however, neither of the novel serotypes seemed to interfere with the others. If Iquitos begins to sustain simultaneous transmission of all four serotypes, the maintenance of longitudinal cohort studies will provide valuable data for confirming the patterns we identified and/or reveal further complexity in the interplay among serotypes.

Conclusions

Beyond clear intra-annual, seasonal variation, the observed temporal variation in epidemiological parameters (especially from year to year) implies that the transmission dynamics of DENV in Iquitos are complex and cannot be summarized with synoptic data or assumptions of time-independent transmission parameters. In addition to informing dengue prevention strategies, connecting the variation of these estimates to other processes, such as measures of entomological risk (i.e., mosquito abundance) and climatic variation, will inform local control strategies. The minimal vaccine coverage required to effectively control dengue varies by serotype. Given a potentially limited number of doses, efficiently distributing a vaccine within and between communities can only be optimized when these variations are understood and taken into account. Because vaccines may not have perfect efficacy (9), the incorporation of accurate, serotype-specific estimates of critical transmission parameters will be crucial for selecting delivery strategies and determining the optimal mix of vaccination and vector control for sustainable prevention of dengue.

ACKNOWLEDGMENTS. We thank Neil Ferguson and an anonymous reviewer for comments that improved this manuscript. In particular, we acknowledge Dr. Ferguson's helpful suggestions regarding our calculations of R0. We thank Tom Lindström for insightful comments on our Bayesian approach. This work was supported by the Research and Policy for Infectious Disease Dynamics program of the Science and Technology Directory, Department of Homeland Security, and Fogarty International Center, National Institutes of Health (NIH); NIH Grants RO1 AI-42332 and RO1 AI069341; Innovative Vector Control Consortium; US Department of Defense Global Emerging Infections Systems Research Program Work Unit 847705.82000.25GB.B0016; Military Infectious Disease Research Program Work Units 6000 RAD1.S.B0302, S0002 04 LI, DOD S0017 03LI, DOD 32519, and S0088 06 NM; Deployed Warfighter Protection Program DOD S0002 04; and Wellcome Trust Grant 08571. A.L.L. acknowledges support from NIH Grant R01AI091980 and National Science Foundation Grant DMS 1246991. E.S.H. and T.J.K. are military service members and B.M.F., S.V., H.A., I.B., A.L., and A.C.M. are employees of the US Government. This work was prepared as part of their official duties. Title 17 U.S.C. §105 provides

1. Muench H (1934) Derivation of rates from summation data by the catalytic curve. *J Am Stat Assoc* 29(185):25–38.
2. Grenfell BT, Anderson RM (1985) The estimation of age-related rates of infection from case notifications and serological data. *J Hyg (Lond)* 95(2):419–436.
3. Hens N, et al. (2010) Seventy-five years of estimating the force of infection from current status data. *Epidemiol Infect* 138(6):802–812.
4. Ferguson NM, Donnelly CA, Anderson RM (1999) Transmission dynamics and epidemiology of dengue: Insights from age-stratified sero-prevalence surveys. *Philos Trans R Soc Lond B Biol Sci* 354(1384):757–768.
5. Anderson R, May R (1992) *Infectious Diseases of Humans: Dynamics and Control* (Oxford Univ Press, Oxford).
6. Fraser C, Riley S, Anderson RM, Ferguson NM (2004) Factors that make an infectious disease outbreak controllable. *Proc Natl Acad Sci USA* 101(16):6146–6151.
7. Brady OJ, et al. (2012) Refining the global spatial limits of dengue virus transmission by evidence-based consensus. *PLoS Negl Trop Dis* 6(8):e1760.
8. Simmons CP, Farrar JJ, Nguyen W, Wills B (2012) Dengue. *N Engl J Med* 366(15): 1423–1432.
9. Sabchareon A, et al. (2012) Protective efficacy of the recombinant, live-attenuated, CYD tetravalent dengue vaccine in Thai schoolchildren: A randomised, controlled phase 2b trial. *Lancet* 380(9853):1559–1567.
10. Reiner RC, Jr., et al. (2013) A systematic review of mathematical models of mosquito-borne pathogen transmission: 1970-2010. *J R Soc Interface* 10(81):20120921.
11. Morrison AC, et al. (2010) Epidemiology of dengue virus in Iquitos, Peru 1999 to 2005: Interepidemic and epidemic patterns of transmission. *PLoS Negl Trop Dis* 4(5):e670.
12. Nisalak A, et al. (2003) Serotype-specific dengue virus circulation and dengue disease in Bangkok, Thailand from 1973 to 1999. *Am J Trop Med Hyg* 68(2):191–202.
13. Rodriguez-Barraquer I, et al. (2011) From re-emergence to hyperendemicity: The natural history of the dengue epidemic in Brazil. *PLoS Negl Trop Dis* 5(1):e935.
14. Balmaseda A, et al. (2010) Trends in patterns of dengue transmission over 4 years in a pediatric cohort study in Nicaragua. *J Infect Dis* 201(1):5–14.
15. King AA, Ionides EL, Pascual M, Bouma MJ (2008) Inapparent infections and cholera dynamics. *Nature* 454(7206):877–880.
16. Endy TP, et al. (2002) Epidemiology of inapparent and symptomatic acute dengue virus infection: A prospective study of primary school children in Kamphaeng Phet, Thailand. *Am J Epidemiol* 156(1):40–51.
17. Burke DS, Nisalak A, Johnson DE, Scott RM (1988) A prospective study of dengue infections in Bangkok. *Am J Trop Med Hyg* 38(1):172–180.
18. Eamchan P, Nisalak A, Foy HM, Chareonsook OA (1989) Epidemiology and control of dengue virus infections in Thai villages in 1987. *Am J Trop Med Hyg* 41(1):95–101.
19. Cummings DA, et al. (2009) The impact of the demographic transition on dengue in Thailand: Insights from a statistical analysis and mathematical modeling. *PLoS Med* 6(9):e1000139.
20. Thai KT, et al. (2011) Age-specificity of clinical dengue during primary and secondary infections. *PLoS Negl Trop Dis* 5(6):e1180.
21. Cuong HQ, et al. (2011) Quantifying the emergence of dengue in Hanoi, Vietnam: 1998-2009. *PLoS Negl Trop Dis* 5(9):e1322.
22. Egger JR, et al. (2008) Reconstructing historical changes in the force of infection of dengue fever in Singapore: Implications for surveillance and control. *Bull World Health Organ* 86(3):187–196.
23. Rothman A (2010) *Dengue Virus* (Springer, Berlin).
24. Scott T, Morrison A (2010) Longitudinal field studies will guide a paradigm shift in dengue prevention. *Vector Biology, Ecology and Control*, ed Atkinson PW (Springer, Berlin), pp 139–161.
25. Phillips I, Need J, Escamilla J, Colán E, Sánchez S, Rodríguez M, Vásquez L, Seminario J, Betz T, da Rosa AT (1992) First documented outbreak of dengue in the Peruvian amazon region. *Bull Pan Am Health Organ* 26(3):201–207.
26. Watts DM, et al. (1999) Failure of secondary infection with American genotype dengue 2 to cause dengue haemorrhagic fever. *Lancet* 354(9188):1431–1434.
27. Forshey BM, et al. (2009) Dengue virus serotype 4, northeastern Peru, 2008. *Emerg Infect Dis* 15(11):1815–1818.
28. Stoddard ST, et al. (2013) House-to-house human movement drives dengue virus transmission. *Proc Natl Acad Sci USA* 110(3):994–999.
29. Olkowski S, et al. (2013) Reduced risk of disease during postsecondary dengue virus infections. *J Infect Dis* 208(6):1026–1033.
30. Forshey BM, et al.; NMRCD Febrile Surveillance Working Group (2010) Arboviral etiologies of acute febrile illnesses in Western South America, 2000-2007. *PLoS Negl Trop Dis* 4(8):e787.
31. Meeker WQ, Escobar LA (1998) *Statistical Methods for Reliability Data* (Wiley, New York).
32. Ziv S, Marc A, Geert M, Philippe B, Pierre Van D (2003) Modelling forces of infection by using monotone local polynomials. *J R Stat Soc Ser C Appl Stat* 52(4):469–485.
33. Ramsay J (2005) *Functional Data Analysis,* Springer Series in Statistics (Springer, New York).
34. Tierney L (1994) Markov chains for exploring posterior distributions. *Ann Stat* 22(4): 1701–1728.
35. Roberts GO, Rosenthal JS (2009) Examples of adaptive MCMC. *J Comput Graph Statist* 18(2):349–367.
36. Gelman A, Rubin D (1992) Inference from iterative simulation using multiple sequences. *Stat Sci* 7(4):457–472.
37. Brooks SP, Gelman A (1998) General methods for monitoring convergence of iterative simulations. *J Comput Graph Statist* 7(4):434–455.
38. R Development Core Team (2012) *R: A Language and Environment for Statistical Computing* (R Foundation for Statistical Computing, Vienna). Available at www.R-project.org. Accessed May 16, 2013.
39. Ramsay, JO, Wickham H, Graves S, Hooker G. (2012) fda: Functional data analysis. R package version 2.2.8. Available at http://CRAN.R-project.org/package=fda. Accessed May 16, 2013.
40. Plummer M, Best N, Cowles K, Vines K (2006) CODA: Convergence diagnosis and output analysis for MCMC. R package version 2.2.8. Available at http://CRAN.R-project.org/doc/Rnews. Accessed May 16, 2013.
41. Aldstadt J, et al. (2012) Space-time analysis of hospitalised dengue patients in rural Thailand reveals important temporal intervals in the pattern of dengue virus transmission. *Trop Med Int Health* 17(9):1076–1085.
42. Nisalak A, et al. (2003) Serotype-specific dengue virus circulation and dengue disease in Bangkok, Thailand from 1973 to 1999. *Am J Trop Med Hyg* 68(2):191.
43. Nguyen MN, et al. (2013) Host and viral features of human dengue cases shape the population of infected and infectious *Aedes aegypti* mosquitoes. *Proc Natl Acad Sci USA* 110(22):9072–9077.
44. Johansson MA, Hombach J, Cummings DA (2011) Models of the impact of dengue vaccines: A review of current research and potential approaches. *Vaccine* 29(35): 5860–5868.
45. Nagao Y, Koelle K (2008) Decreases in dengue transmission may act to increase the incidence of dengue hemorrhagic fever. *Proc Natl Acad Sci USA* 105(6):2238–2243.
46. Wallinga J, Teunis P (2004) Different epidemic curves for severe acute respiratory syndrome reveal similar impacts of control measures. *Am J Epidemiol* 160(6):509–516.
47. Mills CE, Robins JM, Lipsitch M (2004) Transmissibility of 1918 pandemic influenza. *Nature* 432(7019):904–906.
48. Fine PE (1993) Herd immunity: History, theory, practice. *Epidemiol Rev* 15(2):265–302.
49. Adams B, et al. (2006) Cross-protective immunity can account for the alternating epidemic pattern of dengue virus serotypes circulating in Bangkok. *Proc Natl Acad Sci USA* 103(38):14234–14239.
50. Vazquez-Prokopec GM, et al. (2013) Using GPS technology to quantify human mobility, dynamic contacts and infectious disease dynamics in a resource-poor urban environment. *PLoS ONE* 8(4):e58802.
51. Perkins TA, Scott TW, Le Menach A, Smith DL (2013) Heterogeneity, mixing, and the spatial scales of mosquito-borne pathogen transmission. *PLOS Comput Biol* 9(12): e1003327.
52. Liebman KA, et al. (2012) Spatial dimensions of dengue virus transmission across interepidemic and epidemic periods in Iquitos, Peru (1999-2003). *PLoS Negl Trop Dis* 6(2):e1472.
53. Lloyd-Smith JO, Schreiber SJ, Kopp PE, Getz WM (2005) Superspreading and the effect of individual variation on disease emergence. *Nature* 438(7066):355–359.
54. Thomas SJ, et al. (2009) Dengue plaque reduction neutralization test (PRNT) in primary and secondary dengue virus infections: How alterations in assay conditions impact performance. *Am J Trop Med Hyg* 81(5):825–833.
55. Rainwater-Lovett K, Rodriguez-Barraquer I, Cummings DA, Lessler J (2012) Variation in dengue virus plaque reduction neutralization testing: Systematic review and pooled analysis. *BMC Infect Dis* 12:233.
56. OhAinle M, et al. (2011) Dynamics of dengue disease severity determined by the interplay between viral genetics and serotype-specific immunity. *Sci Transl Med* 3:114ra128.
57. Sabin AB (1952) Research on dengue during World War II. *Am J Trop Med Hyg* 1(1): 30–50.

Supplementary Information Appendix for Time-varying, serotype-specific force of infection of dengue virus

Robert C. Reiner, Jr., Steven T. Stoddard, Brett M. Forshey, Aaron A. King, Alicia M. Ellis, Alun L. Lloyd, Kanya C. Long, Claudio Rocha, Stalin Vilcarromero, Helvio Astete, Isabel Bazan, Audrey Lenhart, Gonzalo M. Vazquez-Prokopec, Valerie A. Paz-Soldan, Philip J. McCall, Uriel Kitron, John Elder, Eric Halsey, Amy Morrison, Tadeusz J. Kochel Thomas W. Scott

correspondence to: rcreiner@ucdavis.edu

SECTION S1 Longitudinal cohorts

Seroconversion data used in our analysis were collected from five longitudinal cohort studies carried out between January 1999 and December 2010 (Table S1). When participants left the study, sometimes temporarily, they were replaced by recruiting other residents from the same geographic area. Individual participants provided between 1-13 samples separated typically by 6-9 months. In Figure S1, we plotted the frequency of individuals entering and leaving the study, as indicated by their first and last blood sample, respectively. Enrollment numbers were highest at the initiation of individual cohort studies, specifically January-September 1999, April-May 2004, August-November 2006, November 2007-May 2008 and August-October 2009. Numbers were high throughout the 1999-2005 cohort because sampling and recruitment were staggered temporally (Fig. S1a). Most participants left the studies at the end of each cohort (Fig. S1b), but individuals were lost to follow up at other times for various reasons including: moving away from the study area, opting to drop out of the study, and death. Although each cohort study had distinct objectives, for each we collected blood samples longitudinally and tested them by plaque reduction neutralization test ($PRNT_{70}$) to identify seroconversion to all 4 DENV serotypes.

SECTION S2 Serotype identification of infections and alternative seroconversion identification algorithms

The plaque reduction neutralization test (PRNT) is considered the gold standard for DENV serology. Although specific for each DENV serotype, interpretation of PRNT results is complicated by cross-reactions among DENV-neutralizing antibodies. A novel infection by one serotype will thus cause an increase in titers of neutralizing antibodies to other serotypes. Moreover, an individual infected by a heterologous serotype may have a more robust antibody response to the first than second serotype with which they were infected; i.e., 'original antigenic sin' [1, 2]. Analyzing multiple samples longitudinally is, however, a way to ameliorate uncertainty due to cross-reaction, immunological 'noise', and test error; i.e., sensitivity/specificity [3, 4].

Serotype identification of infections

Serum samples were analyzed for serotype-specific neutralizing antibodies using a plaque reduction neutralization test (PRNT), modified from Morens et al [3, 5, 6]. Test sera were heat inactivated at $56°C$ for 30 minutes prior to dilution. Diluted test sera (0.2 mL) were mixed with 0.2 mL diluted media [Earle's minimal essential medium (E-MEM) with 2% fetal bovine serum (FBS) and antibiotic/antimycotic] containing 40-80 PFU of assay virus and then incubated at $4°C$ for 15 hours. Virus-serum mixture (0.1 mL) was added in triplicate to 0.5 mL

media containing 1.5x105 baby hamster kidney-21 (BHK21) cells and then added to a well of a 24 well tissue culture plate. Plates were incubated at $37°C$ with 5% CO_2 for approximately 3 hrs. Overlay media (0.5 mL of 0.6% carboxymethyl Cellulose, E-MEM w/o phenol Red, 10% FBS, 0.075% $NaHCO_3$ and antibiotic/antimycotic) was added to the adhered cells and incubated at $37°C$ in 5% CO_2 for multiple days (depending on the serotype). Following incubation, the overlay media was removed, and the cells were rinsed (with water) and stained [0.5 mL of 0.1% (w/v) Naphthol Blue Black, 1.36% (w/v) Sodium Acetate, and 6% (v/v) Glacial Acetic Acid] for 30 min. Stain was then removed, the BHK-21 monolayers were washed and air dried, and plaques were counted manually. Between 1999 and 2005, sera were tested at dilutions (after the addition of virus) of 1:60 and 1:120 for DENV-1 and DENV-2, and 1:30 and 1:60 or 1:60 and 1:120 for DENV-3. From 2006 to 2010, sera were tested at dilutions of 1:40, 1:80, 1:160, and 1:640 (after the addition of virus). Results were expressed as the serum dilution (based on a linear fit (1999-2005) or a probit regression fit (2006-2010)) that reduced the number of plaques by 70% (i.e., $PRNT_{70}$) relative to normal human serum at the same dilution. Between 1999 and 2005, for DENV-2, linear regression models were fit to estimate the percent reduction at a cut-off dilution of 1:80, whereas a cutoff dilution of 1:60 was used for DENV-1 and DENV-3. Between 2006 and 2010, titers were based on probit regression fit to the four dilution series (1:40, 1:80, 1:160, and 1:640). To address continuity and comparability between methods used for the two times frames (1999-2005 and 2006-2010), we compared classification from linear regression models of two dilutions with probit models of four dilutions. We focused on samples that fell between the two dilutions and thus would be closer to the cutoff dilution and more difficult to properly classify. We estimate a concordance of 87% between the two dilution and four dilution approaches (84% sensitivity and 95% specificity, using four dilution as a gold standard). Positive and negative control human sera were included with each set of samples analyzed.

Viruses utilized in the assay were amplified in *Ae. albopictus* C6/36 cell culture and frozen in aliquots at $-70°C$ at various points over the course of the study to increase standardization. Test viruses were DENV-1 16007 (DHF case from Thailand, 1964), DENV-2 16681 (DHF case from Thailand, 1964), DENV-3 IQD1728 (DF case from Peru, 2002), and DENV-4 1036 (DF case from Indonesia, 1976). Cut-off dilutions were set at 1:60 for DENV-1, 1:80 for DENV-2, 1:60 for DENV-3, and 1:40 for DENV-4. The cut-offs were selected to balance maximizing sensitivity and specificity, based on results from our laboratory as described in [7, 3, 4, 8]. Seroconversions were based on an increase in reciprocal neutralizing titers from below the cutoff to above the cutoff between paired blood samples.

Alternative seroconversion identification algorithms

Prior to analysis the raw serology data was processed to identify putative DENV infections based on the titer of serotype-specific, neutralizing antibodies. Because DENV serology data is notoriously noisy [9], our approach aimed to reduce uncertainty. Our algorithm was designed to account for the fact that each DENV serotype (and genotype) is a unique virus with its own (biological) PRNT assay and that neutralizing DENV antibodies cross-react on short and long time scales, although the exact nature of these interactions remain poorly understood. In this regard, it is important to note that the dengue season in Iquitos is usually ≤ 6 months, which is consistent with the time frame of temporary, heterologous cross-protection and elevated IgM antibodies; something that would limit multiple, sequential infections with different serotypes in the same transmission season. This, in combination with Iquitos clinic data showing that almost all viruses recovered from dengue patients during a given transmission season were a single serotype, this means that infection with more than one DENV serotype in the same person in a single season was unlikely. Our base algorithm was thus as follows:

1. If a single antibody titer (described in the methods of the main text) exceeded the serotype specific threshold, the results was considered positive. If the result was below the threshold, it was considered negative.

2. Any transiently positive result in a series of samples from the same individual (i.e., if a person presented as positive - negative positive) the positive result was considered to be false and converted to a negative result.

3. If a person appeared to seroconvert to more than one serotype between two serial samples (i.e., they were positive to DENV-1 in the first sample and positive to DENV-2 and DENV-3 in the second sample) that person was removed from the study.

This cleaning process eliminated potentially confounding, false positive results. Because we expect that some results categorized this way were not false, this algorithm was conservative because it retained fewer seroconversions than actually occurred. Nevertheless, we considered a number of alternative algorithms that were both more and less restrictive than the algorithm described above. Generally, with the exception of the most restrictive algorithms, results were comparable to those we present in the main text. Moreover, in all cases we observed seroconversions to multiple serotypes in the same year, which conflicts with Iquitos clinic data. The alternative algorithms, organized from least to most restrictive, focused on the following three key issues.

Multiple serotype seroconversion Our base algorithm eliminated any instances of multiple serotype seroconversion. There were, however, individuals from whom blood samples were separated by long ($>$10 months) intervals. In these instances the person could have been infected twice in two different transmission seasons, which would have looked like a multiple seroconversion in their serology. We, therefore, relaxed our criterion in two ways: (1) by allowing multiple serotype seroconversions if the serial interval was $\leq$10 months and (2) by allowing all multiple serotype conversions. The latter was included primarily to assess the sensitivity of our results to the elimination of all individuals who appeared to seroconvert to multiple serotypes in the base algorithm.

PRNT sensitivity/specificity Prior to their introduction into Iquitos, we detected almost no individuals with antibodies to either DENV-3 or DENV-4. These assays are thus highly specific, although their sensitivity was relatively low (for details see Olkowski et al. [4]). We are thus confident that any instance of a positive DENV-3 or DENV-4 result was an indication of infection with that serotype. Our base algorithm would nevertheless eliminate transient positive results for these serotypes. We, therefore, relaxed this criterion in two separate algorithms so that all positive results for DENV-3 or DENV-4 were considered a seroconversion.

Clinical serotype dominance Clinic-based surveillance data from the same period indicates that single serotypes dominated during a given transmission season. Between 2003 and 2008 the vast majority of cases were caused by DENV-3 and between 2008 and 2010 by DENV-4. Our results, however, suggest that DENV-1 and DENV-2 were continuously circulating during these times. To reconcile these differences, we evaluated two different algorithms. The first considered an individual's first seroconversion between 2003 and 2008 to be a DENV-3 infection. The second did the same for DENV-4 between 2008 and 2010. Infection with other serotypes was only possible if subsequent to a DENV-3 or DENV-4 infection the individual's serohistory showed evidence of seroconversion to DENV-1 or DENV-2.

To evaluate the impact of these alternative cleaning algorithms on the final number of seroconversions to each serotype, we implemented each one in isolation and in concert with the others, resulting in 47 alternate cleaning procedures. Those that were less conservative allowed for more overall seroconversions and appeared qualitatively similar to the main results . The least restrictive cleaning method allowed for multiple seroconversions within an interval of any length and assumed that a positive test to both DENV-3 and DENV-4 was a true seroconversion independent of later tests. This method naturally resulted in more seroconversions (Fig. S33a versus Fig. 1) and while the resulting *FoI* estimates were correspondingly larger, we obtained the same qualitative results; i.e. synchronization among serotypes.

The less restrictive cleaning methods did not address the discordance between our results and patterns observed in Iquitos clinics. Restrictions of the third type (attempting to alter the data to match clinical incidence patterns) removed a considerable number of infections to DENV-1 and DENV-2. Figure S33b plots the number of seroconversions by month when an individual's first seroconversion from 2003 to 2008 was declared DENV-3 unless the individual already appeared to have seroconverted to DENV-3. That analysis resulted in fewer DENV-1 and DENV-2 seroconversions during that interval (Fig. S33b versus Fig. 1), but importantly there were still some

seroconversions those viruses. Even under the artificially restrictive third type of cleaning regimes we could not force the cohort data to match the transmission patterns of the cohort data. This result highlights the need to consider differences between clinically apparent and inapparent transmission dynamics. We saw the same outcome for DENV-4 (Fig. S33c); there were fewer seroconversions to the other serotypes than without this restriction, but no serotype completely disappeared. Unlike estimates generated by the least restrictive cleaning method, these two cleaning methods markedly lowered our *FoI* estimates (Fig. S33b, S33d).

SECTION S3 Mathematical derivations

FoI

The simplest definition of the *FoI*, denoted λ, comes from the so called 'catalytic' model [10], where the change in the proportion of the initially susceptible class (denoted s) is governed by the following differential equation:

$$\frac{ds(t)}{dt} = -\lambda s(t) \tag{S1}$$

The solution to this differential equation is:

$$s(t) = s(t_0)\exp\{-\lambda t\} \tag{S2}$$

Perhaps the easiest way to see the effect of the *FoI* is by considering the ratio of the proportion of the study population that is still susceptible in two consecutive days. Using Eq. (S2) we have

$$\lambda = -\ln\left(\frac{s(t+1)}{s(t)}\right) \tag{S3}$$

If we consider the proportion of the initial susceptible class that have already been infected by day t (denoted $F(t) = 1 - s(t)$), we have

$$\frac{dF(t)}{dt} = \lambda(1 - F(t)) \tag{S4}$$

whose solution is

$$F(t) = 1 - \exp\{-\lambda t\} \tag{S5}$$

In the above, the *FoI* is constant. If we allow the *FoI* to vary in time (denoted $\lambda(t)$, using day as the unit of time) we can rewrite Eq. (S3) as

$$\lambda(t) \approx -\ln\left(\frac{s(t+1)}{s(t)}\right) \tag{S6}$$

Eq. (S4) as

$$\frac{dF(t)}{dt} = \lambda(t)(1 - F(t)) \tag{S7}$$

and Eq. (S5) as

$$F(t) = 1 - \exp\left\{-\int_0^t \lambda(u)du\right\} \tag{S8}$$

From Eq. (S7), writing $\frac{dF(t)}{dt} = f(t)$ and defining κ as

$$\kappa = \int_{-\infty}^{t_0} f(u)du \tag{S9}$$

where t_0 is a constant, we have

$$s(t) = 1 - F(t) = 1 - \int_{-\infty}^{t} f(u)du = 1 - \left(\kappa + \int_{t_0}^{t} f(u)du\right) \tag{S10}$$

And finally solving Eq. (S7) for $\lambda(t)$, and substituting appropriately for both $\frac{dF(t)}{dt}$ and $1 - F(t)$, we have arrived at Eq. (2).

$R(t)$ and $\mathcal{R}_0$

The *FoI* quantifies the rate at which individuals leave the susceptible pool. Our *FoI* estimates are based on, and apply to, our sample population. Under the assumption that at any moment in time the *FoI* for our sample population is the same as the population in general, the *FoI* is a function of time, but not age. To use our *FoI* estimates to calculate, for all of Iquitos, $R(t)$ and $\mathcal{R}_0$ we need to account for the difference between our sample population and the whole population. Given the presence of births, at any moment in time the age structure of the whole population will be different than that of the sample population and because individuals of different ages will have lived under the risk of dengue infection for different amounts of time, the fraction susceptible in each age class will likewise be different (even under the assumption that age has no impact on the *FoI*). If we calculate, for each age group, the fraction susceptible at any point in time and then weight those fractions by the overall fraction of the population within that age group, we can estimate the fraction of the entire population susceptible (denoted $s_P(t)$). Following [11], if we define $s_P(a,t)$ as the fraction of the individuals within the whole population that are age a and susceptible at time t, we have:

$$\frac{\partial s_P}{\partial a} + \frac{\partial s_P}{\partial t} = -\lambda(t) s_P(a,t), \tag{S11}$$

whose solution is:

$$s_P(a,t) = \exp\left\{-\int_0^a \lambda(t-a')da'\right\}. \tag{S12}$$

We assume a stable age-structure within Iquitos from 1999 through 2010 and let $p(a)$ and $P(a)$ denote the pdf and survival function of the age distribution respectively ($P(a)$ is the fraction of the population whose age is at least a, also known as the complementary cumulative distribution function). Using $s_P(a,t)$ and $p(a)$, we calculate $s_P(t)$ as:

$$s_P(t) = \int_0^\infty s_P(a',t)p(a')da', \tag{S13}$$

Note that we do not have to include a term for death within Eq. S11 or Eq. S13 because deaths are implicitly accounted for within $p(a)$.

As noted in the discussion of κ, $\lambda(t)$ can not be estimated directly from the data before t_0 (the beginning of the study period). For DENV-3 and DENV-4, because they invaded Iquitos after t_0, we can set their *FoI*s to 0 before t_0. For DENV-1 and DENV-2, we use both their respective estimates of κ and date of invasion to estimate λ before t_0. For the purpose of calculating $s_P(a,t)$ for $t > t_0$, we assume that $\lambda(t)$ is constant before t_0. For a given serotype, letting t_I represent the date of invasion, and setting $\lambda(t) = \lambda_0$ for $t_I < t < t_0$ (and 0 for $t < t_I$), we can rewrite Eq. (S12) evaluated at $t = t_0$ as:

$$s_P(a,t_0) = \begin{cases} \exp\left\{-\int_{a-(t_0-t_I)}^a \lambda_0 da'\right\}, & a \geq t_0 - t_I; \\ \exp\left\{-\int_0^a \lambda_0 da'\right\}, & a < t_0 - t_I, \end{cases} \tag{S14}$$

$$= \begin{cases} \exp\left\{-(t_0-t_I)\lambda_0\right\}, & a \geq t_0 - t_I; \\ \exp\left\{-a\lambda_0\right\}, & a < t_0 - t_I. \end{cases} \tag{S15}$$

Recalling that $s(t_0)$ denotes the fraction of the sample population that is susceptible at time t_0 (i.e., those born before 1995 and thus whose age at time t_0 is at least 5) we have:

$$\kappa = s(t_0) \tag{S16}$$

$$= \frac{1}{P(5)} \int_5^\infty s_P(a', t_0) p(a') da' \tag{S17}$$

$$= \frac{1}{P(5)} \left(\int_5^{t_0 - t_I} \exp\{-a'\lambda_0\} p(a') da' + \exp\left\{-(t_0 - t_I)\lambda_0\right\} P(t_0 - t_I) \right) \tag{S18}$$

Using the 2007 census in Iquitos [12], we estimate $p(a)$ by year. Letting $\hat{p}(a)$ denote the fraction of the population that is between a and $a+1$ years of age and $\hat{P}(a)$ denote the fraction of the population that is at least a years old, we translate the integrals in Eq. (S18) into summations:

$$\kappa \approx \frac{1}{\hat{P}(5)} \left(\sum_{a'=5}^{\lfloor t_0 - t_I - 1 \rfloor} \exp\{a'\lambda_0\} \hat{p}(a') + \exp\{-(t_0 - t_I)\lambda_0\} \hat{P}\left(\lfloor t_0 - t_I \rfloor\right) \right) \tag{S19}$$

where $\lfloor \cdot \rfloor$ is the floor function. Finally, using $\hat{p}$ and the appropriate estimates of t_I and κ, we numerically solve Eq. (S19) for λ_0 for DENV-1 and DENV-2.

As discussed in the main text, the effective reproductive number, $R(t)$, is the number of secondary infections caused by an individual who is infected at time t. If we denote the force of infection on day d as $g(d)$, then we have:

$$g(d) = \int_d^{d+1} \lambda(t) dt, \tag{S20}$$

and for Iquitos (using the fact that the census indicates no individuals within Iquitos are older than 98 years of age), we have

$$s_P(t) \approx \sum_{a'=0}^{98} s_P(a', t) \hat{p}(a'). \tag{S21}$$

If N is the size of the whole population, then $N \cdot s_P(d) \cdot g(d)$ approximates the number of new infections that occured on day d. Letting $\varepsilon(d) = s_P(d) \cdot g(d)$ (i.e., the fraction of the whole population that is infected on day d) and using $w(\Delta d)$ to denote the probability that the time between two successive infections, also called the serial interval, is equal to Δd days, we can write the number of infections caused by those who became infected at time d, denoted $\pi(d)$ as

$$\pi(d) = \sum_{i=d}^{\infty} w(i-d) \cdot N \cdot \varepsilon(i) \tag{S22}$$

Then we can write the effective reproductive number for day d, $R(d)$, as

$$R(d) \approx \frac{\pi(d)}{N \cdot \varepsilon(d)} = \frac{\sum_{i=d}^{\infty} w(i-d) \cdot \varepsilon(i)}{\varepsilon(d)} \tag{S23}$$

For DENV, $w(\Delta d)$ is unknown, however recent work estimates that the most likely serial interval is 15 to 17 days [13]. As such, we approximate $w(\Delta d)$ as follows:

$$w(\Delta d) \approx \hat{w}(\Delta d) = \begin{cases} \frac{1}{3}, & \Delta d\text{=15, 16 or 17;} \\ \\ 0, & \text{otherwise.} \end{cases} \tag{S24}$$

This approximation ascribes one third of infections 15, 16 and 17 days after d to the infections that occurred on day d. Then, by approximating $w(\Delta d)$ in Eq. (S23) by $\hat{w}(\Delta d)$ from Eq. (S24), denoting the approximate value of $R(d)$ as $\hat{R}(d)$, and using the substitution given in Eq. (S20) we derive Eq. (5). An alternative derivation of $R(t)$

follows from [14]. There, using a continuous version of $w(\Delta t)$ to represent the distribution of the serial interval, the substitution of a continuous $\hat{w}(\Delta t)$ analogous to Eq. (S13) results in a similar representation for $R(t)$. Finally, we relate $\hat{R}(d)$ to $\mathcal{R}_0$ through the following equation (where again $s_P(d)$ is the fraction of the whole population susceptible on day d)

$$\hat{R}(d) = s_P(d)\mathcal{R}_0 \tag{S25}$$

Solving Eq. (S25) for $\mathcal{R}_0$, we arrive at Eq. (6).

SECTION S4 MCMC description, convergence checks, model selection and identifiability

Adaptive, Metropolis-within-Gibbs MCMC algorithm

Due to the number of parameters we estimated, as well as the difficulty of computing the required conditional distributions to use a Gibbs sample, we used a Metropolis-within-Gibbs algorithm [15]. For each step in the chain this algorithm cycles through each individual parameter, and proposes updating that parameter's value using the Metropolis algorithm. Specifically, a single draw from a one-dimensional Normal distribution (to be explicitly defined below) is added to the parameter, the likelihood is computed for the new set of parameters (say L^*, with the likelihood before the perturbation denoted L^{old}), and the new proposed parameter is accepted with probability, p, where p is defined as:

$$p = \begin{cases} \frac{L^*}{L^{\text{old}}}, & \text{if } L^* < L^{\text{old}}; \\ \\ 1, & \text{otherwise.} \end{cases} \tag{S26}$$

Every parameter (order randomly chosen), is potentially perturbed using the same rule (but not necessarily the same Normally distributed noise), and at the completion of the proposals, a single step of the MCMC chain has been completed.

To decrease the time the chains take to converge to computationally reasonable times, we also incorporate an adaptive MCMC algorithm [16] (the adaptive algorithm is discussed within the reference). The adaptive aspect of the algorithm concerns the standard deviation of the distribution of the proposal noise. Optimally [17, 18], one would draw the noise for the proposals from the distribution

$$N\left(0, \frac{(2.38)^2\Sigma}{d}\right) \tag{S27}$$

where Σ denotes the covariance structure of the target distribution and d is the number of parameters. Because Σ is unknown, the adaptive MCMC algorithm approximates it from the empirical estimate based on a number of draws.

From an initial estimate of κ and the 72 B-spline coefficients we generated an initial approximation of f. Note that to assess the robustness of our results when starting each parameter of each chain at the same initial value (set to 0.001), we repeated the analysis so that every parameter of every chain was chosen from a uniform [0,0,001] distribution (Fig. S12). There was no appreciable difference between the posterior distributions of the two approaches. Using this initial f, we computed an initial likelihood. We initially started our MCMC chain using the d-dimensional identity matrix, I_d, as the null estimate, Σ_0, of Σ. Then we selected one of the 73 parameters at random, perturbed it by adding Normally distributed noise, and chose to accept the new value of the parameter using the Metropolis-Hastings acceptance rule. Once every parameter was perturbed once (and either the new value was adopted, or the parameter was reverted to its original value), the chain completed a single step. After an initial run of 5000 steps with independent Gaussian noise, we updated this estimate with the empirical covariance of those 5000 runs (plus, as recommended in [16], a small amount of 'nonrandom normal' as a "safety measure" (see Eq. 2.1 in [16])). We ran the Metropolis-within-Gibbs algorithm with this proposal distribution for 5,000 more steps

and then repeated the adaptive step using the last 5,000 steps, and continued. We did this twice more, for a total of 4 adaptive steps, and a total of 20,000 steps. Finally, we then ran the Metropolis-within-Gibbs algorithm with the 5th estimate of Σ for 80,000 more steps. In this final step, we used only the diagonal elements from Σ to re-achieve Markovian chain-steps.

Convergence was assessed through several metrics. We retained the final 15,000 steps for our analysis. We then recombined the steps from 10 different converged chains to arrive at 150,000 draws from the posterior distribution. From these final 150,000 steps, we randomly sampled 1,000 steps from this subset of the chain to remove autocorrelation, and then using Eq. (3) and the mean value of each parameter among those 1,000 steps, we obtained an estimate of f through time. Because the parameters were not independent of each other, to create credible regions for f (and later the *FoI* and $\mathcal{R}_0$), we used the 1,000 sampled steps of the chain to create 1,000 estimates of f. This forms an empirical estimate of the posterior distribution of f. We then, for each day, selected the middle 90% of the estimates to form our credible interval at that point.

Assessing convergence of MCMC chains

We generated 10 chains independently for each set of parameters with the intent to combine them and form one final sequence of parameter sets. In an attempt to ensure convergence of these chains (and due to the relatively quick time a single step in the chain takes to compute), we ran them each 80,000 steps after the final adaptive step. 80,000 was not chosen to minimize the number of steps required before convergence was declared, but rather as an attempt at overkill because convergence can never be truly 'confirmed.' Convergence checks at lower chain lengths appeared to converge, but there was no reason not to compute excessively long chains to increase our confidence in convergence. The convergence checks we used were: (1) visual inspection of the values of multiple parameters as they changed through the chain (trace plot), (2) investigation of proposal noise by calculating parameter-specific empirical estimates of the acceptance probabilities, (3) calculation of Gelman and Rubin's potential scale reduction factor [19], and (4) calculation of Gelman and Brooks' multivariate scale reduction factor [20]. Because we are combining multiple independent chains, these diagnostics seem most appropriate.

For both the potential scale reduction factor of each parameter, as well as the multivariate scale reduction factor, values considerably larger than one indicate a lack of convergence (of either the individual parameter or the entire parameter set as a whole respectively). For each serotype's estimation of f and κ, there were 73 parameters within the model. Below, in Fig. S13, we plotted the potential scale reduction factor (PSRF) for each parameter, by serotype, as the chain progresses. As noted in [20], when a PSRF was below 1.1 we may have believed the parameter has converged, but this low value may be transient and monitoring this value over time increases our confidence that the parameter has converged. For DENV-1, DENV-2, and DENV-3 (Fig. S13a, b, and c respectively), we saw that the PSRF was consistently below 1.1 for all parameters by the 10,000th step in the chain (and were all below 1.02). Interestingly, the PSRF for DENV-3 takes the longest to converge for the parameters that govern f around where the serotype was introduced into Iquitos. For DENV-4 (Fig. S13d), we saw that there were considerably more steps required before we would believe convergence occurred. The PSRF for parameters 60-70 were not consistently below 1.1 until the 30,000th iteration, and for a few parameters it was above 1.02 when the chain ended. The multivariate scale reduction factors were 1.01 for DENV-1, 1.01 for DENV-2, 1.02 for DENV-3 and 1.03 for DENV-4. Again, DENV-4 had the largest factor, but all were well below 1.1 indicating a high level of confidence that the chains have converged.

We also assessed convergence using trace plots and by evaluating the acceptance probabilities. Because there were 73 parameters, we present only a sampling of six of the trace plots (Fig. S14) and acceptance probabilities (Fig. S15). We combined the last 15,000 steps (indicated by the vertical dashed lines in Fig. S14) of 10 chains, but for clarity we have only displayed the values for the first 3 chains. For DENV-4, because its invasion was not until 2008, we selected a different subset of parameters to plot, starting at the 35th parameter. As indicated by

the PSRF analysis, the mixture of some later parameters for DENV-4 (e.g., the 63rd parameter in Fig. S14d) was sub-optimal. The estimated acceptance probabilities were running averages of the ratio of accepted proposals divided by the total number of values proposed. Our adaptive step ends after 20,000 steps and as such, we did not achieve perfect acceptance probabilities for every parameter of every chain for every serotype. Parameters that have relatively poor mixture (e.g., the 63rd parameter of DENV-4) also appeared to have lower than desirable acceptance probabilities (see, e.g., the 63rd parameter of DENV-4, Fig. S15d). As individual chains, they did not all appear appropriate for inference. When considering the set of 10 chains simultaneously, however, the resulting collection of parameters appears adequately converged.

Model selection

The deviation information criterion (DIC) [21] is a measure of a model's out-of-sample predictive power, and as such can be used to select the optimal model. We define the deviance, with respect to the data y and the parameter set θ, (denoted as $D(y, \theta)$) as:

$$D(y, \theta) = -2 \log p(y|\theta) \tag{S28}$$

where $p(y|\theta)$ is the likelihood function. Further, over the set of parameter sets that constitute the posterior distribution obtained through MCMC, we evaluate the deviance for each parameter set and denote their average as $\overline{D}$. Finally, letting $\hat{\theta}$ to be the mean parameter set of the posterior simulations, the DIC is defined as:

$$DIC = 2\overline{D} - D(y, \hat{\theta}) \tag{S29}$$

Because we analyzed 12 years of data, we chose to use our model selection procedure to select the number of splines per year, not in total. We did not alter the locations of the knots that define the centers of the splines from their default positions and as such these two approaches (selecting the number of splines per year versus total number of splines) were analogous. For the purposes of comparing fitted models across serotypes, we used the same number of splines per year for each serotype. As such, we identified the optimal number of splines for each serotype's model and selected the maximum of those for the final set of models. It is important to note that because DENV-4 was not tested for until 2006, the total number of splines used was the selected number of splines per year multiplied by 5 years (as opposed to 12 years for DENV-1, DENV-2, and DENV-3).

From Table S2 3, 4 and 6 splines per year all produced comparable DIC values for DENV-1 and DENV-2, with the model with 4 splines being most preferred. For DENV-3, 6 splines per year was significantly better than any other model, and for DENV-4, 3 splines a year was optimal. As such, we selected 6 splines per year for each model, and acknowledge (especially given the relatively flat fit for DENV-4) that fewer splines would have been sufficient for DENV-4. Because DIC indicated that 4 splines per year was adequate for 3 of the 4 serotypes, we conducted all analyses with 4 splines (Section S6).

Identifiability issues

There were particular continuity issues that occurred at the boundaries of the region over which the B-splines were defined. In the middle of this region, splines were placed at evenly spaced knots. Here, for comparability across serotypes, we did not choose to optimize the location of the interior spline knots by placing more of them where more interval infections were observed. Instead, for all serotypes, knots were placed unevenly at both endpoints (specifically they were spaced closer than usual). The relative effect of the last spline on the function f was minimal. Because there was not much data from the end of the study, it was not surprising that this parameter would be poorly identified. For the purposes of the analysis, we accounted for this difficulty by truncating our estimates accordingly. Graphically, we removed the final 60 days, but within the likelihood we retained this parameter.

The posterior distribution of the final spline parameter was quite wide (Fig. S16). Across serotypes, the median of the posterior for this parameter was considerably larger than for any other parameter. When looking at the actual likelihoods across values of this parameter, the likelihood was maximized when this parameter was essentially zero. Note that the solid lines in Figure S16 were computed holding all other parameters constant at their median posterior value and thus this was not the profile likelihood. The profile likelihood would be flatter, but the maximum would remain in the same place.

In addition to the endpoint issue, another identifiability issue arose for the first spline parameter. The likelihood integrates f and then adds the integral to κ. Thus the value of the first spline parameter was naturally additively confounded with the value of κ; if one was lower, the other could be increased to create essentially identical likelihoods. To illustrate the relationship between the first spline parameter and κ, we plotted the two dimensional posterior distribution of these parameters in Figure S17. For DENV-3 and DENV-4 (Fig. S17c,d respectively), both of the parameters should be exactly 0 and the fact that they weren't 0 was an artifact of the fitting procedure. Although the values were quite small, we still saw the appearance of a linear relationship between the two parameters in that when one was infinitesimally larger, the other was infinitesimally smaller. The relationship was clearer for DENV-1 and DENV-2 (Fig. S17a, b respectively). There was a clear linear relationship between the two parameters. This variation in κ was proportionally small, but the effect of this relationship resulted in considerable increases in the first spline parameter. To avoid over-interpretation of this effect (which, when confronted with our data, was clearly an artifact of our fitting procedure), we truncated the first 100 days' output in the beginning of f for our analysis.

In Figure S19, we plotted, by serotype, our estimates of f. On each panel we indicated the periods of time that we truncated due to the indentifiability issues. Comparing this plot to Figure 1, it is clear that there were no data to support the excessively high values at the beginning and end of each estimate. The magnitude of f was small, and thus the identifiability issue greatly skewed our estimates in the indicated regions.

SECTION S5 Additional results

Due to a limited amount of space in the main text and the multitude of almost equally-critical products of our analysis, we present here additional results.

κ, $s(t)$ and $s_P(t)$

The other outputs of our model are, by serotype, the fraction of the study population that was infected before 1999, κ. In Figure S18 we plotted the posterior distributions of κ, again noting non-zero values for DENV-3 and DENV-4 (Fig. S18 c and d respectively) were artifacts of the fitting method. Using Eq. S10, we combined f and κ to compute, by serotype, the fraction of the study population susceptible at time t, $s(t)$ (Fig. S20). There was a relatively steady decline in susceptible individuals in the two previously circulating serotypes (DENV-1 (orange) and DENV-2 (green)). DENV-3 (blue) and DENV-4 (purple) both experienced sharp declines consistent with the initial outbreaks of a pathogen in a wholly susceptible study population. Relative to the other serotypes, DENV-4 appeared to have been somewhat consistently depleting its pool of susceptible individuals since introduction. Finally, using λ, κ and $\hat{p}(a)$ we estimate $s_P(t)$. The patterns for DENV-3 and DENV-4 are relatively similar (Fig. S21). Conversely, once the differences between the sample population and all of Iquitos were accounted for (namely the addition of new suceptibles through births), the fraction of the population that was susceptible to DENV-1 and DENV-2 are mostly stable. Over the 12 years, the median fraction of the population that is susceptible to DENV-1 and DENV-2 varies by 8% and 6% respectively (36.6%-44.6% for DENV-1 and 40.0%-46.0% for DENV-2).

Robustness of estimates to the 2005-2006 gap

For our primary algorithm, we did not adjust for the gap in cohorts from late-2005 to mid-2006. This gap afforded us an opportunity to investigate the robustness of our estimates by providing a natural splitting point of the data. For this analysis, we cut the data in half (half 1: 1999-2005, half 2: 2006-2010) and performed our analyses on each half separately. The resulting estimated FoIs are plotted in Figure S24. There was considerable agreement between these estimates and our original estimates. There were, however, some noticeable differences. On both sides of the gap, the estimated credible intervals and posterior medians were considerably larger. Because the original estimates were all dependent on each other, the original estimates in mid-2005 were informed by all the data from 2006-2010, and likewise the original estimates in 2006 were informed by the data from 1999-2005. Thus, it was not too surprising that the credible intervals and estimates were larger.

$R(t)$, $\mathcal{R}_0(t)$, $\mathcal{R}_0(t)$'s sensitivity to the serial interval and $\mathcal{R}_0(t)$'s relationship to *FoI*

$\mathcal{R}_0$ is defined as the number of secondary infections generated by a single infectious individual entering an entirely susceptible population. In practice, this is difficult to observe. Conversely, $R(t)$, the effective reproductive number, merely counts the number of secondary infections at any point in time, independent of the number of susceptibles. In Figure S26 we plotted the estimated daily effective reproductive number for each serotype. The highest computed values of $R(t)$ were for DENV-3 in 2002 where it surpassed 3.

As mentioned in the main text, the presence of s_P in the denominator of $\mathcal{R}_0(t)$ allowed the tail of the posterior distribution of $\mathcal{R}_0(t)$ to be quite fat. In the main text we compensated for this by displaying the 50% credible interval from the posterior distribution of $\mathcal{R}_0(t)$ (Fig. 5), but in Figure S27, to be consistent with the credible level displayed in other figures, we display the fitted values of $\mathcal{R}_0(t)$, as well as the 90% credible interval from the posterior distribution. Note that the scale of $\mathcal{R}_0(t)$ had to be considerably increased to allow for the rare, but extremely high values at the upper end of the credible interval. For example, in 2007 and 2010 the upper limit of the 90% credible interval for the $\mathcal{R}_0(t)$ of DENV-3 exceeded 20. When we smoothed the data by computing a weekly $\mathcal{R}_0(t)$ (by taking the number of estimated cases in one week and then the number of cases 15 to 24 days into the future (appropriately scaling)), this extreme behavior disappears, and we preserved the general pattern. Because the time scale of f was daily, we chose to remain consistent across all products that use f in the main text and figures.

To compute the yearly average estimates for $\mathcal{R}_0$ (Fig. S32), within each year we took a weighted average of the daily $\mathcal{R}_0$ values. We weighted these daily values by the relative number of infectious individuals for each of those days. If we denote $\overline{R_0(Y)}$ the yearly average estimate for year Y, we have

$$\overline{R_0(Y)} = \frac{1}{\sum_{t\in Y} f(t)} \sum_{t\in Y} f(t) \cdot R_0(t) \tag{S30}$$

The serial interval between successive infections we used was 15 to 17 days [13]. This resulted in averaging the number of infections over those three days when computing the effective reproductive number. To assess the sensitivity of our results to the particular serial interval we used, we repeated the computation using shorter (just 15 days) and longer serial intervals (15 to 19 days). In both cases, we assumed the distribution of the serial interval was uniform across the interval to compute $\mathcal{R}_0$. In Fig. S28 we plotted estimates for shorter (Fig. S28a) and longer (Fig. S28b) serial intervals. The results were visually comparable, and numerical investigation showed that $\mathcal{R}_0$ estimates were at most 9% lower and 6% higher than those based on the 15-17 day serial interval.

A complete transmission cycle of DENV requires passage through two different latent periods. Starting with an infectious human host, a susceptible mosquito takes a virus-infected blood meal, and the pathogen enters an 'extrinsic incubation period' (EIP) in the mosquito. There are several different published estimates of the duration of the EIP ranging from 7-13 days [22, 23, 24, 25]. Following the EIP, the mosquito is infectious for the remainder of its life. After the infectious mosquito takes a blood meal from a susceptible human host and successfully infects this host, the virus enters an 'intrinsic incubation period' (IIP). There are several different published estimates of

the IIP, ranging from 4-7 days [26, 22, 23, 27, 28]. Using the shortest combination of EIP and IIP estimates, we estimated the shortest possible duration of the serial interval to be 11 days, which is consistent with the empirical data Siler et al reported [26]. We conducted two additional sensitivity analyses of $\mathcal{R}_0$, using first 11-13 days (Fig. S29a) and then combining that minimum (11) with the maximum presented by Aldsadt et al [13] (17), resulting in a relatively wide range for the serial intervals ranging from 11-17 days (Fig. S29b). The results were also visually comparable with slightly lower global and local maxima for estimates based on serial intervals with shorter lower bounds. Numerical investigation showed that $\mathcal{R}_0$ estimates were at most 18% lower and 16% higher than those based on the 15-17 day serial interval.

Also as mentioned in the text, there appeared to be a lag between $\mathcal{R}_0(t)$ and the *FoI* (Fig. S31). In Figure S30, we plotted the correlation (both Pearson (Fig. S30a) and Spearman (Fig. S30b)) between $\mathcal{R}_0(t)$ and variously lagged values of the *FoI*. For both, we used the median estimated daily lag value. In both panels it is clear that the highest correlation was between $\mathcal{R}_0(t)$ and the *FoI* of DENV-1 (orange), but there were relatively high maximum correlations for each serotype. The timing of the maximized correlation for each serotype was between 68 and 75 days for the Pearson correlation and between 64 and 72 days for the Spearman correlation.

Due to the number of B-splines per year used, we also investigated the level of uncertainty of both weekly and monthly estimates of the *FoI* and $\mathcal{R}_0$. In both cases (Fig. S25), the credible intervals remained relatively constant. For the *FoI* the values increased as expected but maintained the patterns of the daily estimates. For $\mathcal{R}_0$, the maximum values decreased slightly for weekly values and monthly values. (Fig. S25c, S25d respectively). For the weekly and monthly $\mathcal{R}_0$ estimates, like the yearly estimates, we took weighted averages of the daily estimates within the corresponding ranges.

Forward simulation using $\lambda(t)$

Using our estimates of λ, κ and $\hat{p}(a)$, we can forward simulate age-structured serotype specific DENV infection dynamics within Iquitos (assuming no interactions between serotypes). Let s_a, e_a, i_a and r_A denote the fraction of individuals between a and $a+1$ years old that is susceptible, exposed, infectious and immune respectively. For each DENV serotype, we can model the transmission dynamics forward using a standard SEIR model with age dependence. In particular, using a system of difference equations, our susceptibility estimates as initial conditions, and our daily estimates of $\lambda(d)$ to drive transmission, we have:

$$s_a(d+1) = \frac{s_{a-1}(d)}{365} + \frac{364}{365}s_a(d) - \lambda(d)s_a(d) \tag{S31}$$

$$e_a(d+1) = \frac{e_{a-1}(d)}{365} + \frac{364}{365}e_a(d) + \lambda(d)s_a(d) - \alpha e_a(d) \tag{S32}$$

$$i_a(d+1) = \frac{i_{a-1}(d)}{365} + \frac{364}{365}i_a(d) + \alpha e_a(d) - \gamma i_a(d) \tag{S33}$$

$$r_a(d+1) = \frac{r_{a-1}(d)}{365} + \frac{364}{365}r_a(d) + \gamma i_a(d) \tag{S34}$$

where

$$S(d) = \sum_{a'=0}^{98} s_{a'}(d)\hat{p}(a'), \tag{S35}$$

$$I(d) = \sum_{a'=0}^{98} i_{a'}(d)\hat{p}(a'), \tag{S36}$$

$$s_{-1}(d) = 1 \quad \text{for all } d, \tag{S37}$$

$$e_{-1}(d) = i_{-1}(d) = r_{-1}(d) = 0 \quad \text{for all } d, \tag{S38}$$

$1/\gamma$ is the average infectious period, and $1/\alpha$ is the average latent period. To match our serial interval estimates, we approximate $1/\gamma$ at 15 days. Following historical estimates of the average infectious period [29], we set $1/\alpha$ to 4 days.

Using the median output from our six B-Spline per year model, we deterministically simulate forward the age-structured SEIR model. In Figure S22 the estimated total number of infectious individuals within Iquitos by age and day is plotted (calculated by multiplying $I(d)$ by the population size of Iquitos). Similar to Figure 3, the high level of immunity for DENV-1 and DENV-2 limits the total number of infectious individuals on any day. As such, the majority of infections that occur are with young children. The estimated age-distribution of DENV infections for October 1, 2008 (indicated by the red line in Fig. S22) is plotted separately in Figure S23. This date is near the estimated invasion of DENV-4 and as such the age-distribution of infectious individuals is almost exactly the same as the age-distribution of individuals within Iquitos (Fig. S23d indicated by the dark grey histogram). Younger children are over-represented in DENV-1 and DENV-2 infections while high levels of immunity cause adults to be under-represented (Fig. S23a,b). DENV-3 infections display slightly different age-distribution patterns than DENV-1 and DENV-2 (Fig. S23c). Although adults are still under-represented, there are proportionally more individuals over the age of 10, indicative of a serotype that has not stabilized within the population.

SECTION S6 Four B-Splines per year

To assess the robustness of our results regarding the decision to use 6 B-splines per year for our estimation algorithm, we recreated all of the primary analyses using 4 B-splines per year. This resulted in a model with 49 parameters per serotype. We used an identical MCMC approach, initializing every chain individually by selecting random initial conditions.

The *FoI*

Analogously to Fig. 3 and Fig. 4 for the 4 spline-per-year model we present Fig. S2 and Fig. S3. The daily results for DENV-1 and DENV-2 were almost identical to those computed using the 6 spline-per-year model. Results were different for DENV-3. Because the DIC for DENV-3 was over 20 points lower for the 6 spline-per-year model, it was not surprising that there was some level of discordance between the two models' output here. At the yearly scale, all results were qualitatively identical. As with the 6 spline-per-year model, there was a high level of correlation between the yearly DENV-1, DENV-2 and DENV-3 estimates for the 4 spline-per-year model. Here the Spearman correlations were $\rho_{12} = 0.78$; DENV-1/DENV-3: $\rho_{13} = 0.73$ and DENV-2/DENV-3: $\rho_{23} = 0.79$, which were very similar to those described in the main text for the 6 spline-per-year model.

$R(t)$ and R_0

Analogous to Fig. S26 and Fig. 5, for the 4 spline-per-year model we present Fig. S6 and Fig. S4. In Fig. S6, it is clear that the fewer splines resulted in slightly smoother estimated daily effective reproductive numbers. The periods when the *FoI* was different for DENV-3 between the 6 spline and the 4 spline model also resulted in differences in R(t). For $\mathcal{R}_0$, the maximum estimated value was for DENV-1 in 2009 (4.27). Also analogous to Fig. S32, we computed the yearly estimate of the average value of $\mathcal{R}_0$ (Fig. S5). As with the daily values these were slightly lower, but overall in agreement with, the 6 spline-per-year model. The maximums of the yearly estimates were significantly lower than the maximums of the daily estimates with the maximum yearly $\mathcal{R}_0$ (DENV-1 in 2010), never exceeding 3.

For $\mathcal{R}_0$ we computed serial interval sensitivity analyses for the 4 spline-per-year model as outlined in SI 4. Conclusions from 6 spline-per-year and 4 spline-per-year models were essentially identical when the serial interval was set at 15 days and between 15 and 19 days (Fig. S9a, b respectively). As with the 6 spline-per-year output,

decreasing the lower bound of the serial interval to 11 days resulted in slightly lower estimates than in the primary analysis (Fig. S10).

κ, and $s(t)$

As with the 6 spline-per-year model, the estimate of κ for DENV-3 and DENV-4 for the 4 spline-per-year model were essentially 0 (Fig. S8c,d). For DENV-1 the estimated fraction of the sample population susceptible in 1999 was 56.3% (Fig. S8a) and 53.5% of the population was estimated susceptible to DENV-2 in 1999 (Fig. S8b). These values were slightly higher than those for the 6 spline-per-year model but both were well within the credible intervals reported in the main text. The trajectory of the fraction of the population susceptible to each serotype over time was similar to that of the 6 spline-per-year model (Fig. S7).

References and Notes

[1] Halstead, S. B, Rojanasuphot, S, & Sangkawibha, N. (1983) Original antigenic sin in dengue. *The American Journal of Tropical Medicine and Hygiene* **32**, 154–156.

[2] Kuno, G, Gubler, D, & Oliver, A. (1993) Use of 'original antigenic sin' theory to determine the serotypes of previous dengue infections. *Transactions of the Royal Society of Tropical Medicine and Hygiene* **87**, 103–105.

[3] Morrison, A, Minnick, S, Rocha, C, Forshey, B, Stoddard, S, Getis, A, Focks, D, Russell, K, Olson, J, Blair, P, Watts, D, Sihuincha, M, Scott, T, & Kochel, T. (2010) Epidemiology of dengue virus in iquitos, peru 1999 to 2005: interepidemic and epidemic patterns of transmission. *PLoS Neglected Tropical Diseases* **4**, e670. 10.1371/journal.pntd.0000670.

[4] Olkowski, S, Forshey, B. M, Morrison, A. C, Rocha, C, Vilcarromero, S, Halsey, E. S, Kochel, T. J, Scott, T. W, & Stoddard, S. T. (2013) Reduced risk of disease during postsecondary dengue virus infections. *Journal of Infectious Diseases* pp. 1026–1033.

[5] Morens, D, Halstead, S, Repik, P, Putvatana, R, & Raybourne, N. (1985) Simplified plaque reduction neutralization assay for dengue viruses by semimicro methods in BHK-21 cells: comparison of the BHK suspension test with standard plaque reduction neutralization. *Journal of Clinical Microbiology*.

[6] Comach, G, Blair, P. J, Sierra, G, Guzman, D, Soler, M, Quintana, M. C. d, Bracho-Labadie, M, Camacho, D, Russell, K. L, Olson, J. G, & Kochel, T. J. (2009) Dengue Virus Infections in a Cohort of Schoolchildren from Maracay, Venezuela: A 2-Year Prospective Study. *Vector-Borne and Zoonotic Diseases* **9**. 10.1089/vbz.2007.0213.

[7] Kochel, T. J, Watts, D. M, Halstead, S. B, Hayes, C. G, Espinoza, A, Felices, V, Caceda, R, Bautista, C. T, Montoya, Y, Douglas, S, et al. (2002) Effect of dengue-1 antibodies on American dengue-2 viral infection and dengue haemorrhagic fever. *The Lancet* **360**, 310–312.

[8] Liebman, K, Stoddard, S, Morrison, A, Rocha, C, Minnick, S, Sihuincha, M, Russell, K, Olson, J, Blair, P, Watts, D, Kochel, T, & Scott, T. (2012) Spatial dimensions of dengue virus transmission across interepidemic and epidemic periods in Iquitos, Peru (1999-2003). *PLoS Neglected Tropical Diseases* **6**, e1472. 10.1371/journal.pntd.0001472.

[9] Thomas, S. J, Nisalak, A, Anderson, K. B, Libraty, D. H, Kalayanarooj, S, Vaughn, D. W, Putnak, R, Gibbons, R. V, Jarman, R, & Endy, T. P. (2009) Dengue plaque reduction neutralization test (PRNT) in primary and secondary dengue virus infections: how alterations in assay conditions impact performance. *The American Journal of Tropical Medicine and Hygiene* **81**, 825.

[10] Muench, H. (year?) Derivation of rates from summation data by the catalytic curve. *Journal of the American Statistical Association* **29**, 25–38.

[11] Ferguson, N, Donnelly, C, & Anderson, R. (1999) Transmission dynamics and epidemiology of dengue: insights from age-stratified sero-prevalence surveys. *Philosophical Transactions of the Royal Society of London. Series B, Biological sciences* **354**, 757–768. 10.1098/rstb.1999.0428.

[12] Instituto Nacional de Estadistica e Informatica. (2007) Censos nacionales 2007 (http://http://censos.inei.gob.pe/Censos2007/redatam/).

[13] Aldstadt, J, Yoon, I.-K, Tannitisupawong, D, Jarman, R, Thomas, S, Gibbons, R, Uppapong, A, Iamsirithaworn, S, Rothman, A, Scott, T, & Endy, T. (2012) Space-time analysis of hospitalised dengue patients in rural thailand reveals important temporal intervals in the pattern of dengue virus transmission. *Tropical Medicine & International Health : TM & IH* **17**, 1076–1085. 10.1111/j.1365-3156.2012.03040.x.

[14] Wallinga, J & Teunis, P. (2004) Different epidemic curves for severe acute respiratory syndrome reveal similar impacts of control measures. *American Journal of Epidemiology* **160**, 509–516. 10.1093/aje/kwh255.

[15] Tierney, L. (1994) Markov chains for exploring posterior distributions. *The Annals of Statistics* **22**, 1635 – 2134.

[16] Roberts, G. O & Rosenthal, J. S. (2009) Examples of Adaptive MCMC. *Journal of Computational and Graphical Statistics* **18**, 349–367. 10.1198/jcgs.2009.06134.

[17] Roberts, G, Gelman, A, & Gilks, W. (1997) Weak convergence and optimal scaling of random walk Metropolis algorithms. *The Annals of Applied Probability* **7**, 110 – 120.

[18] Roberts, G & Rosenthal, J. (2001) Optimal scaling for various Metropolis-Hastings algorithms. *Statistical Science* **16**.

[19] Gelman, A & Rubin, D. (1992) Inference from iterative simulation using multiple sequences. *Statistical Science* **7**, 457–472.

[20] Stephen, P. B & Andrew, G. (1998) General methods for monitoring convergence of iterative simulations. *Journal of Computational and Graphical Statistics* **7**, 434–455. 10.1080/10618600.1998.10474787.

[21] Gelman, A, Carlin, J. B, Stern, H. S, & Rubin, D. B. (2004) *Bayesian Data Analysis*. (Chapman & Hall/CRC).

[22] Newton, E & Reiter, P. (1992) A model of the transmission of dengue fever with an evaluation of the impact of ultra-low volume (ULV) insecticide applications on dengue epidemics. *The American Journal of Tropical Medicine and Hygiene* **47**, 709–720.

[23] Focks, D, Daniels, E, Haile, D, & Keesling, J. (1995) A simulation model of the epidemiology of urban dengue fever: literature analysis, model development, preliminary validation, and samples of simulation results. *The American Journal of Tropical Medicine and Hygiene* **53**, 489–506.

[24] Favier, C, Schmit, D, Mller-Graf, C, Cazelles, B, Degallier, N, Mondet, B, & Dubois, M. (2005) Influence of spatial heterogeneity on an emerging infectious disease: the case of dengue epidemics. *Proceedings of the Royal Society B* **272**, 1171–1177. 10.1098/rspb.2004.3020.

[25] Otero, M, Barmak, D, Dorso, C, Solari, H, & Natiello, M. (2011) Modeling dengue outbreaks. *Mathematical Biosciences* **232**, 87–95. 10.1016/j.mbs.2011.04.006.

[26] Siler, J, Hall, M, & Kitchens, A. (1926) Dengue: Its history, epidemiology, mechanism of transmission, etiology, clinical manifestations, immunity and prevention. *Philippine Bur. Sci.*

[27] Gubler, D & Kuno, G. (1997) *Dengue and dengue hemorrhagic fever*. (Cab International Wallingford, New York).

[28] de Castro Medeiros, L, Castilho, C, Braga, C, de Souza, W, Regis, L, & Monteiro, A. (2011) Modeling the dynamic transmission of dengue fever: investigating disease persistence. *PLoS Neglected Tropical Diseases* **5**. 10.1371/journal.pntd.0000942.

[29] Gubler, D, Suharyono, W, Tan, R, Abidin, M, & Sie, A. (1981) Viraemia in patients with naturally acquired dengue infection. *Bulletin of the World Health Organization* **59**, 623–630.

Study	Time Span	Population	Samples	Study Design	Active surveillance component	IRB protocol numbers and approval*	Related publications	Serotypes tested
Entomological Correlates of Dengue Control (ECDC)	Jan. 1999 to Mar. 2005	Primary school children (78%, 5-17 y/o)	N = 3,903 with 2-12 samples at ∼6 mo intervals	Participants selected from geographically stratified sample of city blocks spanning northern half of Iquitos	School-based in subset of participants	UCD-235832, NMRCD2001.008, INS13-2002 SDSU	Morrison et al. 2004a,b, 2010, Rocha et al. 2009	DENV-1, -2, -3
Dengue Vector Control System (DVCS)	April 2004 to Oct. 2005	Ages 5 and above (77%, >18 years)	N= 1,267 with 2-3 samples at 9 mo intervals	Participants were enrolled from 24 city blocks distributed across 7 of 26 administrative zones located in the northern half of Iquitos	Community-based surveillance, 3 visits per week	UCD-200311958, NMRCD2003.0008, INS-04502003	Rocha et al. 2009	DENV-1, -2, -3
Predictors of Disease Severity (PRED)	August 2006 to June 2010	Ages 5 and above (66%, >18 years)	N=2,555 with 2-7 samples at 6 mo intervals	Cohort members were recruited from 20 city blocks selected (2 per zone) at random from 10 administrative zones in northern half of Iquitos	Community-based surveillance, 3 visits per week	UCD-216811 NMRCD2005.0009 CAY-06017	Forshey et al. 2010 (Influenza)	DENV-1, -2, -3, -4
Measuring Risk across Activity Spaces (AS)	November 2007 to December 2010	Ages 5 and above (76%, >18 years)	N=3,500 with 2-5 samples at 6-12 mo intervals	Cohort members were recruited from contiguous blocks in two neighborhoods: Maynas (20 blocks) and Tupac Amaru (14 blocks).	Community-based surveillance, 3 visits per week	UCD-296683 NMRCD2007.0007 Relying Agreements: TUL, EM	Stoddard et al. 2009, 2013 Vasquez-Prokopec et al. 2009 Paz-Soldan et al. 2010	DENV-1, -2, -3, -4
Insecticide Treated Curtains (ITC)	October 2009-August 2010	Ages 3 and above (71%, >20 years)	N=1,943 with 2 samples 9 mo interval	Cohort was recruited from 20 clusters (90 houses) from a contiguous area located in southern Iquitos	No surveillance component	NMRCD.2009.0007 LSTM, LSTMH Relying Agreements: UCD, TUL		DENV-1, -2, -3, -4

*Institutional Review Board (IRB) abbreviations. University of California (UCD). Naval Medical Research Center Detachment (NMRCD) or Naval Medical Research Unit No. 6 (NAMRU-6) where from 1999-2007 protocols were reviewed by the Naval Medical Research Center (NMRC) IRB located in Bethesda Maryland and assigned NMRCD numbers to protocols carried out by NMRCD which became NAMRU-6 in July 2010. In 2007, NMRCD which later became NAMRU-6 formed their own IRB which is comprised of both Peruvians and military officials and because of its registration with the Peruvian Network of Ethic's Committee provides both DOD and Peruvian approval for reviewed protocols. Studies conducted before 2007 were reviewed by the NMRC and either the Peruvian National Institute of Health (INS) or Cayetano Heredia University (CAY) located in Lima, Peru to obtain Peruvian approval. Additional collaborators, Tulane University (TUL), Emory University (EM), San Diego State University (SDSU) established relying agreements with either UCD or NMRCD/NAMRU-6 IRBs. The ITC project was also approved by the Liverpool School of Tropical Medicine (LSTM) and London School of Tropical Medicine and Hygiene (LSTMH) at the initiation of the study as per European Regulations.

Table S1: **Summary of cohort studies.** For each longitudinal cohort study, we list the time span, population of interest, total number of participants/samples, a brief description of the study design, a brief description of the active surveillance component, IRB protocol numbers, related publications, and the DENV serotypes tested for.

	Number of splines per year				
	2	3	4	6	8
DENV-1	19930.11	19908.29	19904.41	19910.37	19931.03
DENV-2	21009.92	21005.29	21003.36	21007.11	21028.16
DENV-3	23461.92	23397.27	23356.47	23335.02	23342.9
DENV-4*	11535.79	11528.3	11537.6	11551.92	11572.8

* Due to DENV-4 not being tested until 2006, the total number of spline parameters is based on 5 years.

Table S2: **Summary of DIC values.** For each serotype, we utilized deviation information criterion (DIC) to select the appropriate model. For each serotype, we list the DIC value for the model that consisted of 3, 4, 6, or 8 splines per year. For comparability across serotypes, we chose, amongst the recommended models for each serotype, the largest model which resulted in our models each having 6 splines per year.

$P(T < t_L) = \int_{-\infty}^{t_L} f(s)ds$	For left censored individuals who seroconverted before their first observation at time t_L.
$P(T_{I_1} < I < t_{I_2} = \int_{t_{I_1}}^{t_{I_2}} f(s)ds$	For interval censored individuals who seroconverted between observation times t_{I_1} and t_{I_2}.
$P(T > t_R) = 1 - \int_{-\infty}^{t_R} f(s)ds$	For right censored individuals who never seroconverted and were last observed at time t_R.

Table S3: **Likelihood for censored data.** For each type of censored data, the likelihood of that observation is a different function of f , depending also on the timing of the pertinent test(s).

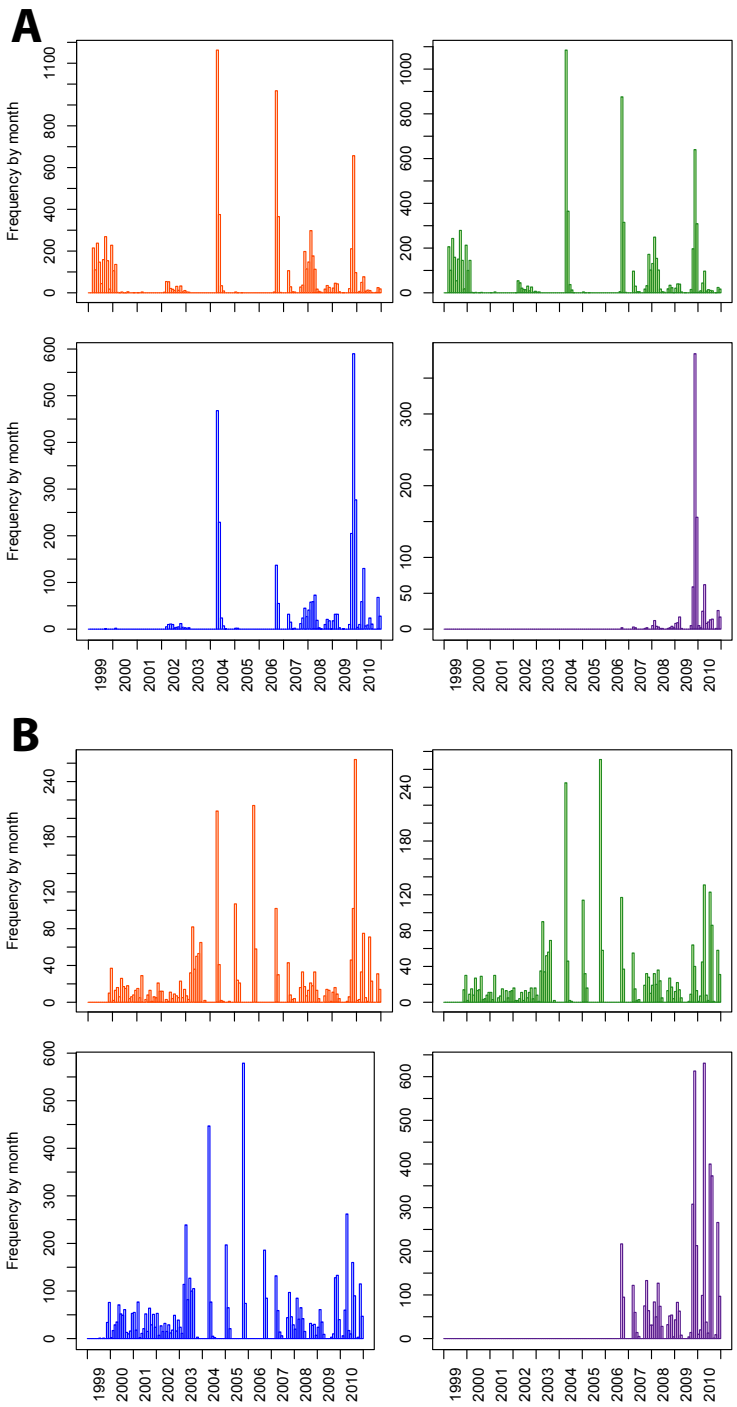

Fig. S1: **Left and right censored data.** (a) The number of left censored infections per month are plotted against time (DENV-1 top panel (orange), DENV-2 second panel (green), DENV-3 third panel (blue) and DENV-4 bottom panel (purple)). The three large spikes in the number of left censored infections correspond to the beginning of three of the cohort studies. (b) The number of right censored infections per month (i.e., the date of the final negative PRNT for an individual before they left the study) are plotted against time (DENV-1 top panel (orange), DENV-2 second panel (green), DENV-3 third panel (blue) and DENV-4 bottom panel (purple)). The DVCS study from April 2004 February 2006 consisted of three tests. Spikes in right censored data in mid-2004, early 2005 and late 2005 corresponded to individuals within that cohort who left after the first, second or third test respectively.

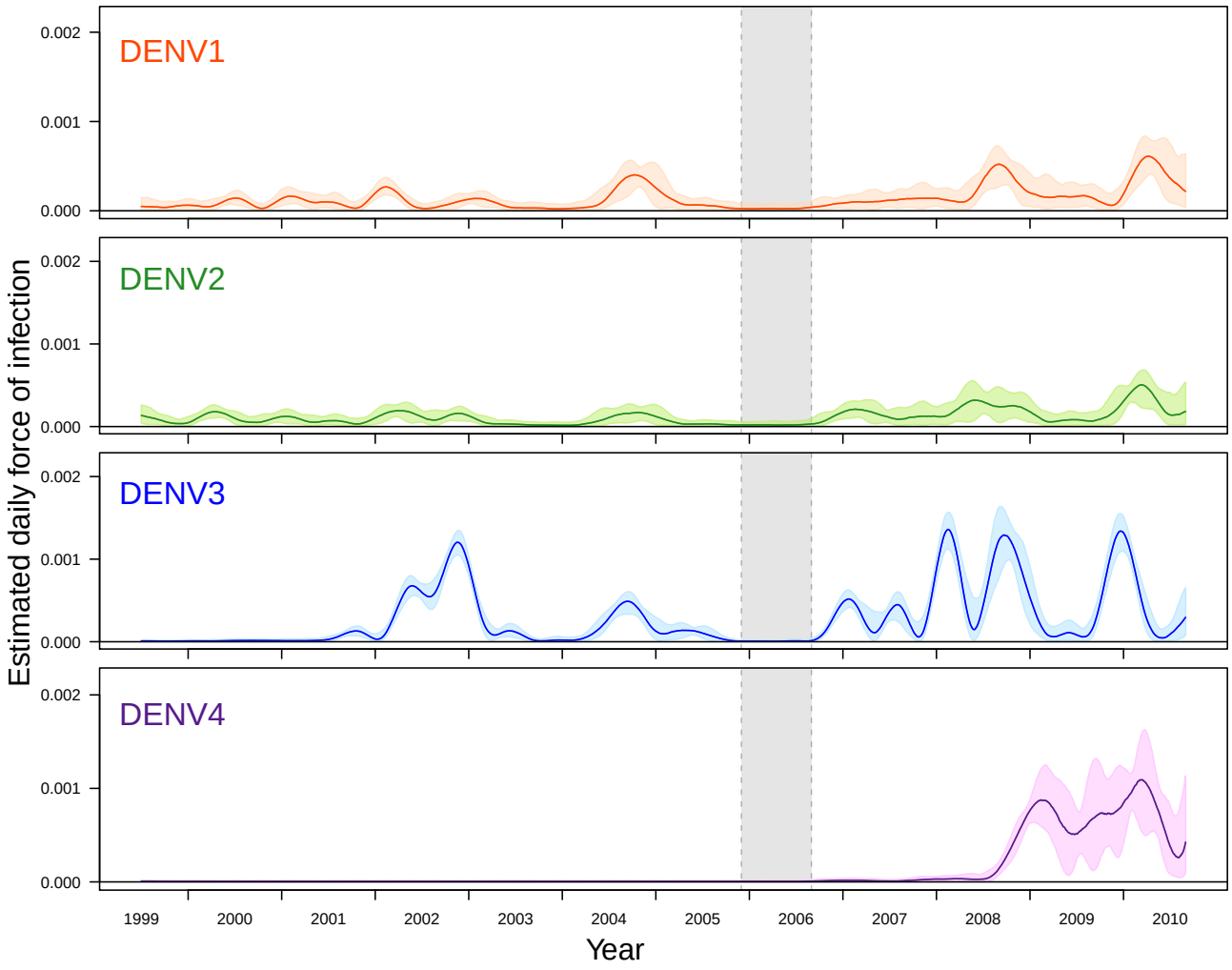

Fig. S2: **4 spline-per-year analysis: Daily estimates of the *FoI*.** For each serotype (DENV-1 top panel (orange), DENV-2 second panel (green), DENV-3 third panel (blue) and DENV-4 bottom panel (purple)), daily estimates of the *FoI* as well as the 90% BCI are plotted against time. The absence of a cohort study from late 2005 to mid-2006 is indicated by the grey shaded region.

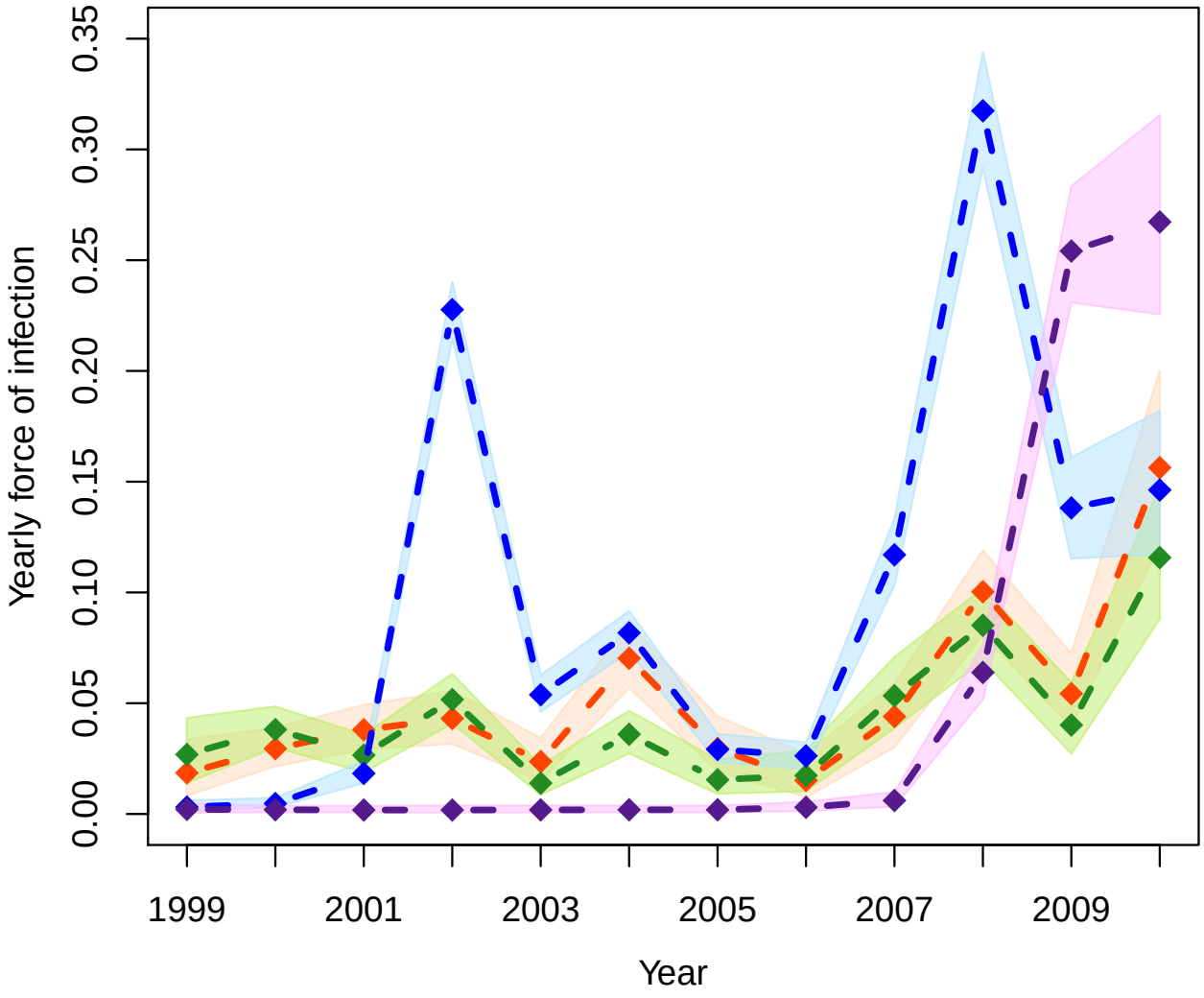

Fig. S3: **4 spline-per-year analysis: Yearly estimates of the *FoI*.** For each serotype (DENV-1 (orange), DENV-2 (green), DENV-3 (blue) and DENV-4 (purple)), yearly estimates of the *FoI* as well as the 90% BCI are plotted against time. The absence of a cohort study from late 2005 to mid-2006 does not preclude the estimation of the yearly *FoI* estimates for either 2005 or 2006 as evidenced by the non-zero *FoI* estimates for the circulating serotypes for both of those years.

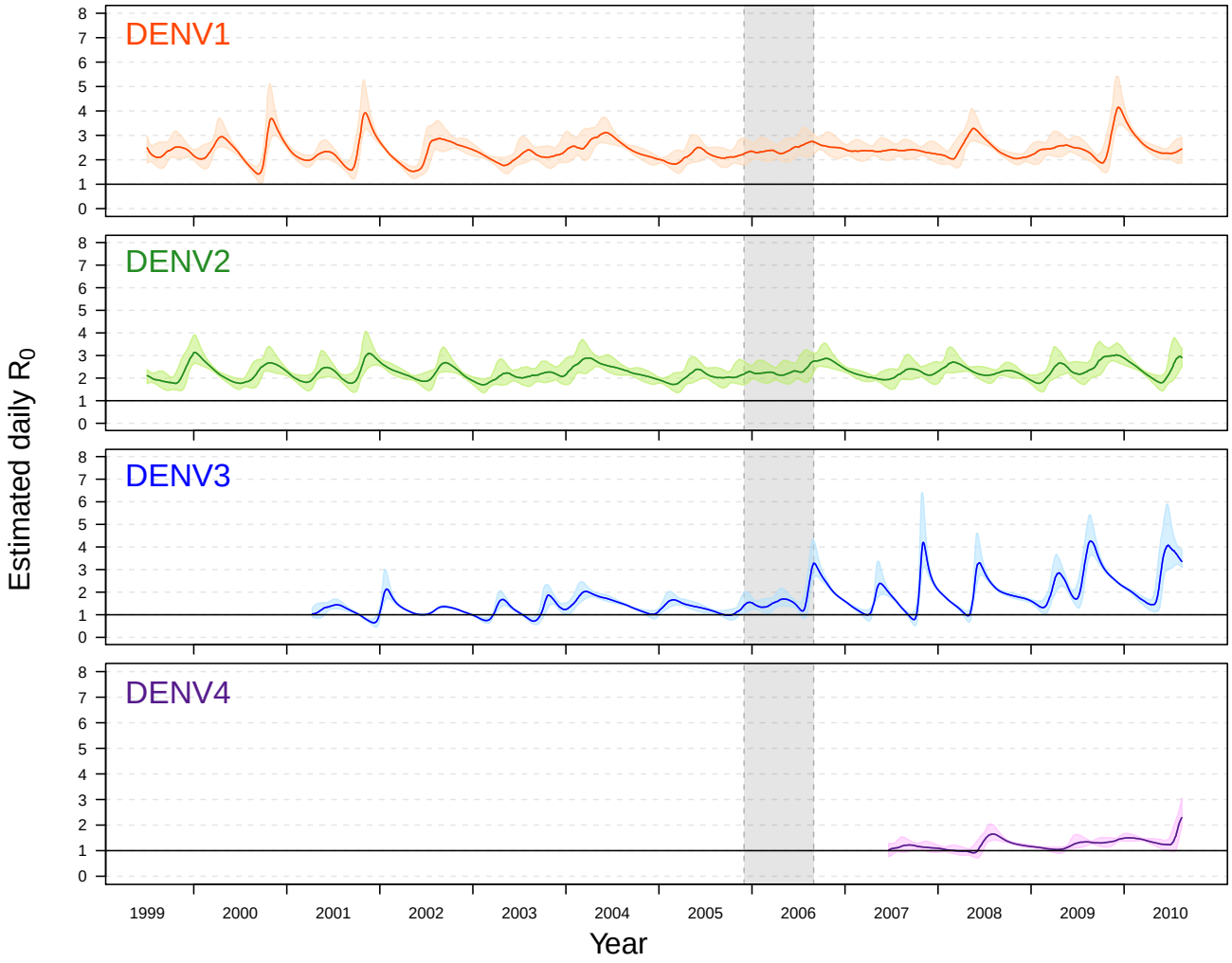

Fig. S4: **4 spline-per-year analysis: Daily estimates of $\mathcal{R}_0$.** For each serotype (DENV-1 top panel (orange), DENV-2 second panel (green), DENV-3 third panel (blue) and DENV-4 bottom panel (purple)), daily estimates of $\mathcal{R}_0$ as well as the 50% BCI are plotted against time. The absence of a cohort study from late 2005 to mid-2006 is indicated by the grey shaded region. The estimates for both DENV-3 and DENV-4 are truncated, excluding estimation before their respective introductions.

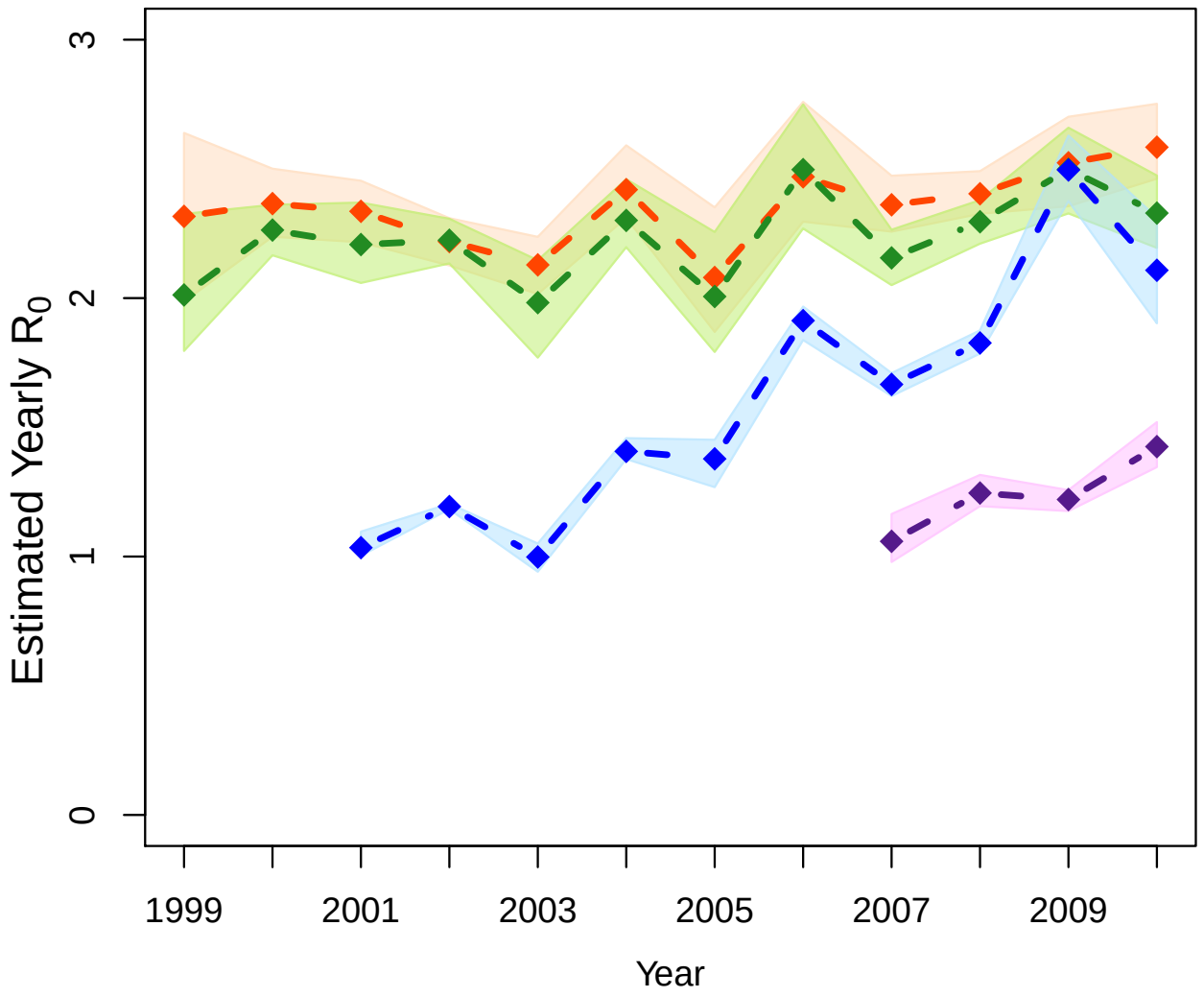

Fig. S5: **4 spline-per-year analysis: Yearly estimates of $\mathcal{R}_0$.** For each serotype (DENV-1 top panel (orange), DENV-2 second panel (green), DENV-3 third panel (blue) and DENV-4 bottom panel (purple)), yearly estimates of $\mathcal{R}_0$ as well as the 90% BCI are plotted against time by computing the yearly mean of the daily estimates. The estimates for both DENV-3 and DENV-4 are truncated, excluding estimation before their respective introductions.

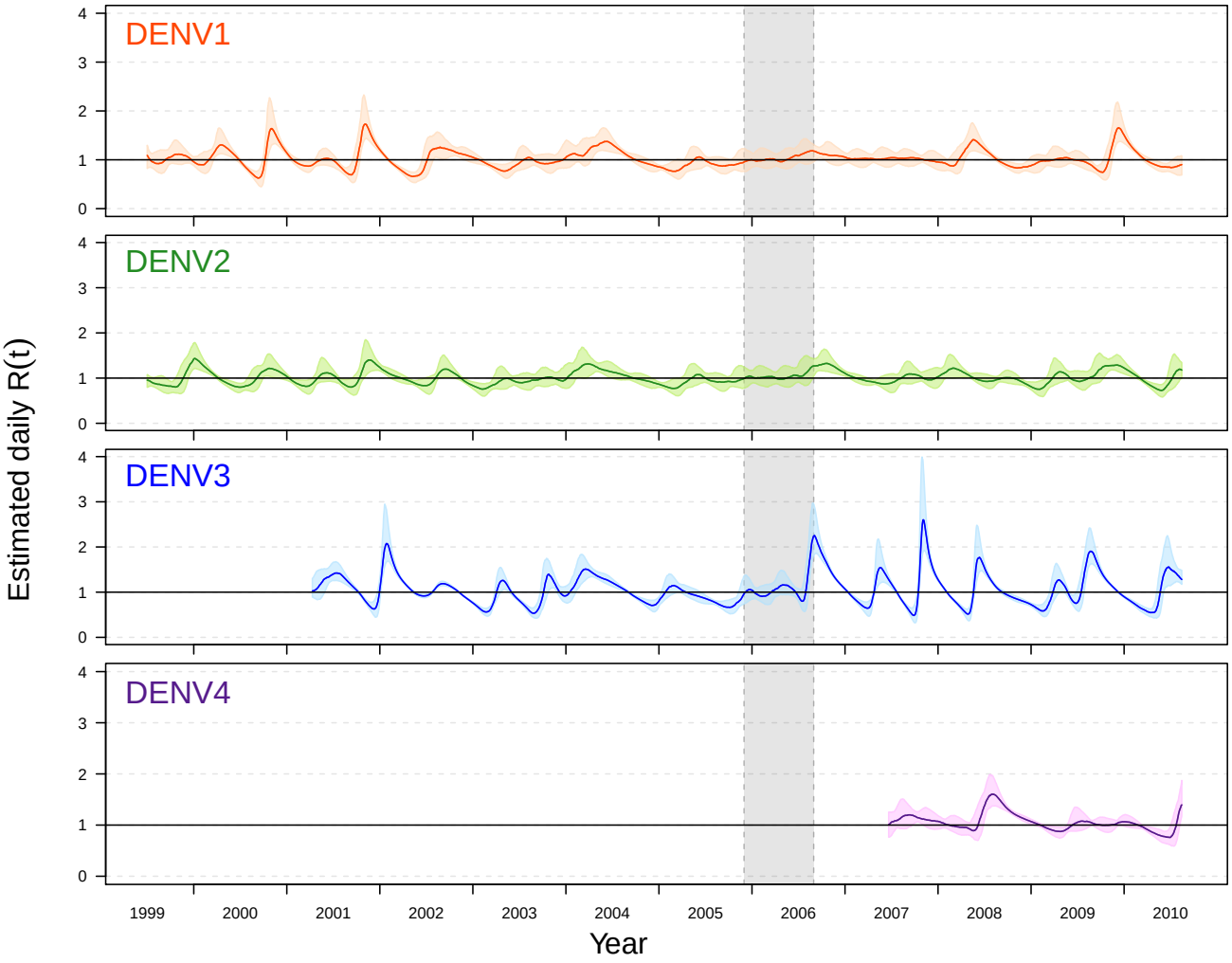

Fig. S6: **4 spline-per-year analysis: Daily estimates of the effective reproductive number, $R(t)$.** For each serotype (DENV-1 top panel (orange), DENV-2 second panel (green), DENV-3 third panel (blue) and DENV-4 bottom panel (purple)), daily estimates of $R(t)$ as well as the 50% BCI are plotted against time. The absence of a cohort study from late 2005 to mid-2006 is indicated by the grey shaded region. The estimates for both DENV-3 and DENV-4 are truncated, excluding estimation before their respective introductions.

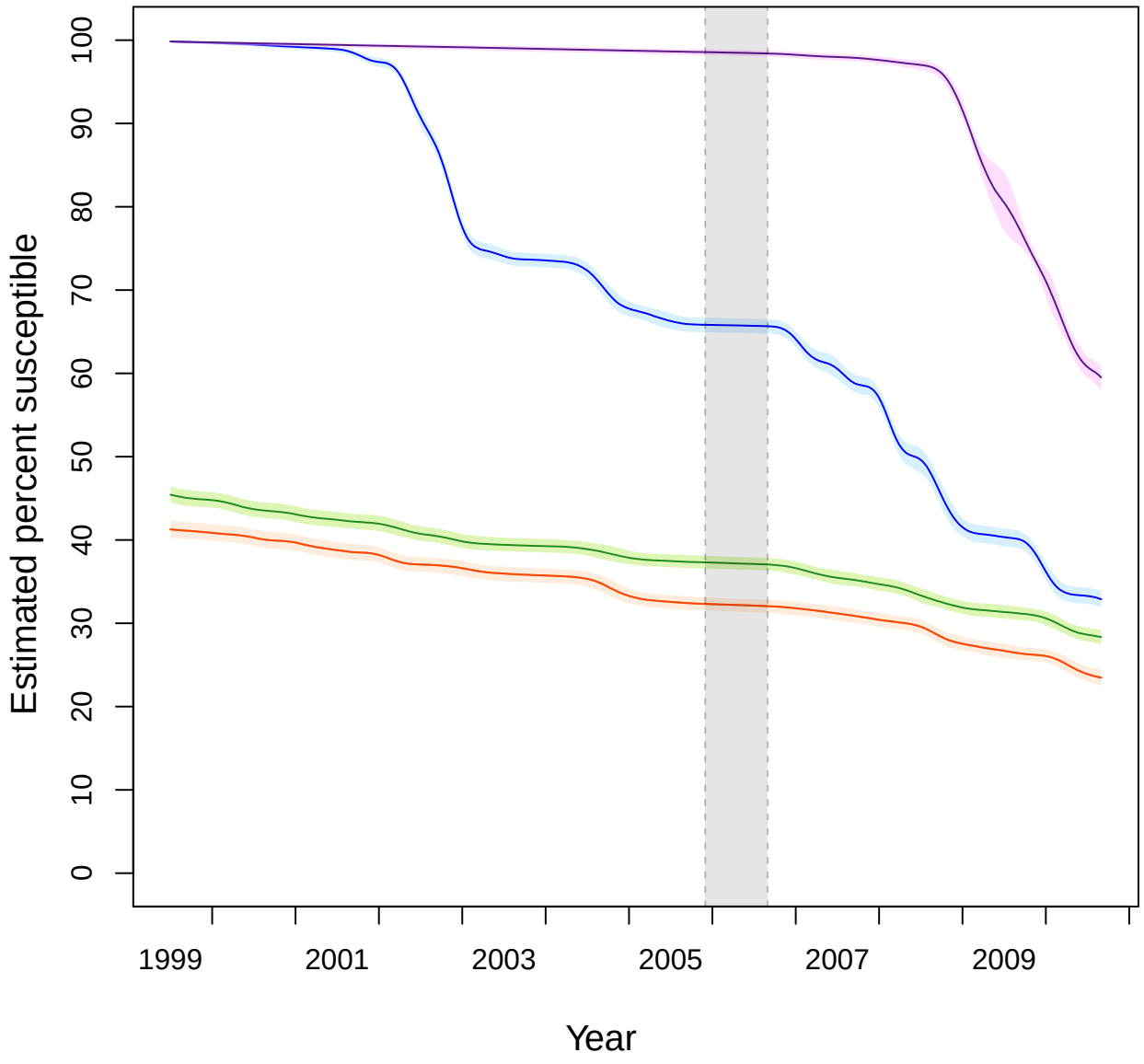

Fig. S7: **4 spline-per-year analysis: Fraction of the study population susceptible over time.** The fraction of the study population that was susceptible over time, $s(t)$, is plotted for (a) DENV-1, (b) DENV-2, (c) DENV-3, and (d) DENV-4. Note that because we define our study population to be those that were born before 1995 (and thus the susceptible pool was never replenished) and each serotype circulates after its introduction, these estimates decreased over time.

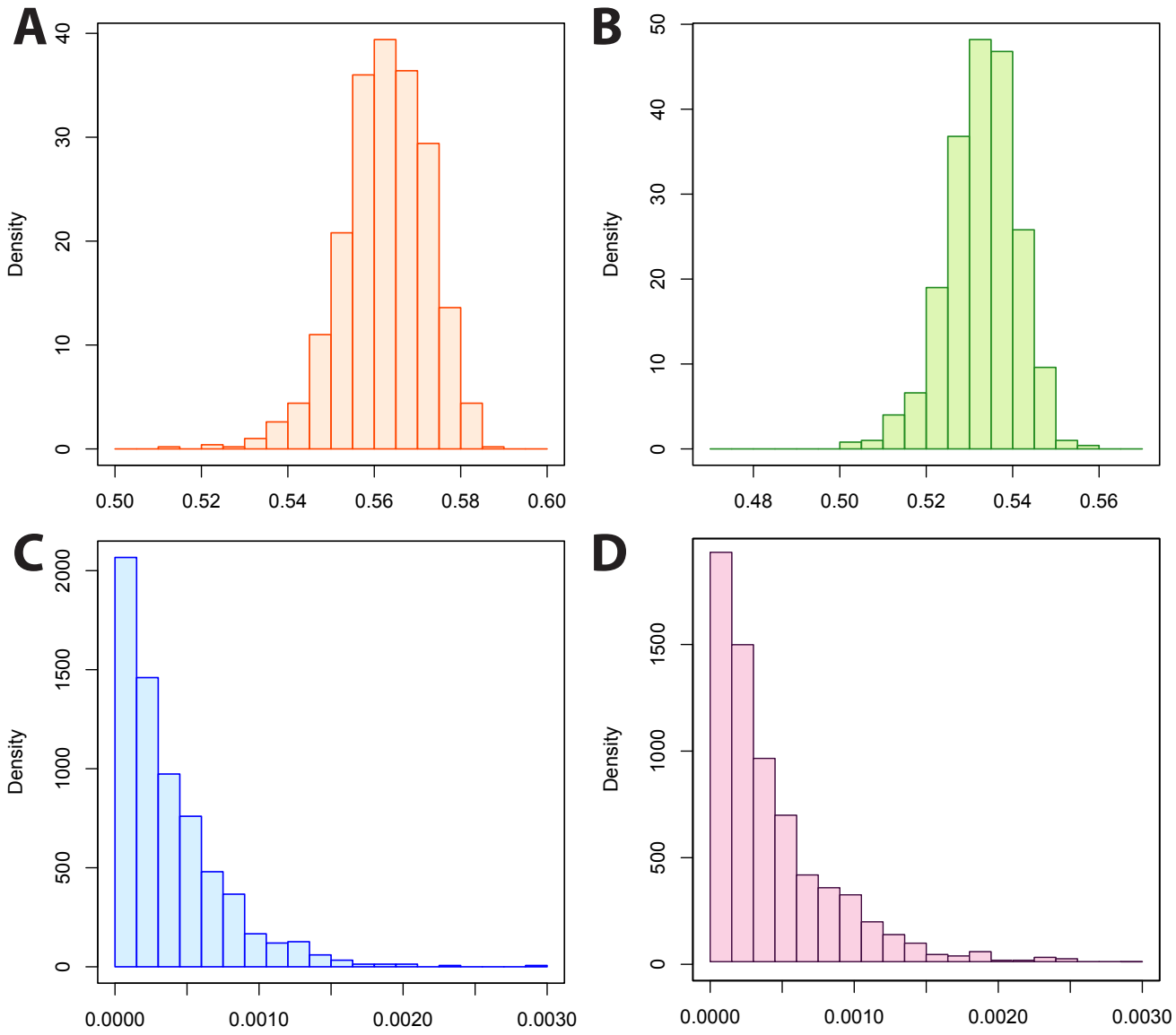

Fig. S8: **4 spline-per-year analysis: Posterior distribution of κ.** The posterior distribution of the fraction of the study population that was susceptible to each serotype at the time of the beginning of the study in 1999 is plotted for (a) DENV-1, (b) DENV-2, (c) DENV-3, and (d) DENV-4. Note that the scale is not the same for each of the figures.

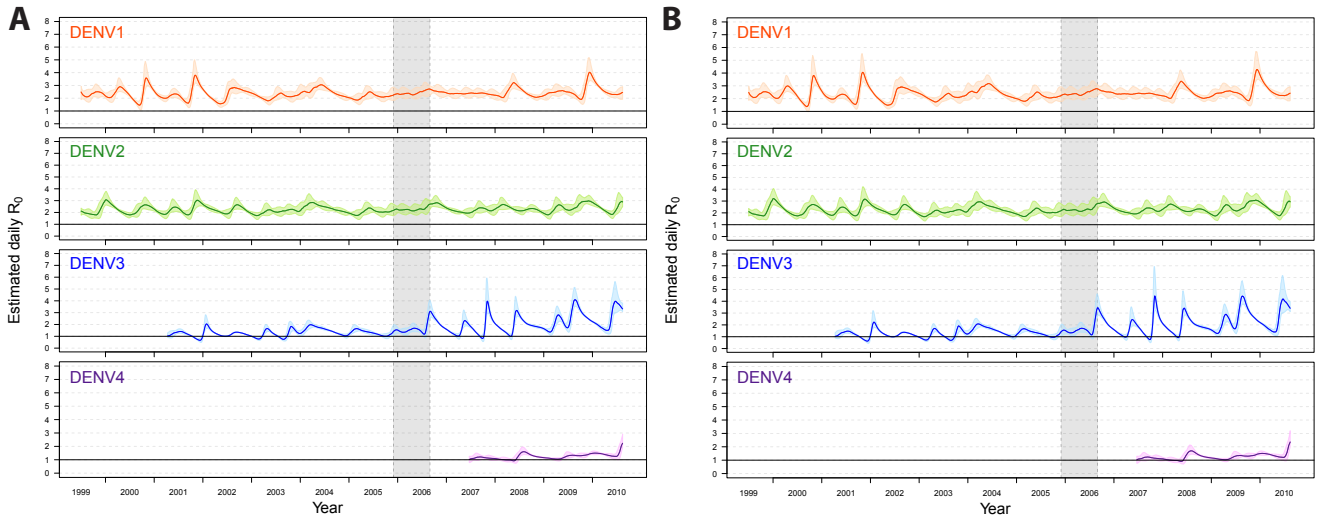

Fig. S9: **4 spline-per-year analysis: Sensitivity of $\mathcal{R}_0$ to the serial interval, part 1.** We recomputed $\mathcal{R}_0$ using both a shorter and longer serial interval than found in [13]. In (a), we assumed that the length of time between primary and secondary infections was exactly 15 days. In (b), we lengthened the serial interval to 5 days, allowing the time between a primary and secondary infection to be between 15 and 19 days. In both (a) and (b), for each serotype (DENV-1 top panel (orange), DENV-2 second panel (green), DENV-3 third panel (blue) and DENV-4 bottom panel (purple)), daily estimates of $\mathcal{R}_0$ as well as the 50% BCI are plotted against time.

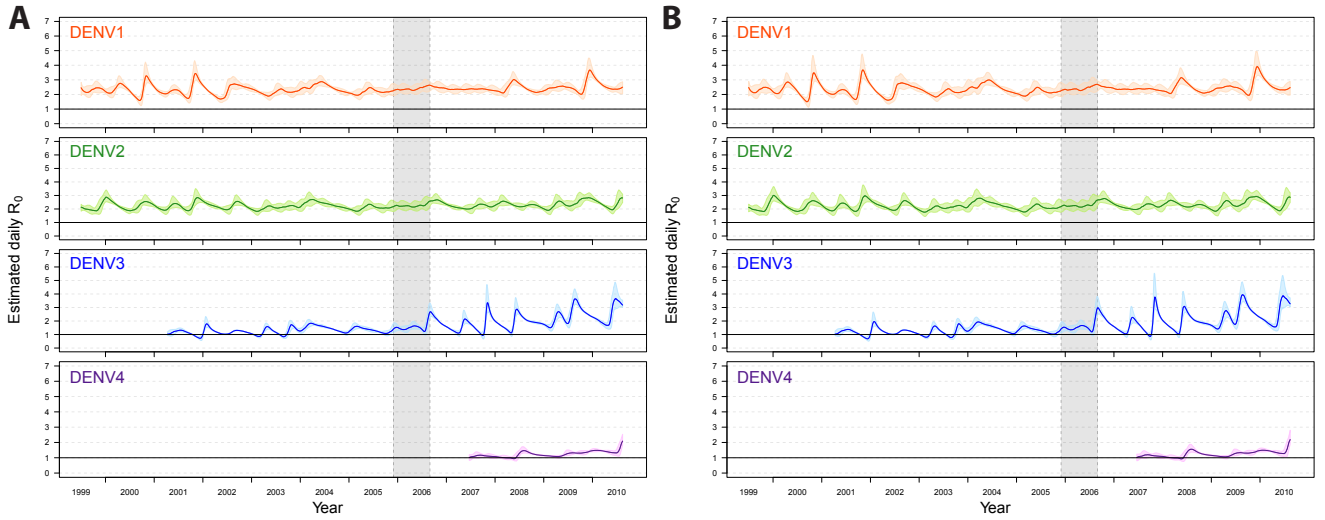

Fig. S10: **4 spline-per-year analysis: Sensitivity of $\mathcal{R}_0$ to the serial interval, part 2.** Using the lower bound on both the EIP and the IIP for DENV reported in the literature, we estimated the shortest serial interval possible as 11 days. Using this value we recomputed $\mathcal{R}_0$. In (a), we assumed that the length of time between primary and secondary infections was between 11 and 13 days. In (b), we combined this lower bound (11 days) with the upper bound found in [13] (17 days), allowing the time between a primary and secondary infection to be between 11 and 17 days. In both (a) and (b), for each serotype (DENV-1 top panel (orange), DENV-2 second panel (green), DENV-3 third panel (blue) and DENV-4 bottom panel (purple)), daily estimates of $\mathcal{R}_0$ as well as the 50% BCI are plotted against time.

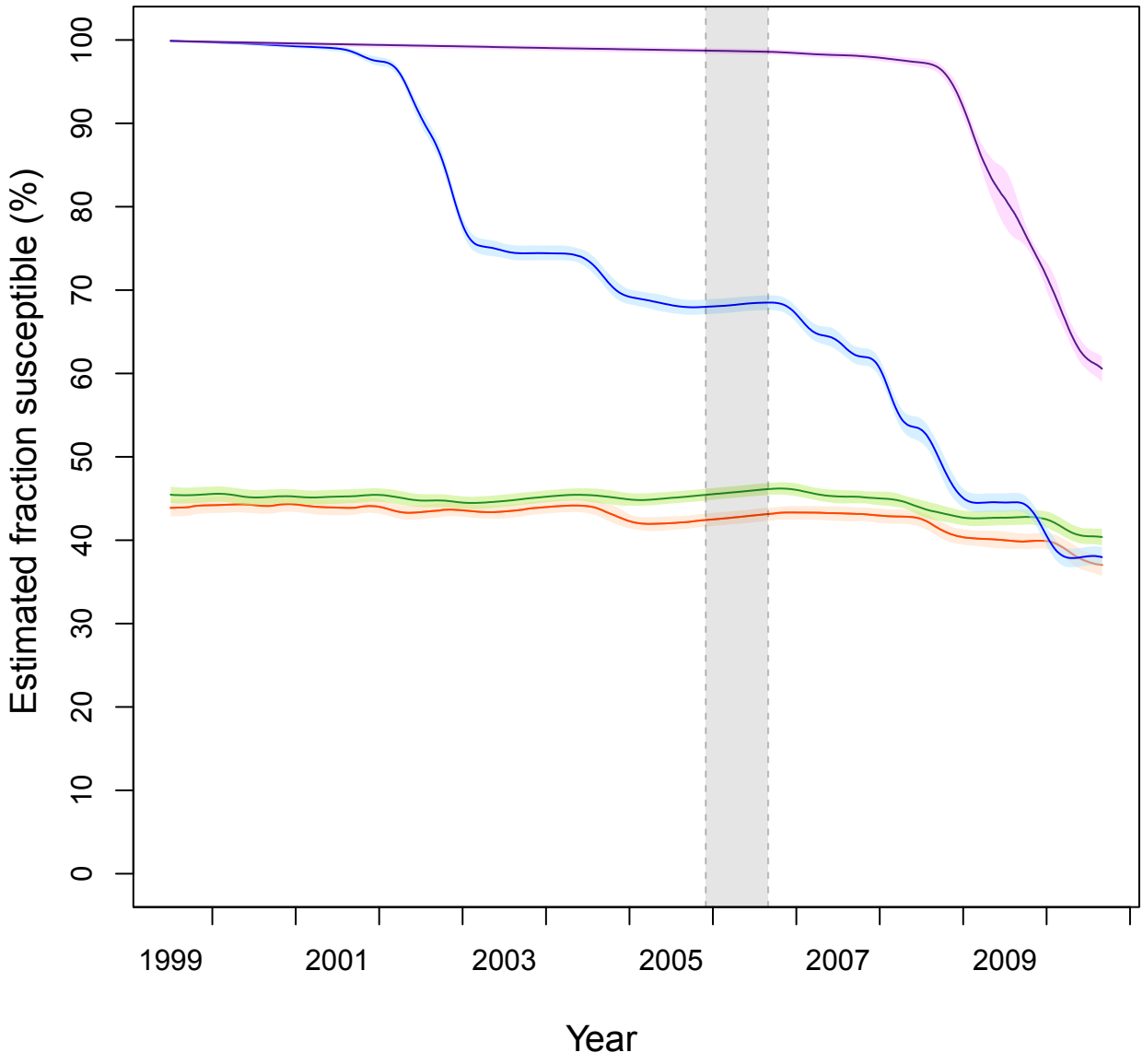

Fig. S11: **4 spline-per-year analysis: Fraction of the entire population susceptible over time.** The fraction of the entire population that was susceptible over time shown as a percentage, $s_P(t)$, is plotted for (a) DENV-1, (b) DENV-2, (c) DENV-3, and (d) DENV-4.

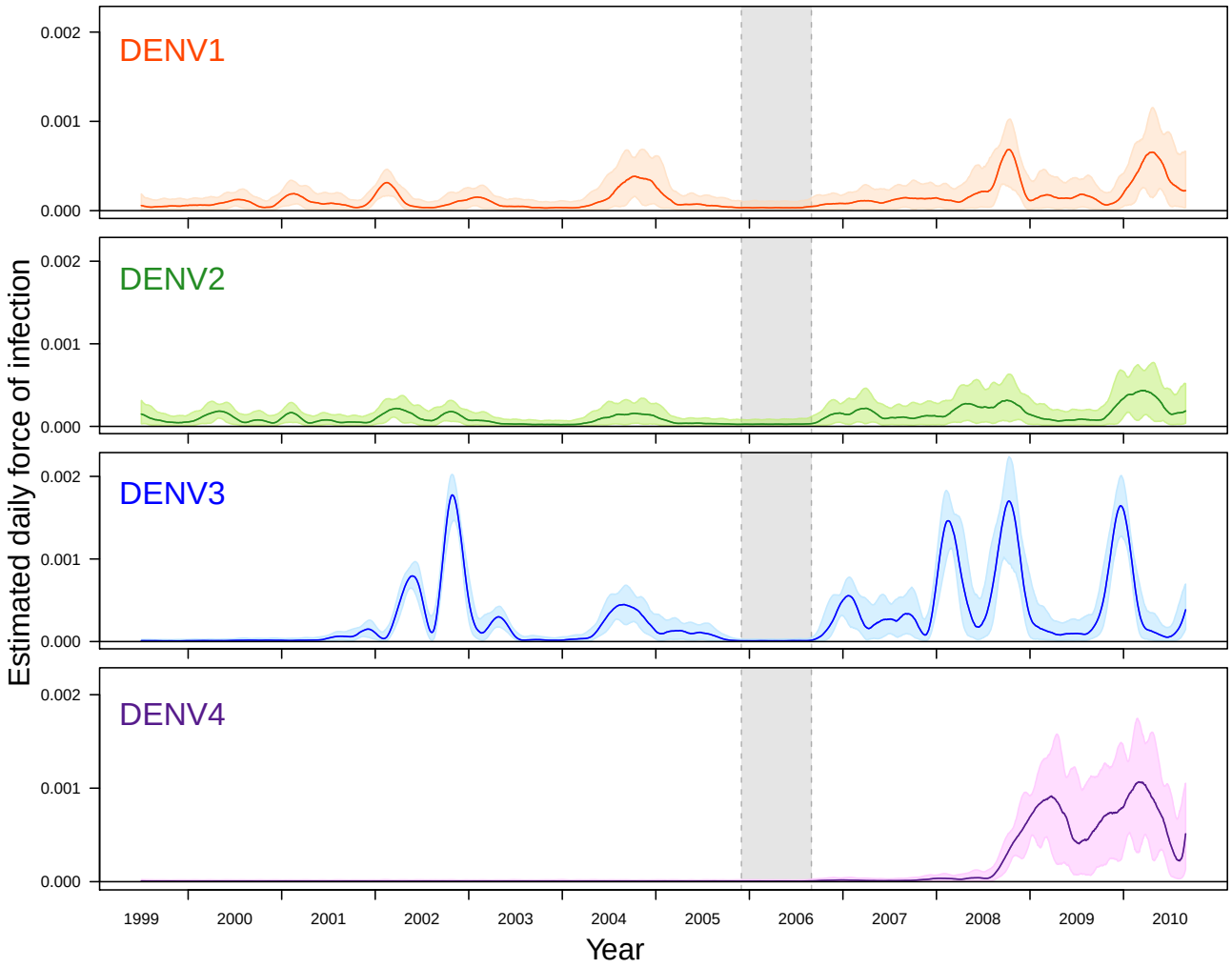

Fig. S12: **Sensitivity of daily estimates of the *FoI* to initial conditions.** Using different initial conditions for every parameter of every chain (uniformly drawing initial conditions from a uniform [0,0.001] distribution), f and then the daily *FoI* estimates were computed. For each serotype (DENV-1 top panel (orange), DENV-2 second panel (green), DENV-3 third panel (blue) and DENV-4 bottom panel (purple)), daily estimates of the *FoI* as well as the 90% BCI are plotted against time. The absence of a cohort study from late 2005 to mid-2006 is indicated by the grey shaded region.

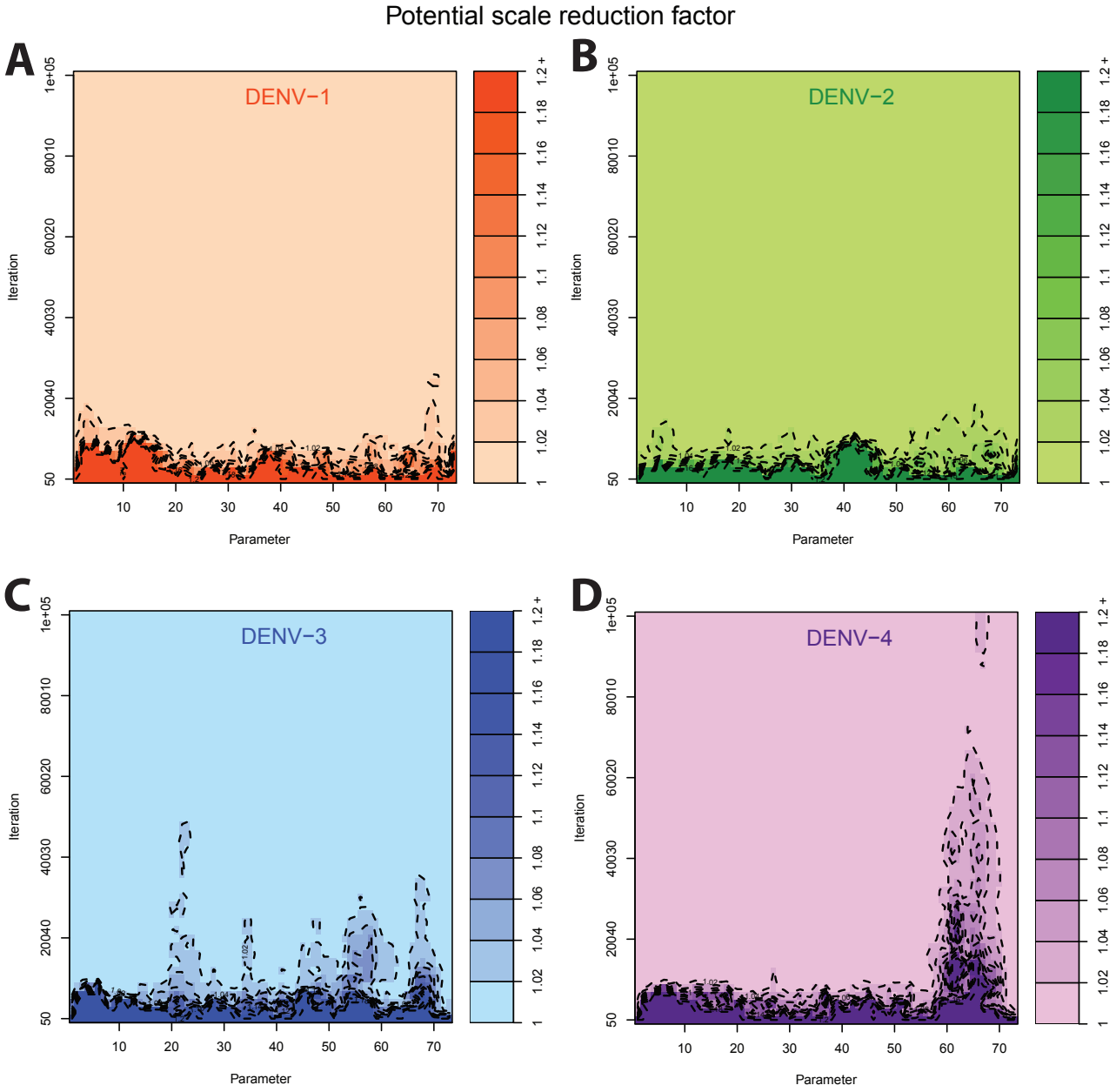

Fig. S13: **Potential scale reduction factors.** The potential scale reduction factors for computed for the MCMC chains corresponding to the parameters of (a) DENV-1, (b) DENV-2, (c) DENV-3, and (d) DENV-4 are plotted against the iteration of the MCMC algorithm. A potential scale reduction greater than 1.1 indicated a lack of convergence for that particular parameter.

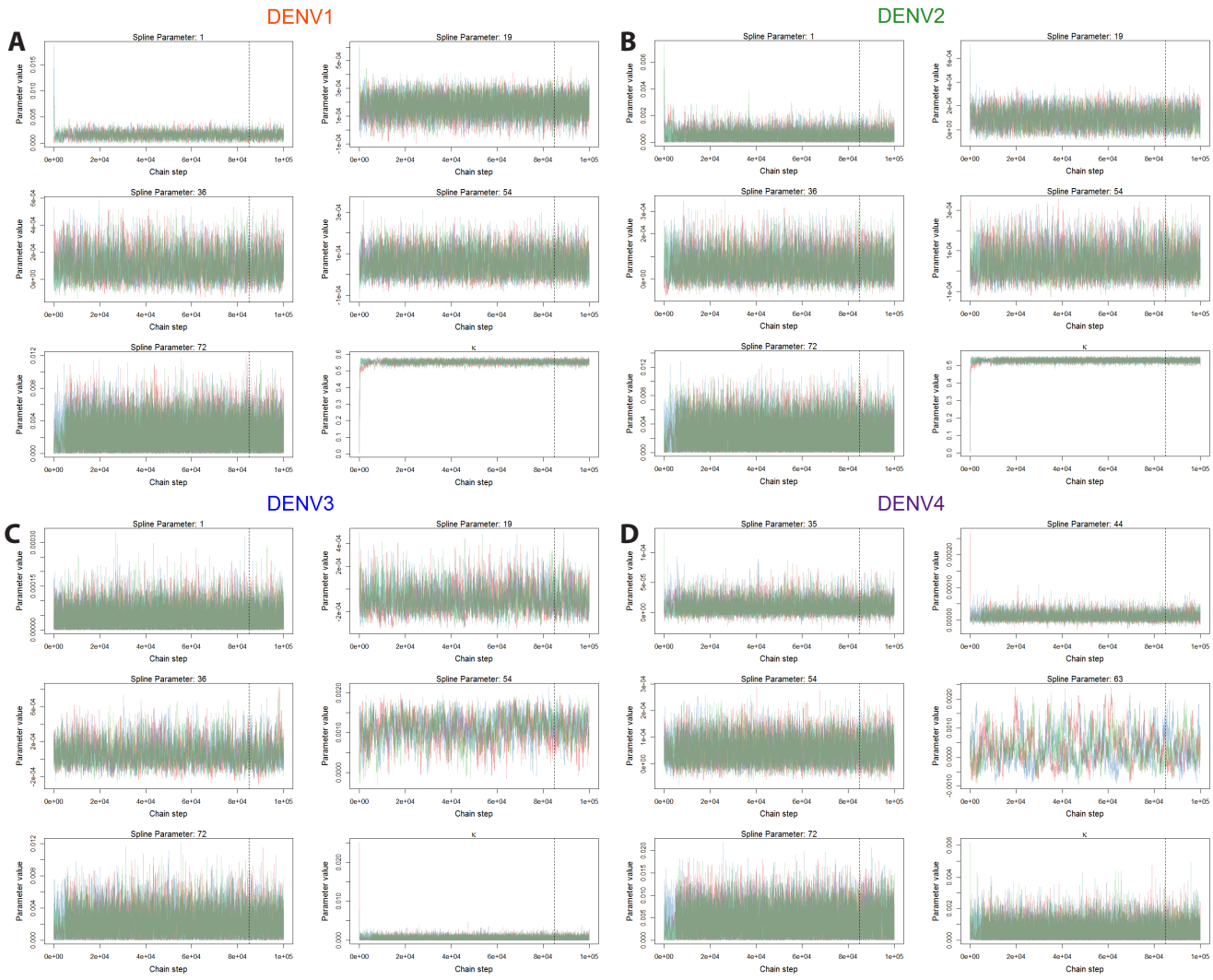

Fig. S14: **Trace plots.** Trace plots of a subset of parameters of the first three chains (red, blue and green lines respectively) are plotted for (a) DENV-1, (b) DENV-2, (c) DENV-3, and (d) DENV-4 against the iteration of the MCMC algorithm. The parameters selected for DENV-4 were altered due to the late invasion date of this serotype.

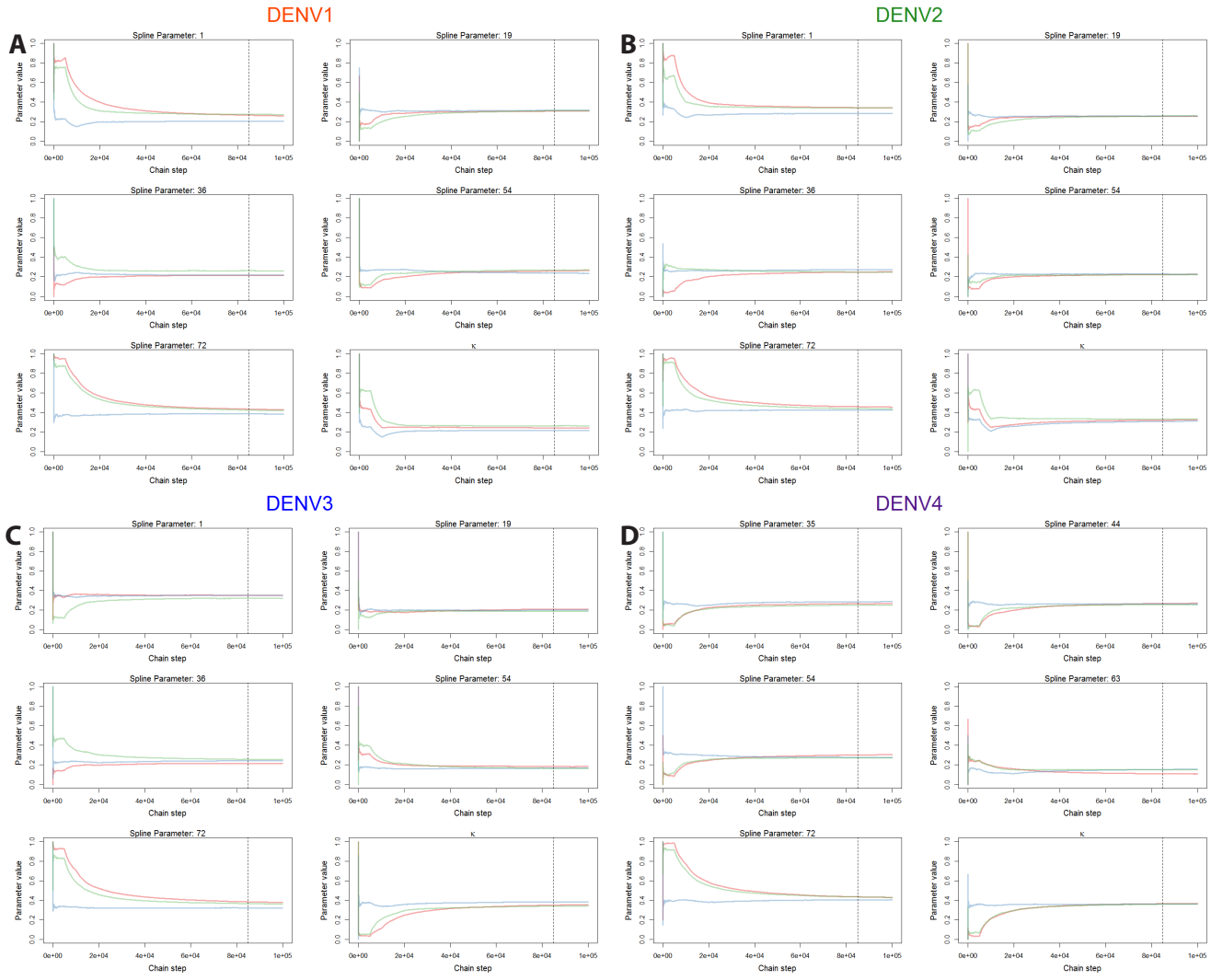

Fig. S15: **Estimates of the acceptance probabilities.** The estimated acceptance probabilities were running averages of the ratio of accepted proposals divided by the total number of values proposed. Estimated acceptance probabilities for a subset of parameters of the first three chains (red, blue and green lines respectively) are plotted for (a) DENV-1, (b) DENV-2, (c) DENV-3, and (d) DENV-4 against the iteration of the MCMC algorithm. The parameters selected for DENV-4 were altered due to the late invasion date of this serotype.

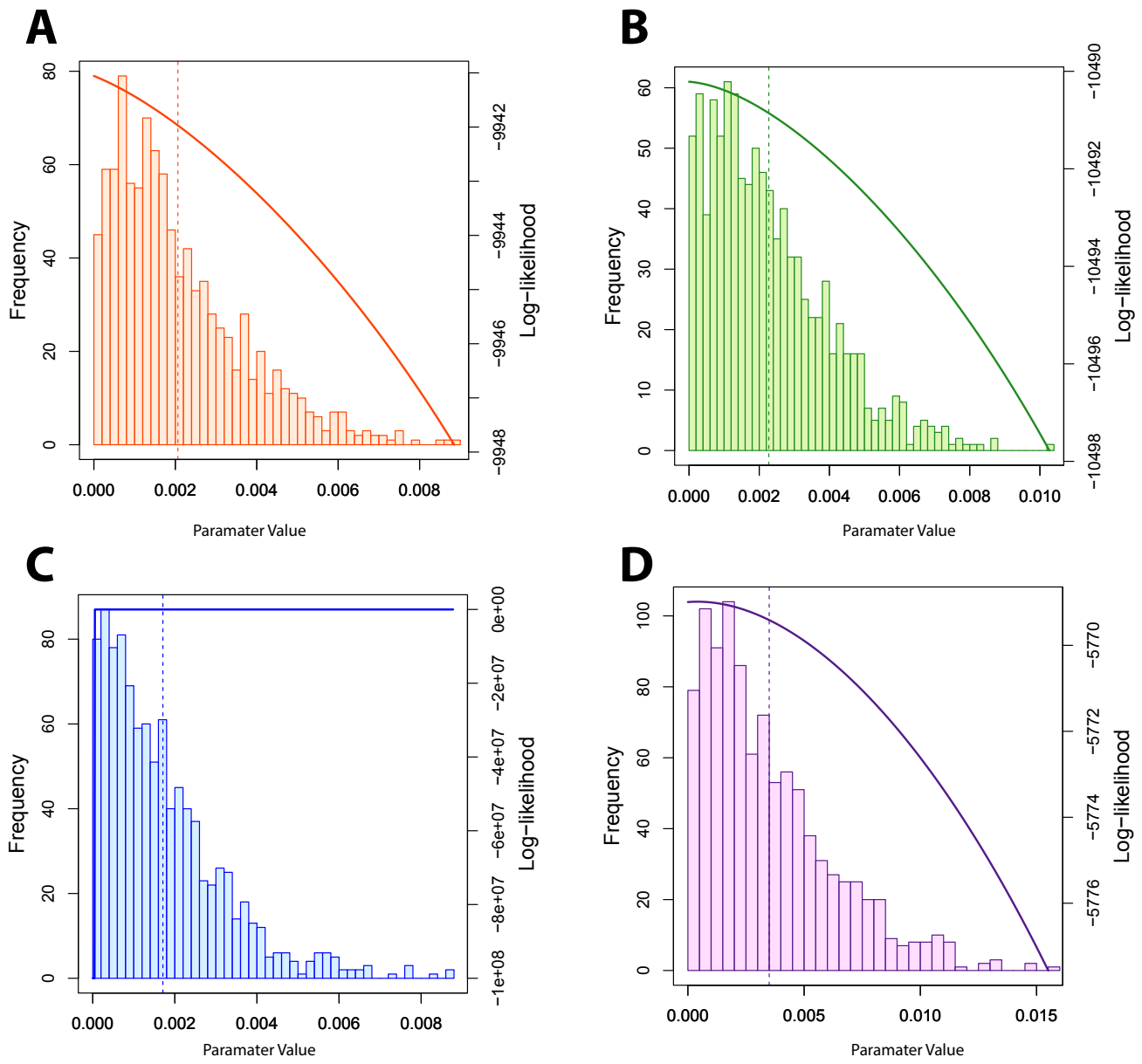

Fig. S16: **Posterior distribution and likelihood of final spline parameter.** The posterior distribution of the final spline parameter (histogram), posterior median of the final spline parameter (dashed line) and likelihood based on keeping all other parameters fixed at their posterior median and varying the final spline parameter (thick solid line) are plotted against values of the final spline parameter for (a) DENV-1, (b) DENV-2, (c) DENV-3, and (d) DENV-4. It is important to note that the solid line is not the profile likelihood, because the profile likelihood would be calculated by optimizing all other parameter values for any suggested value of the final spline parameter (and would thus decrease less sharply than the solid plotted line). In all cases however, it is clear that the same configuration of all other parameters and setting the final parameter equal to 0 (or a value much lower than the posterior median in the case of DENV-4) would have resulted in a better likelihood.

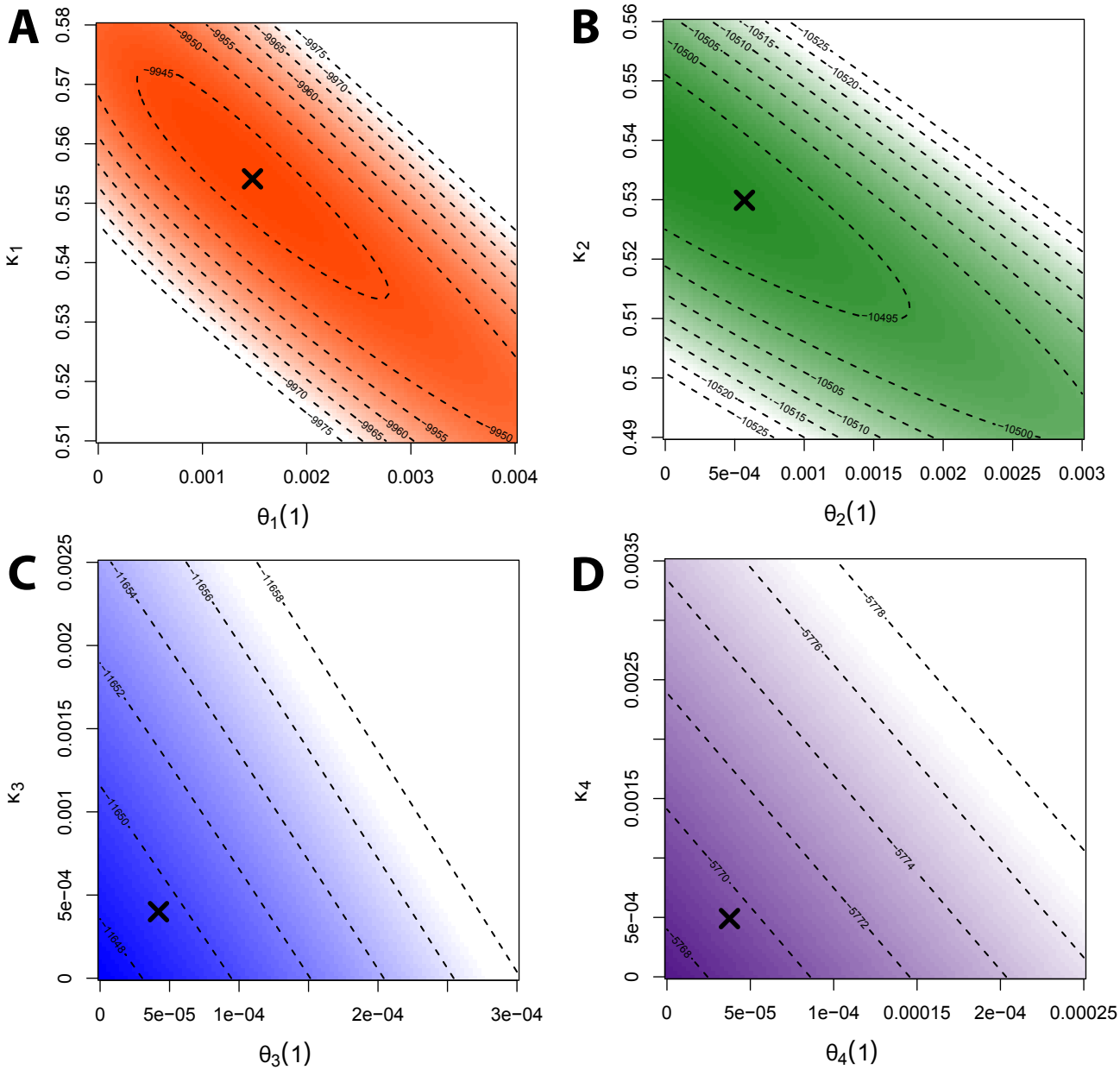

Fig. S17: **Identifiability issues between κ and the first spline parameter.** The 2-dimensional posterior distribution of κ and the first spline parameter are plotted for (a) DENV-1, (b) DENV-2, (c) DENV-3, and (d) DENV-4. In each case, there was a linear relationship between κ and the first spline parameter, especially for DENV-1 and DENV-2, making identification of the true value of the first spline parameter impossible in the current framework.

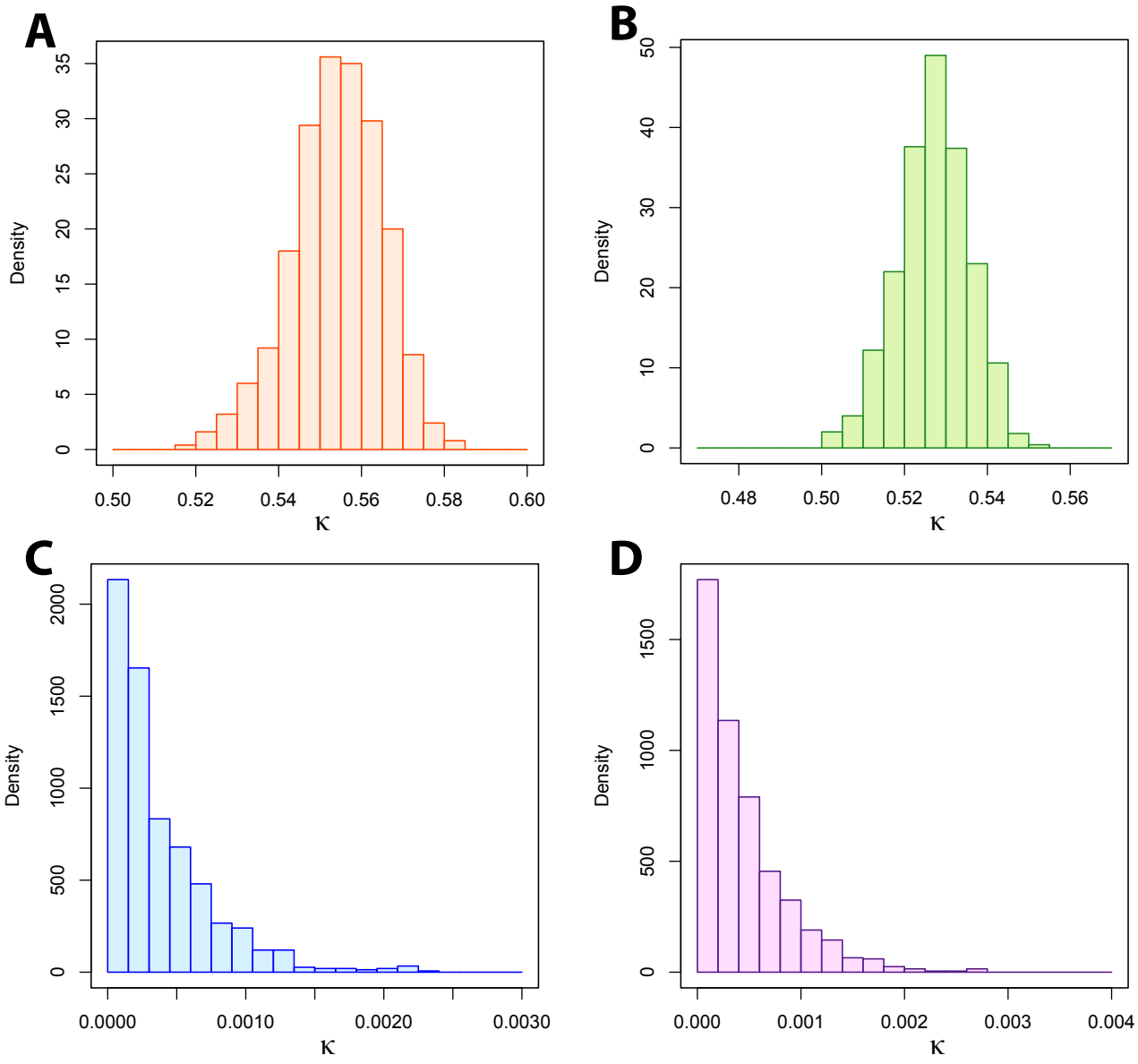

Fig. S18: **Posterior distribution of κ.** The posterior distribution of the fraction of the study population that was susceptible to each serotype at the time of the beginning of the study in 1999 is plotted for (a) DENV-1, (b) DENV-2, (c) DENV-3, and (d) DENV-4. Note that the scale is not the same for each of the figures.

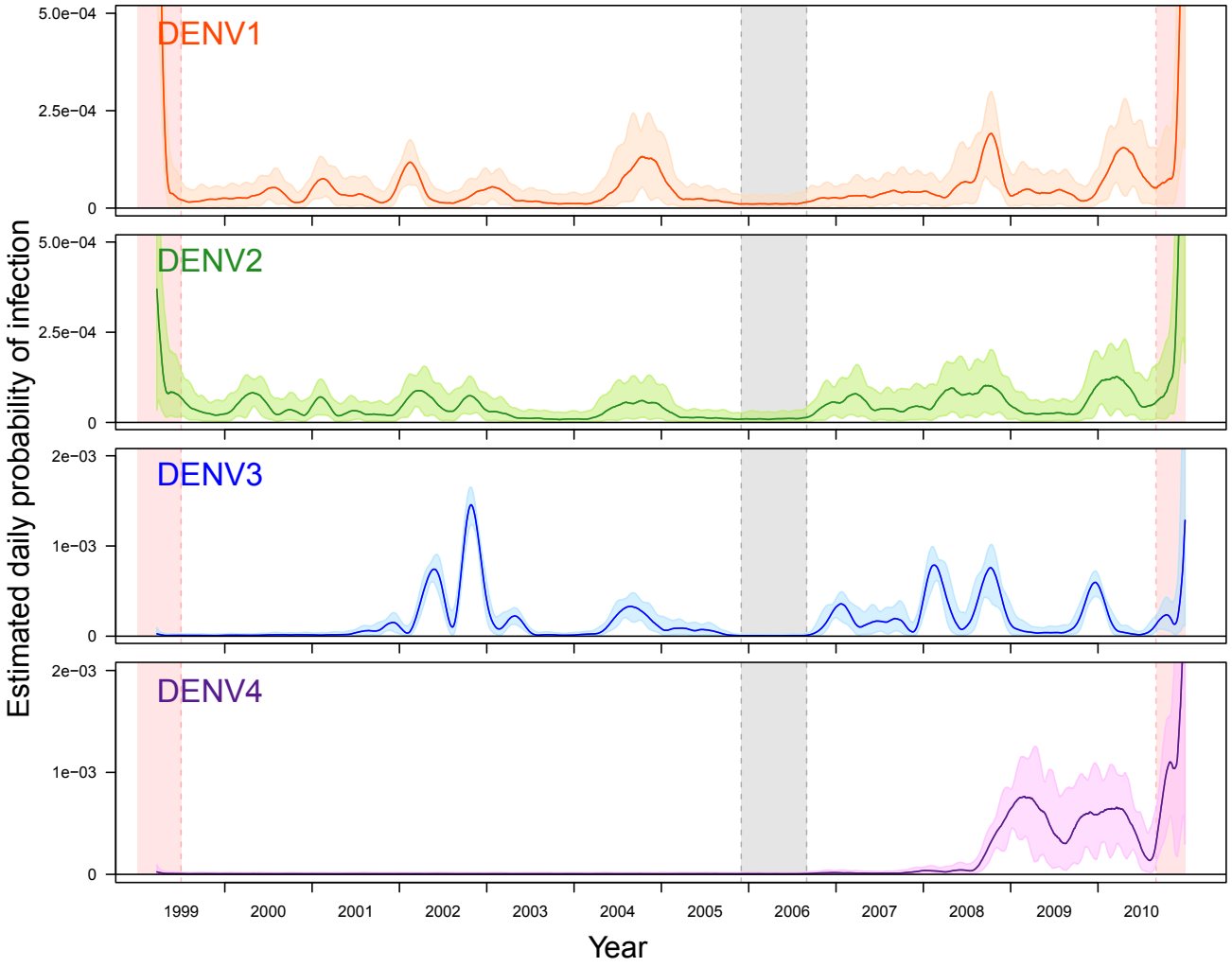

Fig. S19: **Estimated daily probability of infection, f.** For each serotype (DENV-1 top panel (orange), DENV-2 second panel (green), DENV-3 third panel (blue) and DENV-4 bottom panel (purple)), daily estimates of the probability of infection, f, as well as the 90% BCI are plotted against time. The absence of a cohort study from late 2005 to mid-2006 is indicated by the grey shaded region. The red regions at the beginning and end of the plots indicate where the identifibility issues for the first and last spline parameter greatly affected the results.

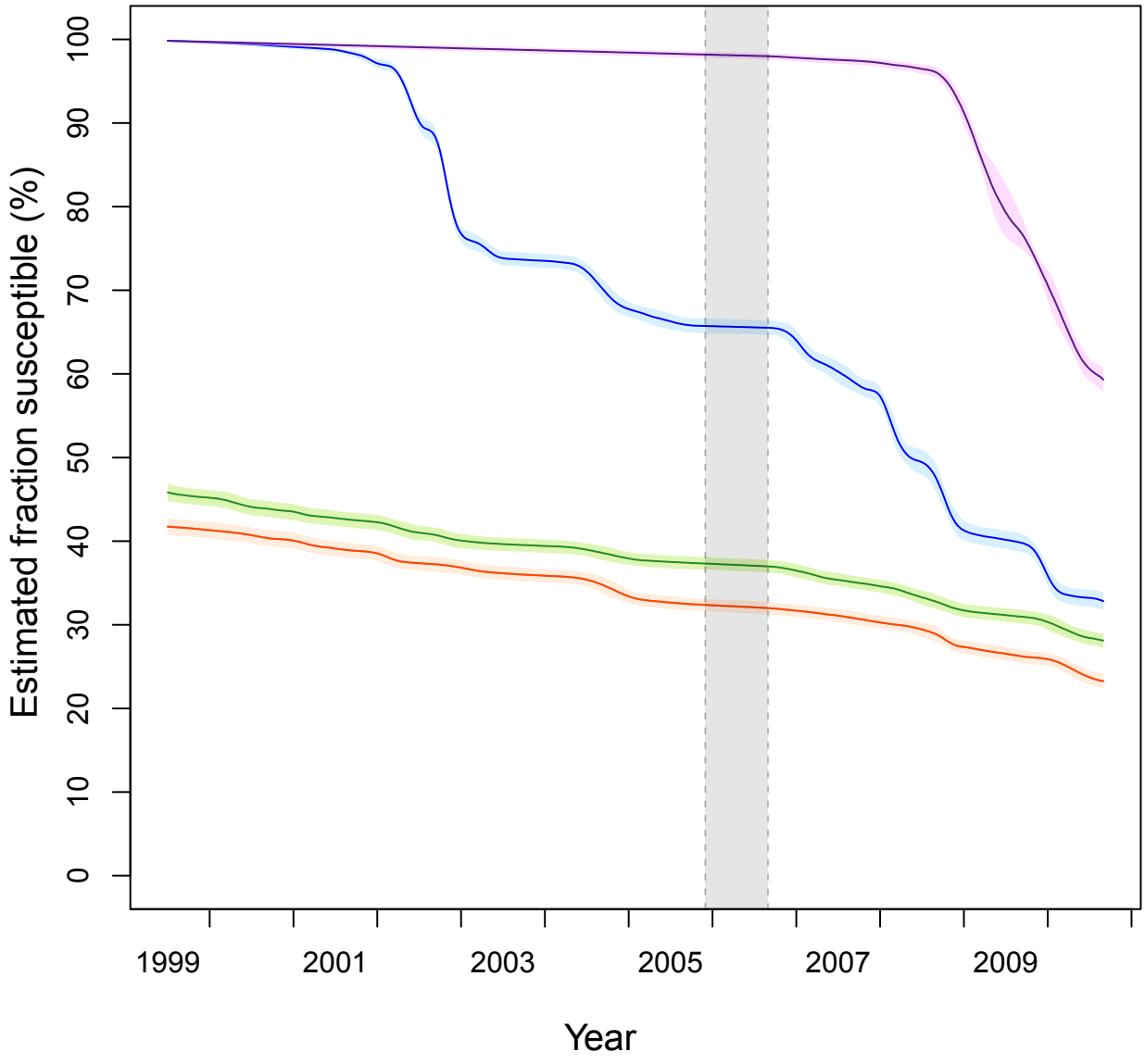

Fig. S20: **Fraction of the study population susceptible over time.** The fraction of the study population that was susceptible over time, $s(t)$, is plotted as a percentage for (a) DENV-1, (b) DENV-2, (c) DENV-3, and (d) DENV-4. Note that because we defined our study population to be those that were born before 1995 (and thus the susceptible pool was never replenished) and each serotype circulated after its introduction, these estimates decreased over time.

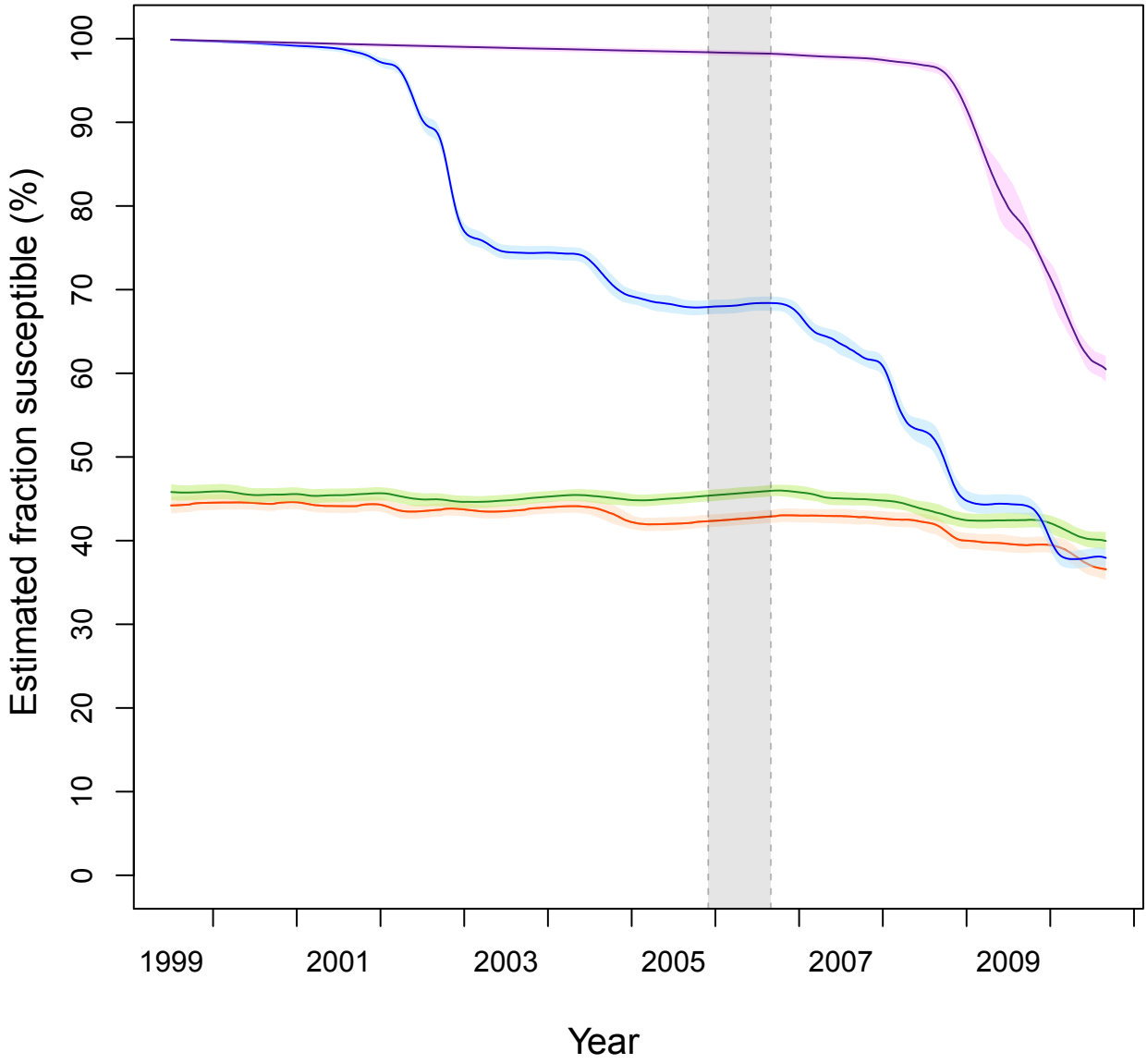

Fig. S21: **Fraction of the entire population susceptible over time.** The fraction of the entire population that was susceptible over time, $s_P(t)$, is plotted as a percentage for (a) DENV-1, (b) DENV-2, (c) DENV-3, and (d) DENV-4.

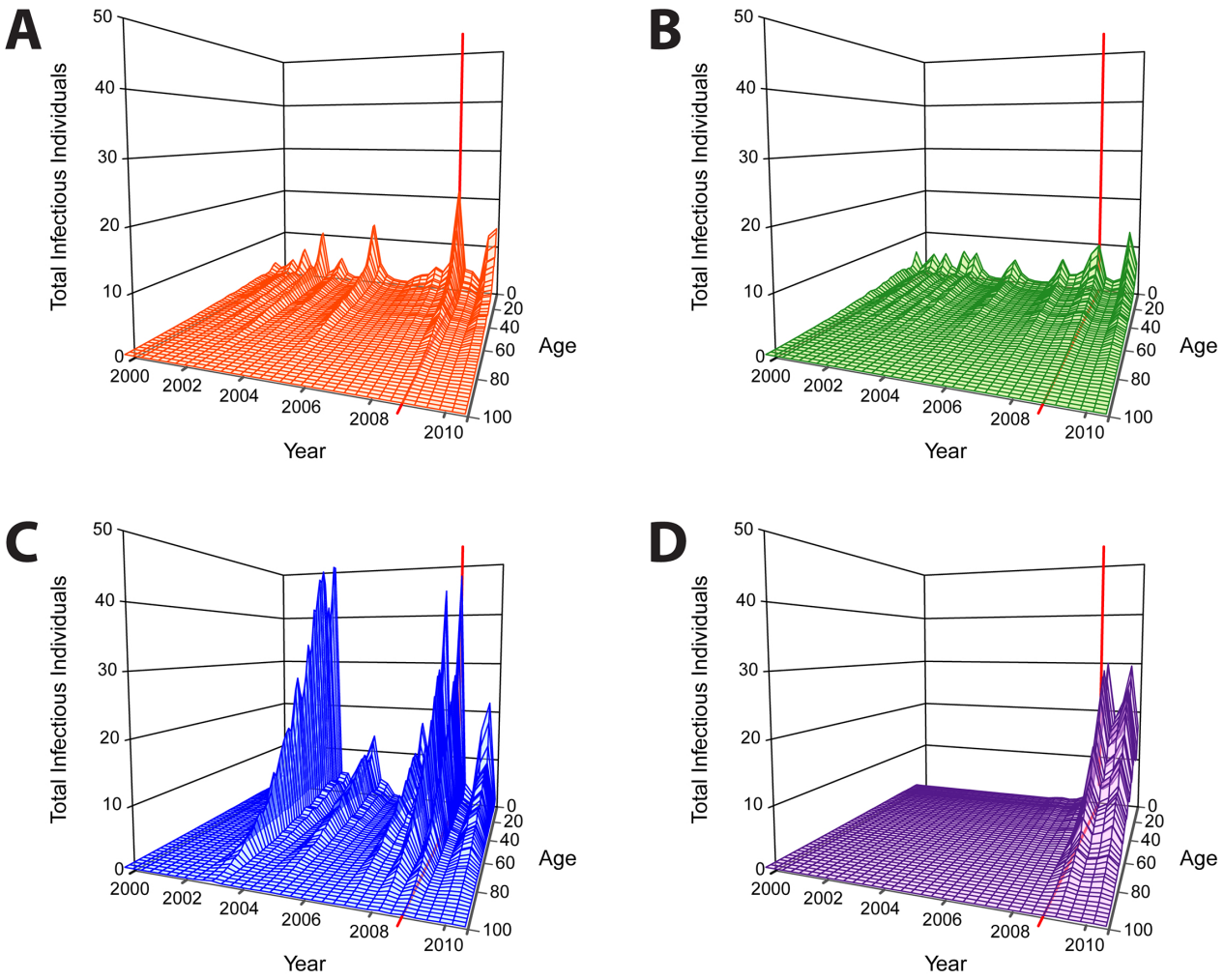

Fig. S22: **Estimated number of infectious individuals within Iquitos by age and day.** Using an age-structured SEIR model driven by the *FoI* estimates, the estimated number of individuals that are infectious on any given day are plotted by age for (a) DENV-1, (b) DENV-2, (c) DENV-3, and (d) DENV-4. The red line indicates October 1, 2008

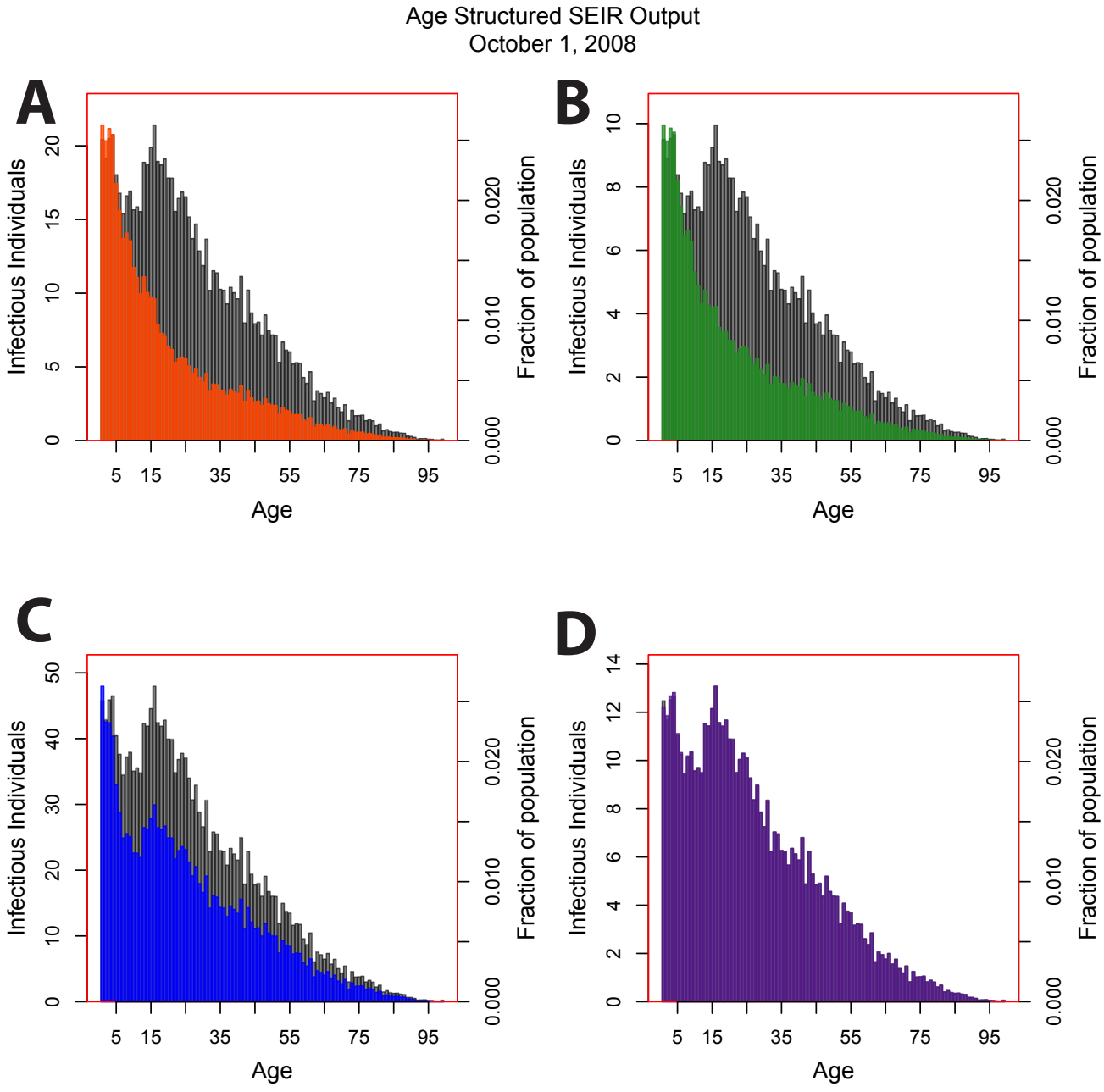

Fig. S23: **Predicted age distribution of infectious individuals within Iquitos.** The age distribution of infectious individuals on October 1, 2008, predicted from an age-structured SEIR model driven by the *FoI* estimates, is plotted for (a) DENV-1, (b) DENV-2, (c) DENV-3, and (d) DENV-4. The age distribution of the Iquitos population is plotted in dark gray.

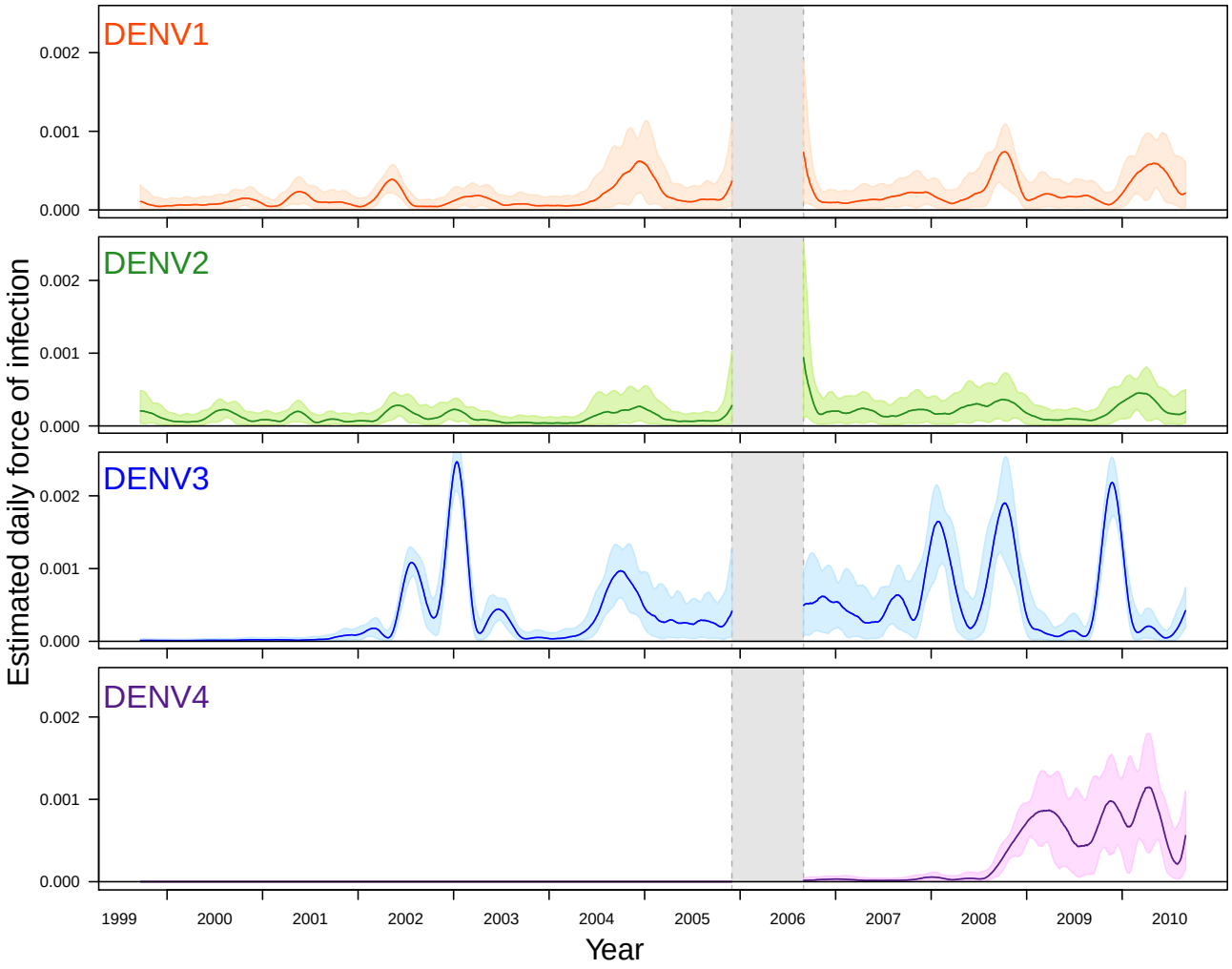

Fig. S24: **Robustness of daily estimates of the *FoI* to 2005-2006 gap.** Fitting two different models to the two halves of the data, using the gap from 2005-2006 to split the data, the resulting estimates of the *FoI* are plotted along with the 90% BCIs against time (DENV-1 top panel (orange), DENV-2 second panel (green), DENV-3 third panel (blue) and DENV-4 bottom panel (purple)). The absence of a cohort study from late 2005 to mid-2006 is indicated by the grey shaded region.

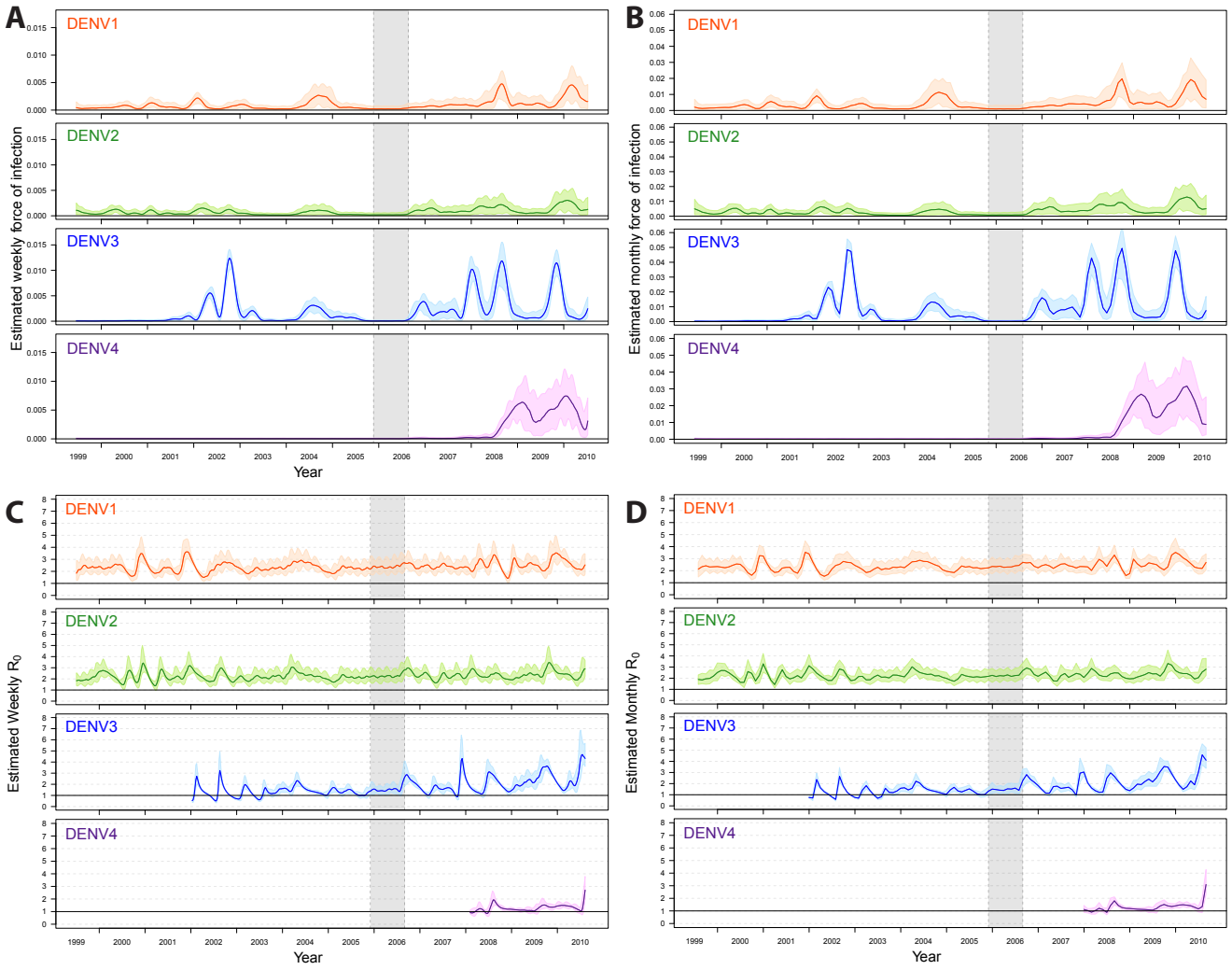

Fig. S25: **Weekly and monthly estimates of the *FoI* and $\mathcal{R}_0$.** In panel (a) and (b) respectively, weekly and monthly estimates of the *FoI* are plotted along with 90% BCIs. In panels (c) and (d) respectively, weekly and monthly averages of $\mathcal{R}_0$ are plotted along with 50% BCIs. For each panel, DENV-1 is plotted in the top sub-panel (orange), DENV-2 in the second sub-panel (green), DENV-3 in the third sub-panel (blue) and DENV-4 is plotted in the bottom sub-panel (purple)). The absence of a cohort study from late 2005 to mid-2006 is indicated by the grey shaded region.

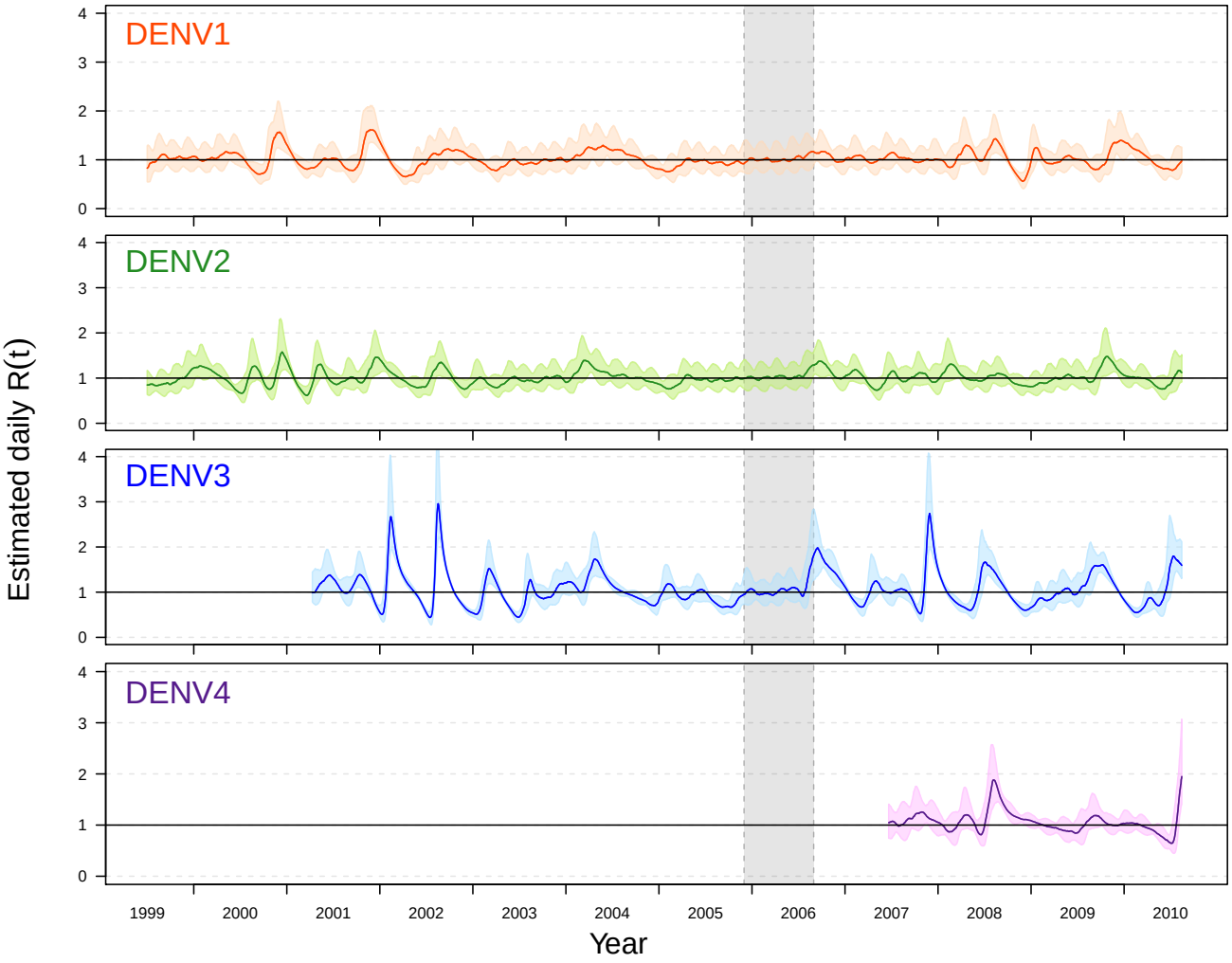

Fig. S26: **Daily estimates of the effective reproductive number,** $R(t)$**.** For each serotype (DENV-1 top panel (orange), DENV-2 second panel (green), DENV-3 third panel (blue) and DENV-4 bottom panel (purple)), daily estimates of R(t) as well as the 50% BCI are plotted against time. The absence of a cohort study from late 2005 to mid-2006 is indicated by the grey shaded region. The estimates for both DENV-3 and DENV-4 are truncated, excluding estimation before their respective introductions.

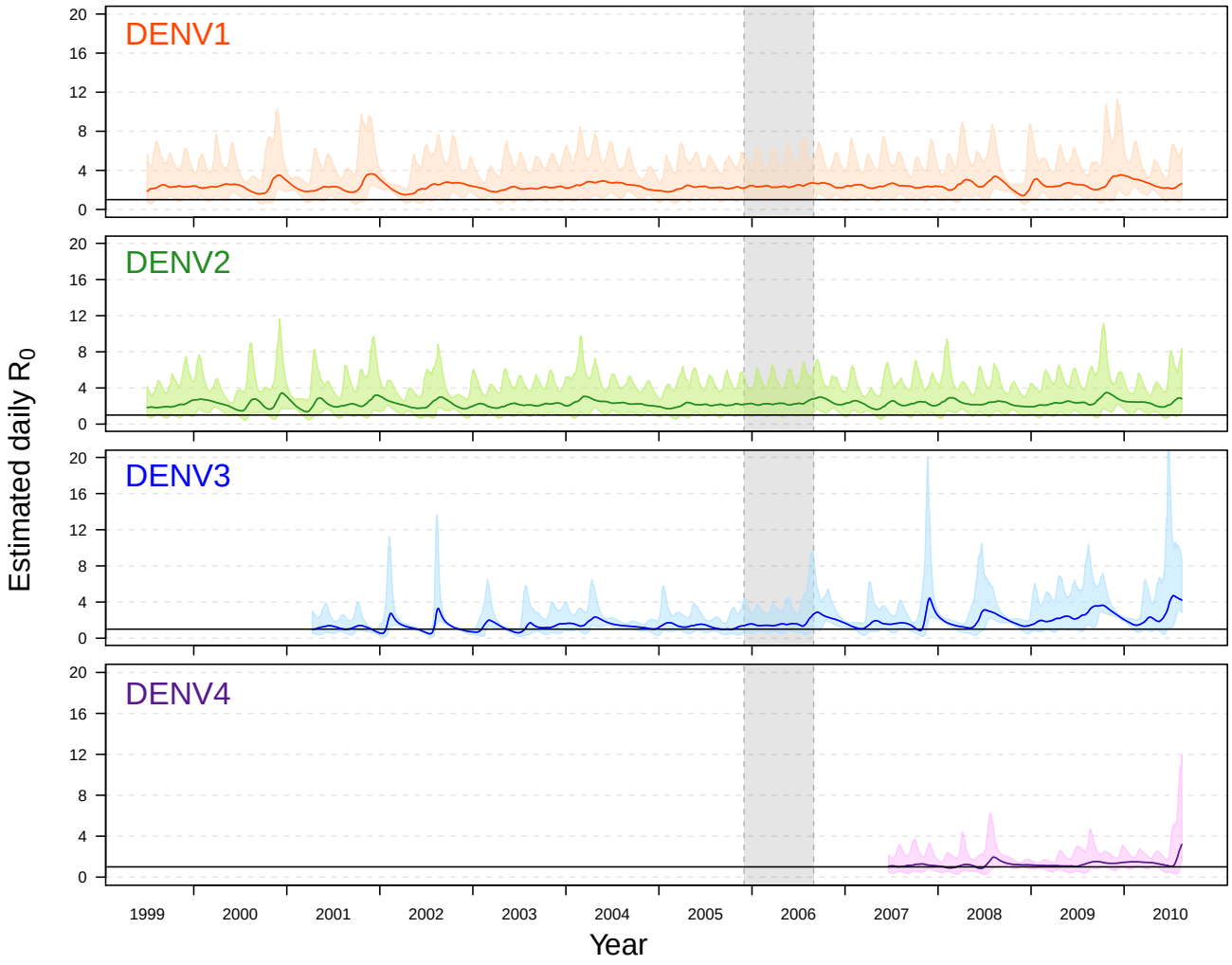

Fig. S27: **Daily estimates of $\mathcal{R}_0$.** For each serotype (DENV-1 top panel (orange), DENV-2 second panel (green), DENV-3 third panel (blue) and DENV-4 bottom panel (purple)), daily estimates of $\mathcal{R}_0$ as well as the 90% BCI are plotted against time. The absence of a cohort study from late 2005 to mid-2006 is indicated by the grey shaded region. The estimates for both DENV-3 and DENV-4 are truncated, excluding estimation before their respective introductions. While the lower bound of the 90% BCI was comparable to that of the 50% BCI (Figure 5), the upper bound was considerably larger, in the extreme suggesting $\mathcal{R}_0$ values that exceeded 20 as being within the credible interval.

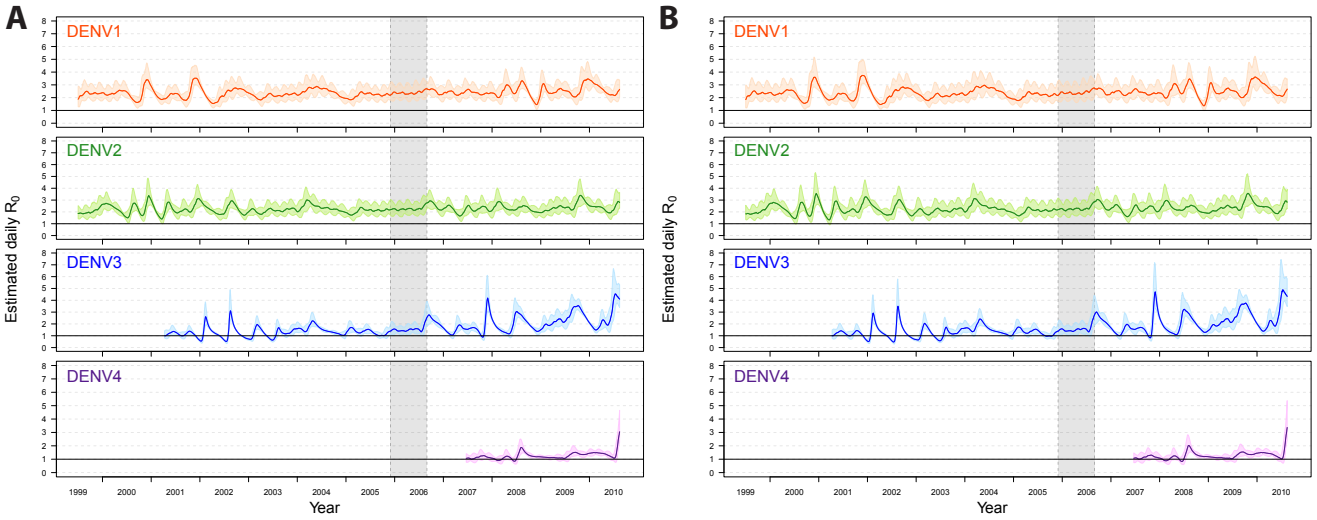

Fig. S28: **Sensitivity of $\mathcal{R}_0$ to the serial interval, part 1.** We recomputed $\mathcal{R}_0$ using both a shorter and longer serial interval than found in [13]. In (a), we assumed that the length of time between primary and secondary infections was exactly 15 days. In (b), we lengthened the serial interval to 5 days, allowing the time between a primary and secondary infection to be between 15 and 19 days. In both (a) and (b), for each serotype (DENV-1 top panel (orange), DENV-2 second panel (green), DENV-3 third panel (blue) and DENV-4 bottom panel (purple)), daily estimates of $\mathcal{R}_0$ as well as the 50% BCI are plotted against time.

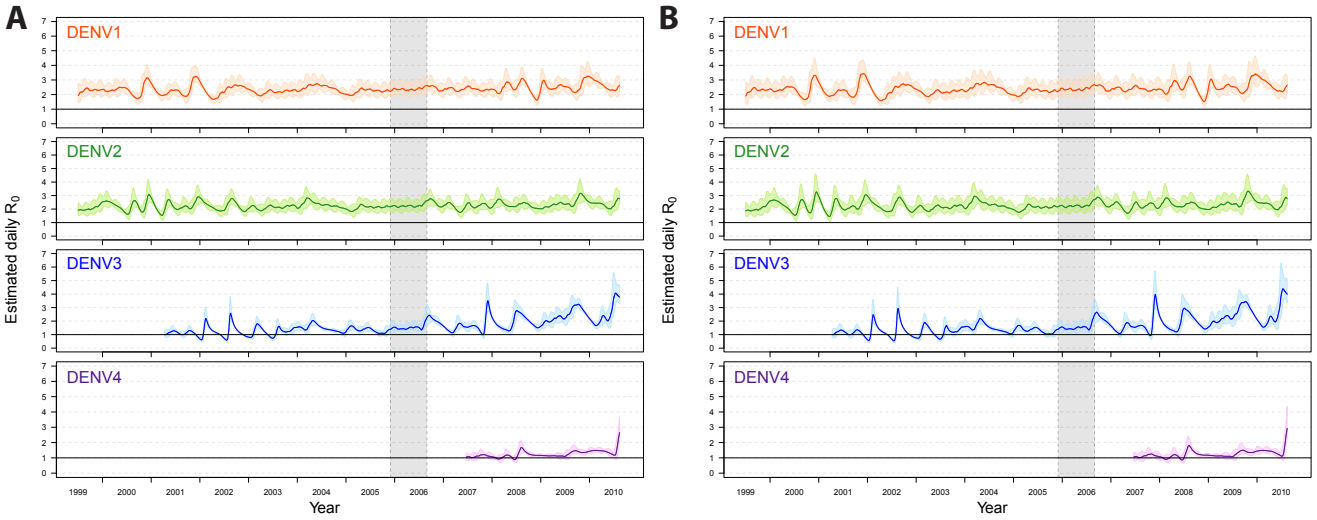

Fig. S29: **Sensitivity of $\mathcal{R}_0$ to the serial interval, part 2.** Using the lower bound on both the EIP and the IIP for DENV reported in the literature, we estimated the shortest serial interval possible as 11 days. Using this value we recomputed $\mathcal{R}_0$. In (a), we assumed that the length of time between primary and secondary infections was between 11 and 13 days. In (b), we combined this lower bound (11 days) with the upper bound found in [13] (17 days), allowing the time between a primary and secondary infection to be between 11 and 17 days. In both (a) and (b), for each serotype (DENV-1 top panel (orange), DENV-2 second panel (green), DENV-3 third panel (blue) and DENV-4 bottom panel (purple)), daily estimates of $\mathcal{R}_0$ as well as the 50% BCI are plotted against time.

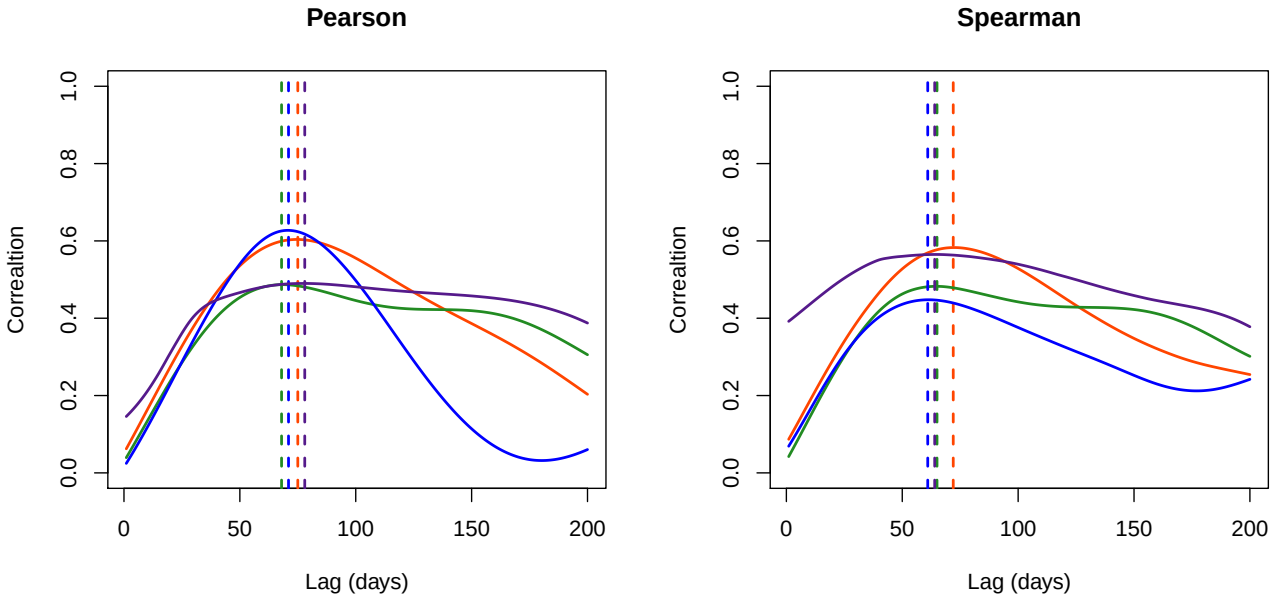

Fig. S30: **Lagged relationship between the *FoI* and $\mathcal{R}_0$.** The Pearson and Spearman rank correlations (left and right panel respectively) are plotted for various lags between the *FoI* and $\mathcal{R}_0$ for each serotype (DENV-1 (orange), DENV-2 (green), DENV-3 (blue) and DENV-4 (purple)). The maximum lags (illustrated by vertical dashed lines) were comparable for each serotype and were between 55 and 75 days.

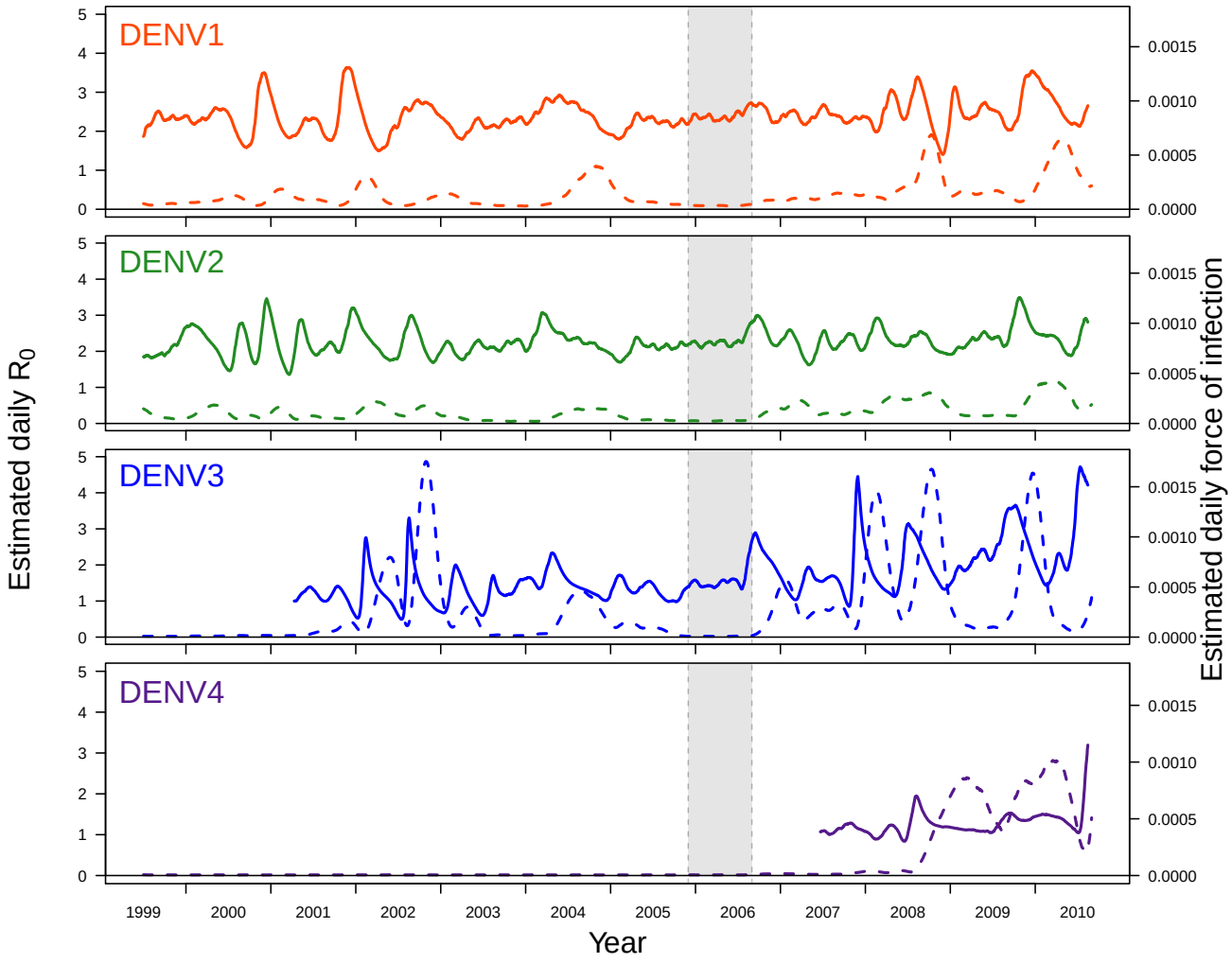

Fig. S31: **Relationship between the *FoI* and $\mathcal{R}_0$.** For each serotype (DENV-1 top panel (orange), DENV-2 second panel (green), DENV-3 third panel (blue) and DENV-4 bottom panel (purple)), daily estimates of the *FoI* (dashed lines) and $\mathcal{R}_0$ (solid lines) are plotted each other against time. The absence of a cohort study from late 2005 to mid-2006 is indicated by the grey shaded region. Every increase in the *FoI* was preceded by a sharp spike in $\mathcal{R}_0$.

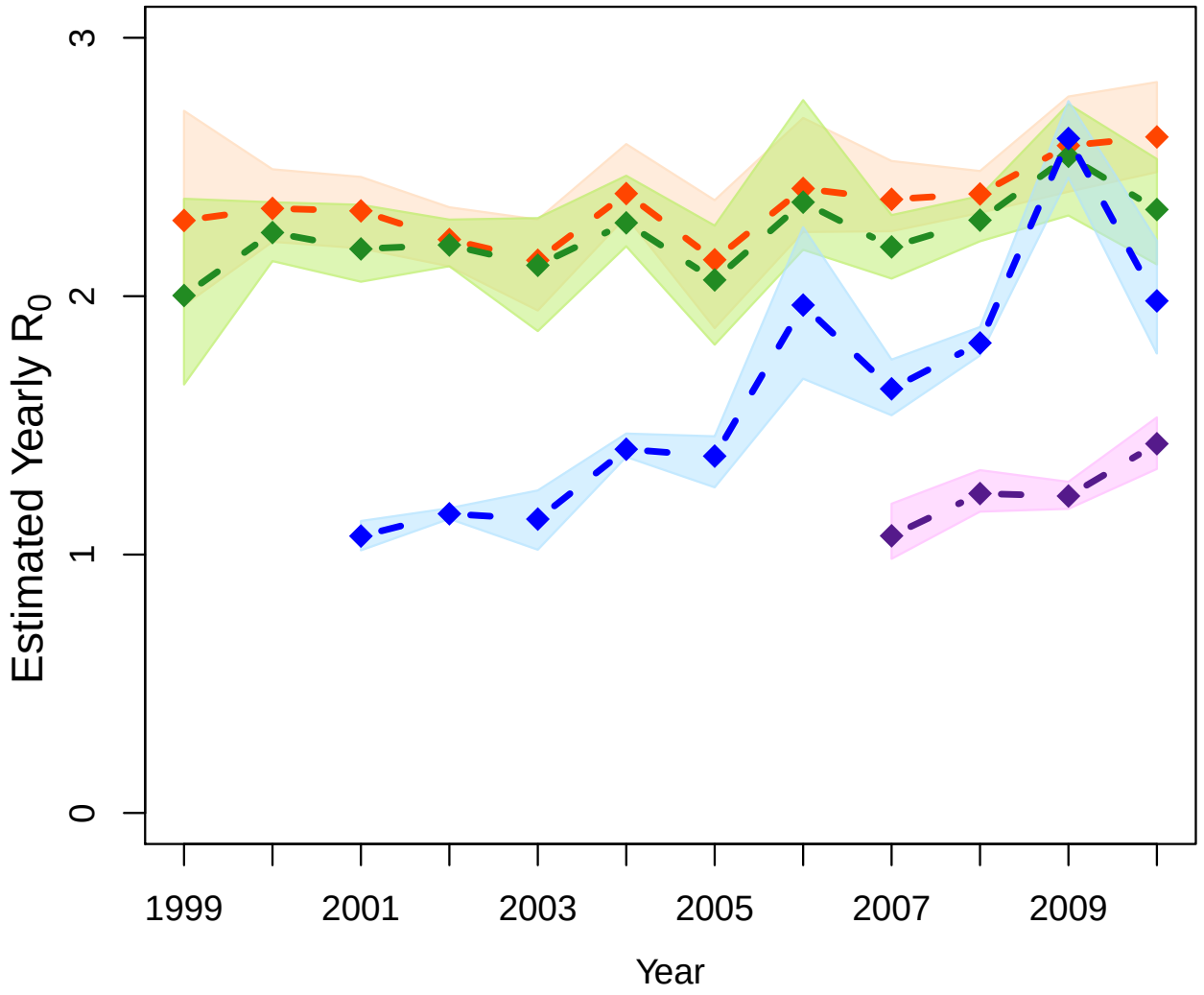

Fig. S32: **Yearly estimates of $\mathcal{R}_0$.** For each serotype (DENV-1 top panel (orange), DENV-2 second panel (green), DENV-3 third panel (blue) and DENV-4 bottom panel (purple)), yearly estimates of $\mathcal{R}_0$ as well as the 90% BCI are plotted against time by computing the yearly mean of the daily estimates. The estimates for both DENV-3 and DENV-4 are truncated, excluding estimation before their respective introductions.

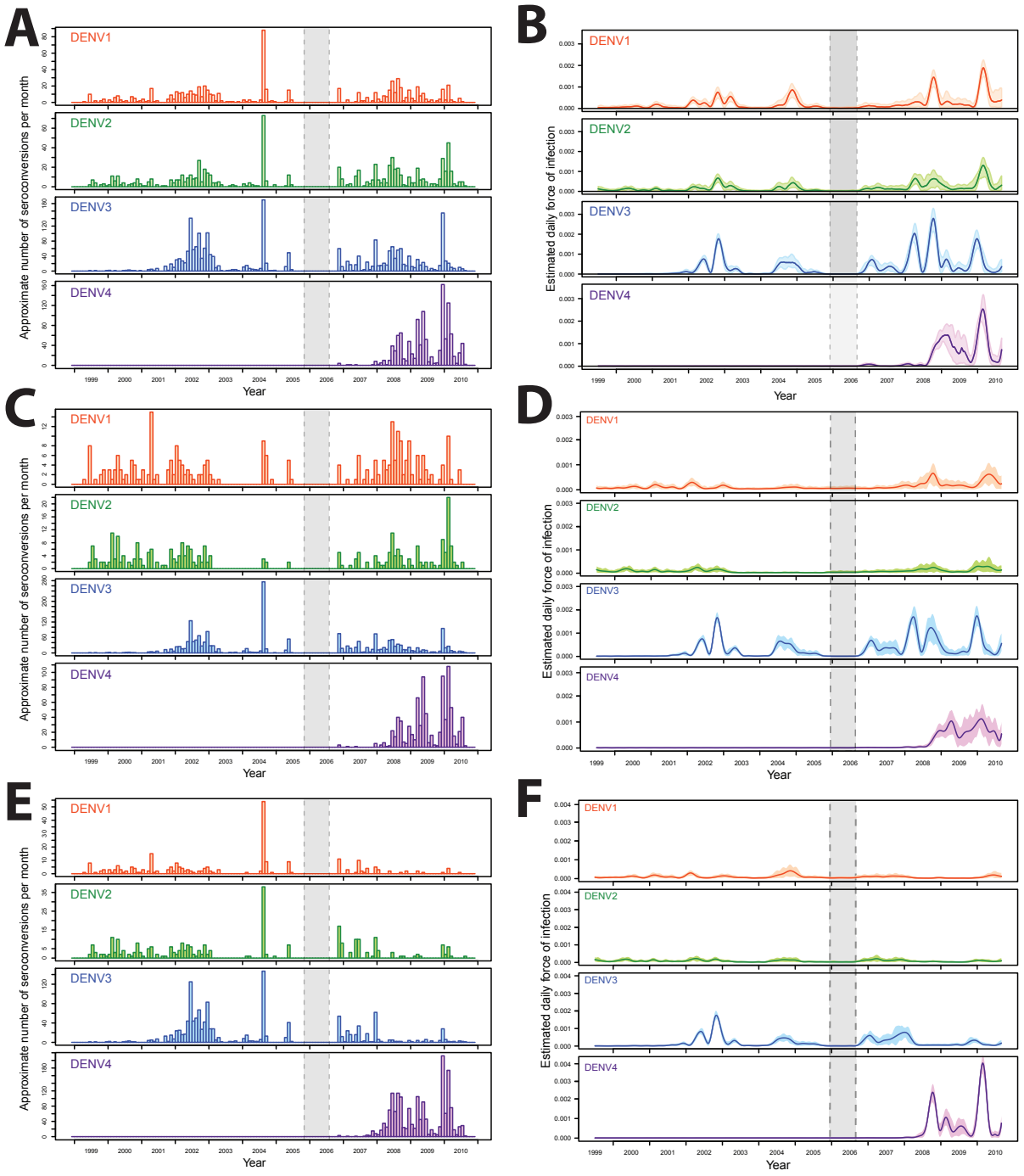

Fig. S33: **Results using three alternative data cleaning methods.** We repeat our analysis under different data cleaning approaches. Analogous to Figure 1 we plotted the number of interval censored infections by serotype against time, where the midpoint of the interval over which the infection was censored was used to time infections in (a), (c) and (e). Analogous to Figure 3, for each serotype (DENV-1 top panel (orange), DENV-2 second panel (green), DENV-3 third panel (blue) and DENV-4 bottom panel (purple)), daily estimates of the *FoI* as well as the 90% BCI are plotted against time in (b), (d) and (f). In (a) and (b) we used the least conservative cleaning method which allows for multiple seroconversions within any interval as well as automatically assuming any positive DENV-3 and DENV-4 test cannot be a false positive. In (c) and (d) we implement the restrictive assumption that any individual's first seroconversion from 2003 to 2008 was declared DENV-3 unless the individual already appeared to have seroconverted to DENV-3. In (e) and (f) we implement the restrictive assumption that any individuals' first seroconversion from 2008 to 2010 was declared DENV-4 unless the individual already appeared to have seroconverted to DENV-4.